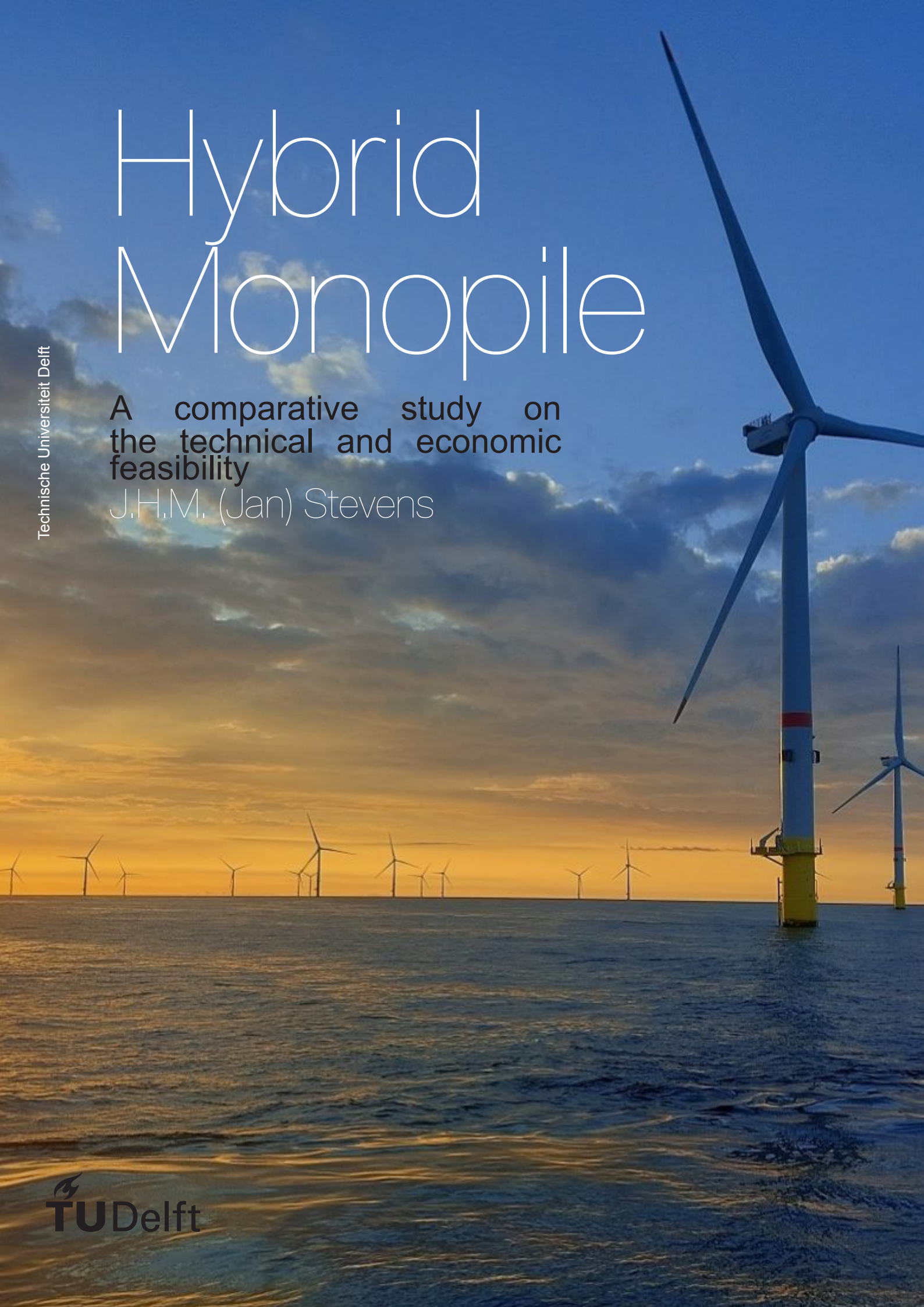

Hybrid Monopile

A comparative study on the technical and economic feasibility

J.H.M. (Jan) Stevens

Technische Universiteit Delft

TU Delft

Hybrid Monopile

A comparative study on the technical and economic feasibility

by

J.H.M. (Jan) Stevens

to obtain the degree of Master of Science,

in the field of Civil Engineering,

at the Delft University of Technology,

to be defended publicly on Wednesday August 28, 2024 at 2:30 PM.

Student number:	5647258	
Project duration:	March 1, 2024 – August 28, 2024	
Thesis committee:	Dr. J.O. Colomes Gene,	TU Delft
	Dr. A. Tsouvalas,	TU Delft
	Ir. T. Balder,	Heerema Engineering Solutions
	Ir. A. Adriaenssens,	Heerema Engineering Solutions

An electronic version of this thesis work is available at: `http://repository.tudelft.nl/`.

Cover image credited to Deltares [1].

The work in this thesis was supported by Heerema Engineering Solutions
Their cooperation is hereby gratefully acknowledged.

TU Delft Delft University of Technology

Preface

This thesis marks the end of my study at Delft University of Technology. It represents the final step toward obtaining my Master of Science degree in Civil Engineering, with a focus on Hydraulic and Offshore Structures. Throughout my studies, I have been deeply interested in the offshore world, and this thesis has allowed me to explore this passion further by contributing to the development of innovative solutions for offshore wind energy.

Conducting my research in collaboration with Heerema Engineering Solutions (HES) has been an great opportunity. Working alongside experts in the field of offshore engineering has enriched my understanding and provided practical insights into the challenges and advancements within the industry. This collaboration allowed me to investigate new ideas and contribute to more sustainable practices in offshore wind development.

I am truly thankful to Thomas Balder and Arthaud Adriaenssens for their support and guidance throughout this project. Our regular meetings were essential in improving my research and work on various challenges. Their expertise, along with the assistance of the entire HES team, has greatly enhanced the quality of this thesis.

Special appreciation goes to my supervisors from the TU Delft, Oriol Colomes Gene and Apostolos Tsouvalas. Their constructive feedback, academic mentorship, and dedication have been crucial in shaping the direction and outcome of this research. The bi-weekly meetings we had were particularly valuable in keeping my work focused and continuously improving.

I am also grateful to my friends and peers for their support. Our coffee breaks and study sessions were not only enjoyable but also provided a space to discuss and resolve engineering challenges, often leading to new insights and solutions.

Lastly, I want to express my deepest gratitude to my family. Your unconditional support, encouragement, and belief in me have been the driver of my journey. This achievement would not have been possible without your unconditional support.

Jan Stevens
Delft, August 2024

Abstract

To meet the ambitious targets outlined in the Paris Climate Agreement of limiting global temperature rise to 1.5 degrees Celsius, global renewable power generation must triple by 2030, with offshore wind energy expected to increase exponentially to 500 GW—a fourteen-fold rise from 2020. Despite a 48% cost reduction from 2010 to 2020, offshore wind energy remains more costly per megawatt-hour than fossil fuels, highlighting the need for cost-effective innovations in offshore wind farm foundations in the North Sea.

Offshore wind farms are increasingly moving into deeper waters and utilizing larger turbines, which arise challenges for traditional monopile foundations. The Hybrid Monopile (HMP) is a promising alternative. It integrates features from traditional monopiles and jackets, potentially enhancing structural stability, reducing environmental impact, and optimizing costs in deeper waters. This thesis evaluates the technical and economic feasibility of the HMP compared to traditional foundation types such as the traditional monopile and jacket structure, aiming to accelerate development of offshore wind energy and contribute to global climate objectives.

This study uses a comprehensive methodology to assess the HMP's structural integrity, installation feasibility, and cost-effectiveness relative to traditional monopiles and jackets. The structural analysis begins with a preliminary design phase to establish input parameters for the finite elements analysis in Abaqus. This analysis evaluates natural frequencies and stress levels under varied conditions such as water depth, soil types, and turbine sizes, assessing the HMP's feasibility across different conditions.

The installation procedures are investigated, evaluating various strategies for HMP's and compare it with the installation strategies of traditional monopiles and jackets. The most efficient way of installation is determined for the installation of the Hybrid Monopile while considering various options. This is compared to industry standards for the installation of the traditional monopile and jacket structure. The economic evaluation involves cost modeling. This analysis provides a cost comparison based on the manufacturing and installation of the structures, highlighting the economic advantages of the HMP in deeper waters and with larger turbine.

Structural assessments demonstrate that the HMP is capable of deployment in water depths up to 80 meters and supporting offshore wind turbines of up to 22 megawatts in the North Sea. Design simulations indicate the HMP's resilience against operational stresses caused by various environmental forces. The installation strategies emphasize efficient methodologies for HMP installation. Due to the fact the hybrid monopile requires an increased number of pin piles compared to jackets, the installation cycle of the hybrid monopile is less superior to the jacket, where the traditional monopile outperforms both of them based on installation time. Economic analyses highlight that while traditional monopiles are cost-effective in waters until 40 meter, the HMP emerges as a competitive solution for deeper waters and larger turbine configurations compared to jacket structures.

In conclusion, the HMP represents an advancement over traditional jackets assuming a 20% reduction in interface piece manufacturing costs. Further optimizations in the design of the Hybrid Monopile and installation procedures could enhance its competitiveness in relation with a jacket. The traditional monopile is a more cost-effective solution in environments where possible, however the HMP offers a promising solution where noise and environmental limitation arises.

Contents

List of Figures

List of Tables

Glossary

Acronyms

BBC	Big Bubble Curtain
CEA	Computer-aided Engineering
DAF	Dynamic Amplification Factor
dB	Decibel
DLC	Design Load Case
DOF	Degrees of Freedom
DTU	Danmarks Tekniske Universitet
EOM	Equation of Motion
FEA	Finite Element Analysis
FEM	Finite Element Method
GW	Gigawatt
HES	Heerema Engineering Solutions
HMC	Heerema Marine Contractors
HMP	Hybrid Monopile
IEA	International Energy Agency
IEC	International Electrotechnical Commission
IP	Interface piece
LW	LEANWIND
MDOF	Multiple Degrees of Freedom
mt	Megaton
MW	Megawatt
NREL	National Renewable Energy Laboratory
OSV	Offshore Support Vessel
PP	Pin pile
RNA	Rotor Nacelle Assembly
ROV	Remotely operated vehicle
RPM	Round Per minute
SDOF	Single Degree of Freedom
SEL	Sound Exposure Level
SF	Safety Factor
SSCV	Semi-submersible crane vessel

TP	Transition piece
ULS	Ultimate Limit State
WTG	Wind Turbine Generator

Symbols

Roman

a	Wave crest	$[m]$
A_d	Rotor surface	$[m^2]$
c	Damping constant	$[Ns/m]$
c	Cohesion	$[kPa]$
C_a	Added mass coefficient	[-]
C_d	Drag coefficient	[-]
C_m	Inertia coefficient	[-]
C_T	Thrust coefficient	[-]
D	Diameter	$[m]$
g	Gravity	$[m/s^2]$
F_b	Base shear force	$[N]$
F_T	Thrust force	$[N]$
k	Spring constant	$[N/m]$
k_w	Wave number	$[m^{-1}]$
KC	Keulegan-Carpenter number	[-]
m	Mass	$[N]$
M	Overturning moment	$[Nm]$
r	Pearson correlation coefficient	[-]
Re	Reynolds number	[-]
S	Squared residuals	[-]
t	Thickness	$[m]$
T	Wave period	$[s]$
u	Flow velocity	$[m/s]$
U_{max}	Maximum flow velocity	$[m/s]$
$\dot{u}$	Flow acceleration	$[m/s^2]$
V_{infty}	Free-stream velocity	$[m/s]$

Greek

α	Axial induction factor	[-]
β	Sarpkaya's Beta	[-]
γ	Unit weight	$[kN/m^3]$
ρ_a	Density of air	$[kg/m^3]$
ρ_w	Density of (sea) water	$[kg/m^3]$
σ_N	Axial stress	$[kPa]$
σ_M	Bending Stress	$[kPa]$
υ	Kinematic viscosity of the fluid	[°]
ϕ	Velocity potential	$[m^2/s]$
φ	Friction angle	$[m^2/s]$
ω	Angular frequency	$[rad/s]$
ω_w	Wave frequency	$[rad/s]$
ω_n	Natural Frequency	$[rad/s]$

1 Introduction

1.1. Trend in offshore wind energy

In pursuit of aligning with the Paris Climate Agreement and limiting global temperature rise to 1.5 degrees Celsius, global renewable power generation must triple by 2030. The offshore wind energy sector contributes significant in this effort, with a target of reaching 500 GW globally by 2030, a fourteen-fold increase from 2020 [3]. Currently, fossil fuels like oil, gas, and coal account for 80% of global energy production, while renewable resources meet 29% of global electricity demand. To accelerate the transition to renewables, it is crucial to reduce the costs associated with renewable energy. From 2010 to 2020, the cost of energy from offshore wind turbines decreased by 48% [4]. However, renewable energy costs often remain higher than those of fossil fuels [5].

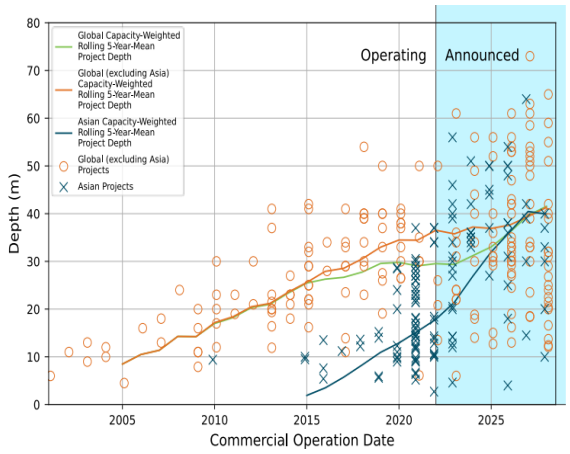

Figure 1.1: Increasing trend of water depth of wind farms [6]

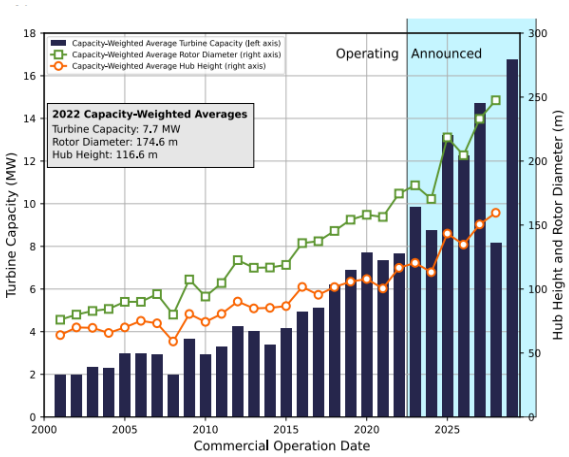

Figure 1.2: Increasing trend of wind turbines sizes offshore [6]

Figure 1.1 shows the increasing water depths of offshore wind farms, while Figure 1.2 depicts the growing sizes of offshore wind turbines [6]. These trends emphasize the need to explore new power generation methods that can handle deeper waters and support larger turbines. As offshore wind development moves towards deeper waters to take advantage of better wind conditions, it also faces more challenging environmental conditions. New methods should overcome the limitations of traditional foundations and reduce the costs of offshore wind turbines.

While the long-term expectation is that the lifetime costs of offshore wind energy will become competitive with or lower than those of oil and gas, current operational costs per MWh still favor fossil fuels [5]. Therefore, there is an urgent need for advancements in bottom-fixed foundations to enhance cost efficiency in offshore wind farms and support the broader shift towards sustainable energy solutions.

1.2. Offshore wind turbine foundation types

An interesting development in the offshore wind industry is the development of the Hybrid Monopile, which integrates the features of both traditional monopiles and jacket structures. In this section, the concept of the Hybrid Monopile is introduced and outlined. Also an overview of the traditional monopile and jacket structure, which will serve as a benchmark for comparison in this research.

1.2.1. Hybrid Monopile

The Hybrid Monopile (HMP) is a new concept for bottom-fixed offshore wind turbines developed by Heerema Engineering Solution (HES) and Heerema Marine Contractors (HMC). It combines the concept of the traditional monopile and jacket structure, although the Hybrid Monopile has differences.

The Hybrid Monopile basically is a traditional monopile supported by six smaller pin piles (PP) with an interface piece (IP) in between to connect the monopile to the pin piles (see Figure 1.3). Installation of the Hybrid Monopile avoids pile driving of heavy (mono)piles into the subsurface.

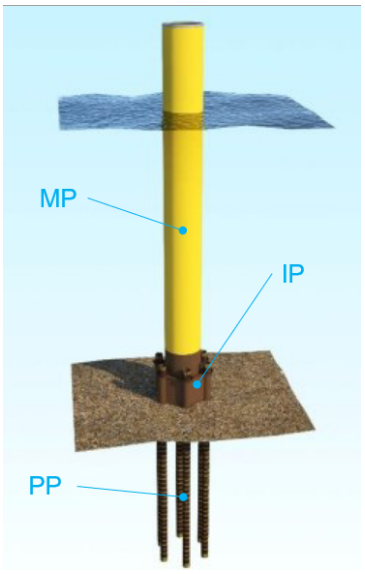

Figure 1.3: Hybrid Monopile concept from HES and HMC [7]

Utilizing pin piles as a foundation for the monopile has the potential to result in smaller monopile diameters. The advantage of smaller diameters lies in the simplified installation process, as it could requires less heavy crane vessels, fewer noise mitigation strategies and equipment. Consequently, the manufacturing and installation of the HMP could be a more cost-effective alternative compared to jacket structures and allow for utilization in deeper water compared to the traditional monopile.

1.2.2. Traditional monopile

The traditional monopile is a large, cylindrical steel tube driven into the seabed to provide a stable and secure foundation for offshore wind turbines. the traditional monopile is widely used due to its straightforward design [8]–[10]. They are suitable for various soil types like clay, sand, and gravel, and can even be installed in rock-socketed layers [11] [12]. However, the feasibility of manufacturing and installation is generally limited to water depths of up to around 45-50 meters [2], [13], [14]. Installation in deeper waters require larger, heavier tradtional monopiles, increasing costs and therefore larger vessels. Despite their technical and economic feasiblity up to water depth of 45-50 meter, the installation process can disrupt the seabed and affect marine ecosystems [15], [16]. Figure 1.4 schematically provides a clear overview of how to traditional monopile foundation looks.

Figure 1.4: Monopile foundation for offshore wind turbine [17]

1.2.3. Jacket structure

The jacket structure, a well-established offshore foundation method dating back to 1947 [18], currently constitutes approximately 10% of all offshore wind turbine foundations [19]. Technically feasible up to depths of around 300 meters, as validated by its extensive use in the oil and gas sector [20], jacket structures are particularly suitable for offshore wind projects starting from depths exceeding 40 meters [15], [21] .

Jacket structures can be installed across various soil types, including stiff clay, and can be installed using piles or suction caissons. They are known for their reliability and relatively labour-expensive manufacturing process, due to the significant welding involved, which contributes to higher production costs compared to other foundation types. Figure 1.5 schematically shows the jacket structure for an offshore wind turbine.

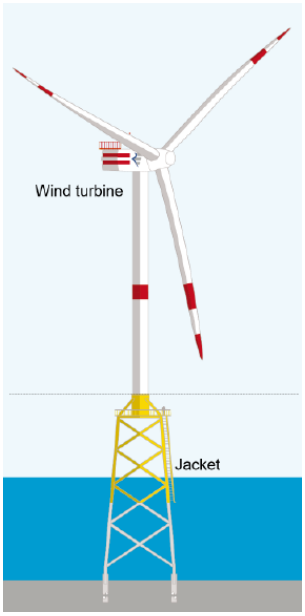

Figure 1.5: Jacket foundation for offshore wind turbine [22]

1.3. Research gap

the majority of the existing wind farms worldwide are installed in shallow and intermediate waters. About 80% of offshore wind turbines use monopiles as their foundation, followed by jacket structures, which account for nearly 10%, as shown in Figure 1.6 [19], [21].

Even though the offshore wind energy sector has grown significantly, current foundation options face challenges that limit their effectiveness in different water depths. Traditional monopiles are cost-effective in shallow waters but becomes challenging around 50 meters of water depth [23], requiring expensive alternatives like jacket structures [19]. The high costs of jackets highlight the need for new solutions that are both cost-efficient and technically feasible in deeper waters with more severe environmental conditions [15], [24].

The deployment of foundations in deeper water for offshore wind turbines correlates with an increase of expenditures. To compare, for an installation of a wind turbine, around 19-36% corresponds to the costs for the foundation specifically dependent of the water

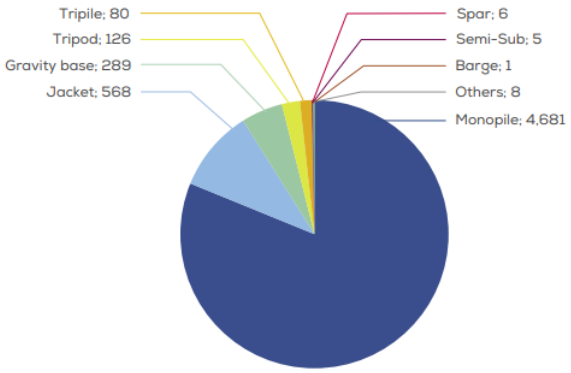

Figure 1.6: Share of foundation types for offshore wind turbines in 2020 [19]

depth. Figure 1.7 shows the ratio of costs for the foundation and its installation compared to other expenses in establishing an offshore wind turbine project. To make the offshore wind energy sector competitive to more traditional energy production industries, such as the oil and gas industry, new foundation concepts and installation solutions should be investigated (and developed) to lower the foundation and installation cost that are associated with deep water deployment of wind turbines

The development of the Hybrid Monopile (HMP) represents a promising advancement aimed at overcoming these limitations [7]. By combining aspects of monopiles and jackets, the HMP aims to extend installation depths, mitigate environmental impacts such as noise pollution, and reduce manufacturing and installation costs compared to traditional options [23], [25].

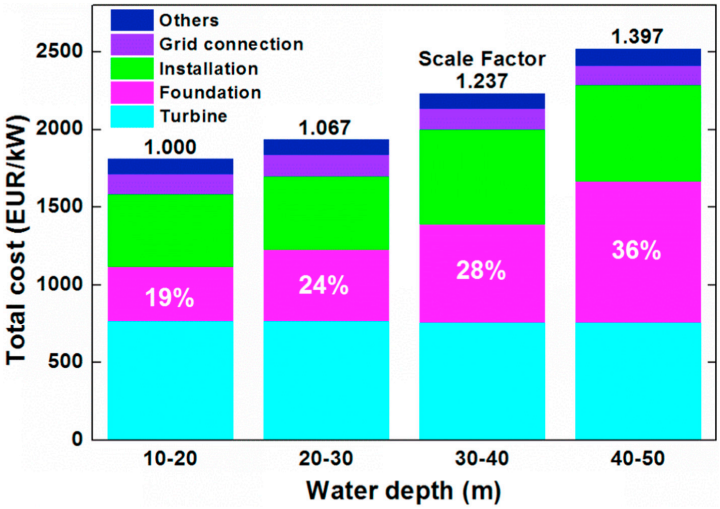

Figure 1.7: Comparison total costs per kW for offshore wind turbines [2]

Comprehensive evaluations comparing the technical and economic feasibility of hybrid monopiles against traditional monopiles and jacket structures in real-world conditions are limited. Existing studies often focus on retrieving forces [26], [27], soil-stiffness curves [28]–[34], limitations regarding noise [35], [36], and the manufacturing and installation of structures [37] comparable to hybrid monopiles, without providing a comprehensive assessment of structural design, installation efficiency, and overall cost-effectiveness compared to traditional foundation methods for offshore wind foundations.

This research aims close these gaps through a comparative analysis of the HMP alongside traditional foundation methods. By assessing structural integrity, installation feasibility, and costs, this study investigates the potential benefits of integrating HMPs into offshore wind projects. The findings provides answers about the viability and practicality of HMPs as a pioneering solution for the offshore wind energy industry.

1.4. Research question

The research question of this research is formulated as follows:

"Can the technical and economic aspects of bottom-fixed foundations be improved by implementing the Hybrid Monopile as a bottom-fixed foundation in comparison to jacket structures and traditional monopiles in the North Sea?"

Subquestions:

1. *Up to what water depths, soil conditions, and wind turbine sizes can the Hybrid Monopile be feasibly manufactured and installed?*
2. *Is it possible to reduce the installation cycle time of the Hybrid Monopile compared to traditional monopiles and jacket structures*
3. *Are there achievable cost savings in manufacturing and installation processes of the Hybrid Monopile compared to traditional monopiles and jacket structures?*

1.5. Research objectives and scope

This study focuses on to assess the technical and economic feasibility of the Hybrid Monopile compared to foundation methods commonly used by the industry such as the traditional monopile and jacket structures. The scope of this feasibility study is on structural design, installation assessment, and manufacturing and installation costs. The research aims to determine what conditions are required to make the HMP technically superior to - and more cost-effective than traditional foundation methods, allowing it to be used wide-spread for offshore wind turbine solutions in the North Sea.

For the design assessment, sea state conditions of the North Sea are taken as input parameters. This includes water depths, wave heights, and wave periods, which are critical to evaluate the structural performance of the Hybrid Monopile. The comparison of the Hybrid Monopile with traditional monopile and jacket structures based on data from projects that were conducted in the North Sea, providing an equal comparison for the evaluation. The design analysis will consider various factors such as the load-bearing capacity, the natural frequency and the stress magnitude in relation to the ultimate limit state of the Hybrid Monopile.

Installation considerations are a significant aspect of this research. The installation time for the Hybrid Monopile is primarily focused on the time a vessel needs to install a single foundation, irrespective of location, transport logistics, and yard accessibility. This approach isolates the installation process, allowing for a direct comparison of efficiency and practicality between the Hybrid Monopile and other foundation types. Factors such as installation speed, equipment requirements, and potential challenges during the installation process will be thoroughly examined.

The economic feasibility analysis will cover overall costs, including manufacturing and installation expenses. This research aims to provide a cost-effective analysis, highlighting the economic advantages or disadvantages of the Hybrid Monopile compared to traditional monopile and jacket structures.

1.6. Thesis outline

This research is structured into three main components to assess the overall feasibility of the Hybrid Monopile compared to traditional monopiles and jacket structures. Firstly, a comprehensive literature review is conducted to gather relevant research on structural analysis, installation assessment strategies and cost-engineering.

Secondly, the methodology outlines how these components (structural analysis, installation assessment, and economic evaluation) are executed. A framework is established to sequence these steps logically, indicating how results from each model influence one another.

The structural analysis of the Hybrid Monopile is the initial focus. It determines details for each step, including the approach and assumptions taken, to ensure reliable results that accurately reflect the designs of the Hybrid Monopile, the traditional monopile, and jacket structure.

Next, the installation assessment examines the feasibility of installing the Hybrid Monopile, considering it as a novel concept. Various installation possibilities are analyzed, and criteria are applied to determine the optimal method. This assessment is compared with installation cycles for traditional monopiles and jacket structures according to industry standard. This provides a detailed installation time per foundation.

Lastly, the economic evaluation is derived from the outputs of the structural analysis and installation assessment. Foundation costs are broken down into manufacturing costs, largely derived from the

structural model, and installation costs, based on the installation assessment.

The research concludes with results from each assessment, addressing by sub-questions given in this study, resulting in a final conclusion that summarizes findings and provides insights into the overall feasibility of the Hybrid Monopile compared to the two alternatives.

2

Literature review

This chapter provides an overview of the theoretical background necessary for understanding the environmental loads impacting the design of the Hybrid Monopile. It begins by the hydrodynamic loading and thrust forces acting on the structure, which are critical in determining the overall performance and stability under varying environmental conditions, considering factors such as the dynamic amplification. The chapter accordingly explores the soil-structure interaction, focusing on how the foundation of the Hybrid Monopile engages with the surrounding soil at the installation site, considering factors such as pile-group effects. Additionally, the chapter delves into the limitations associated with the manufacturing and installation processes, including constraints related to noise pollution and other site-specific challenges that influence the design and deployment of offshore structures.

2.1. Hydrodynamic loading

This section provides an overview of the different wave regimes, emphasizing the validity of the Morison equation within specific regimes. Additionally, it explains the application of the Morison equation and the parameters required to define the forces acting on structures in offshore environments. Furthermore, it determines the drag and inertia coefficients for utilizing the Morison equation effectively. Finally, the linear wave theory is outlined including the Wheeler Stretching method.

2.1.1. Morison equation

The Morison equation is a quasi-static equation used for a fixed body in an oscillatory flow, primarily used to obtain the forces acting on offshore structures. To assess the applicability of the Morison equation for calculating hydrodynamic loading on structures, it is necessary to examine the ratio of diameter to wavelength (x-axis) against the ratio of wave height to diameter (y-axis) within the wave force regime spectrum, as depicted in Figure 2.1. This spectrum shows different hydrodynamic regimes, with the Morison equation being suitable for regions III, IV, and V.

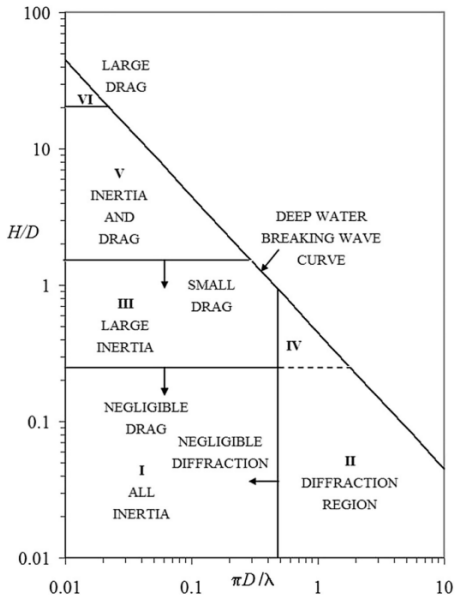

Figure 2.1: Wave forces regimes [38]

Equation 2.1 represents the Morison equation, consisting of a sum of drag and inertia forces. The formula is well-known within the offshore industry, the entire derivation of the Morison theory can be found in Book for the hydrodynamic for offshore structures [26].

$$F_{Morison} = \frac{1}{2}\,\rho_w\,C_d\,D\,u\,|u| + \frac{1}{4}\,\pi\,D^2\,C_m\,\rho_w\,\dot{u} \tag{2.1}$$

Where ρ_w is the density of water, C_d is the drag coefficient, D is the diameter, u is the wave velocity, C_m is the inertia coefficient and $\dot{u}$ is the wave acceleration.

2.1.2. Drag and inertia coefficient

Sarpkaya [27] experimentally investigated the variation of drag and inertia coefficients with smooth cylinders in U-tubes. Figure 2.2 and Figure 2.3 depict the graphs of Sarpkaya's experimental results, where C_d and C_m are functions of dimensionless numbers KC and β. The Sarpkaya Beta (β) depends on the ratio between the Reynolds Number (R_e) and the Keulegan-Carpenter number (KC). The drag and inertia coefficients can be determined based on the KC number, Re, and β. The KC number can be calculated according to Equation 2.2, the Re number is calculated according to Equation 2.3, and the Sarpkaya Beta according to Equation 2.4.

$$KC = \frac{U_{\max} T}{D} \tag{2.2}$$

$$R_e = \frac{U_{\max} D}{\upsilon} \tag{2.3}$$

$$\beta = \frac{D^2}{\upsilon T} \tag{2.4}$$

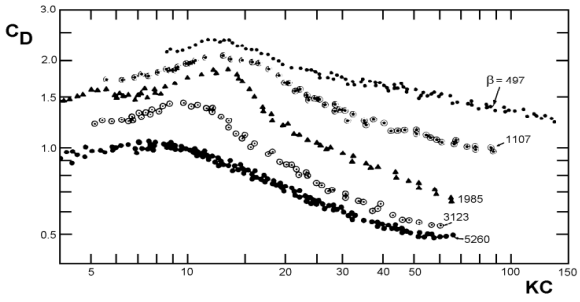

Figure 2.2: C_d as a function of KC according to DNV standards

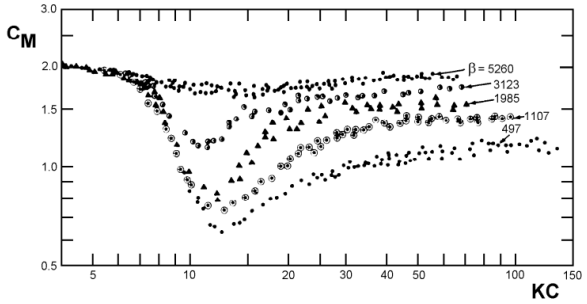

Figure 2.3: C_m as a function of KC according to DNV standards

Figure 2.4: Comparison of C_d and C_m as functions of KC according to DNV standards

As can be seen from the figures, at very low KC numbers, until KC = 10, the inertia coefficient is constant around 2.0 regardless of the Sarpkaya Beta parameter. Nevertheless, for the drag coefficient the influence of the Sarpkaya Beta parameter affects number significant more, even for low KC numbers.

2.1.3. Linear wave theory

To extract the velocity and acceleration from the waves, the linear wave theory is used, also known as the Airy wave theory. The Linear wave theory offers a simplified yet effective framework for understanding the dynamics of waves on fluid surfaces. This theory provides a mathematical description of wave propagation where the wave amplitude is relatively small compared to the wave period and water depth. It is assumed that the wave have a sinusoidal shape and that their interactions are linear. Figure 2.5 represents an overview of the linear/Airy wave theory.

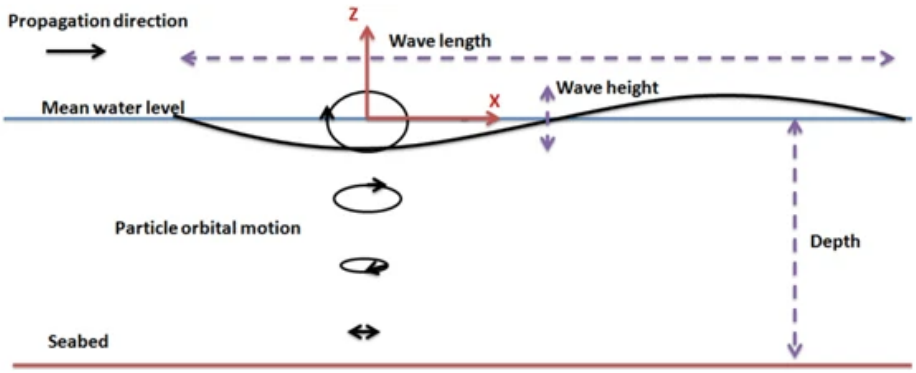

Figure 2.5: Overview of the linear wave theory [39]

Equation 2.5 and Equation 2.6 represents the equation to determine the velocity and acceleration respectively from the propagated waves.

$$u = \omega a \frac{\cosh k(z+h)}{\sinh(kh)} \sin(\omega t - kx) \tag{2.5}$$

$$\dot{u} = \omega^2 a \frac{\cosh k(z+h)}{\sinh(kh)} \cos(\omega t - kx) \tag{2.6}$$

The associated velocity potential and dispersion relation are formulated respectively according to Equation 2.7 and Equation 2.8.

$$\phi = \frac{\omega a}{k} \frac{\cosh[k(z+h)]}{\sinh(kh)} \cos(\omega t - kx) \tag{2.7}$$

$$\omega^2 = gk \tanh(kh) \tag{2.8}$$

In the four equations related to the linear wave theory, u is the wave velocity, $\dot{u}$ is the wave acceleration, k is the wave number, z is the observation depth, h is the water depth, ω is the angular frequency, a is the wave crest, t is the observation time, x is the observation space, ϕ is the velocity potential and g is the standard acceleration of gravity.

The linear wave theory regularly models wave motion only up to the mean sea level, providing a useful but incomplete picture of the forces exerted by waves on structures. To address this limitation, Wheeler Stretching can be used. Wheeler Stretching is a method used to enhance the accuracy of wave impact predictions on structures that extend above the mean sea level. It effectively adapts the linear wave theory to account for the vertical motion of waves as they interact with structures extending beyond the mean sea level. This method adapts the calculated wave elevations by stretching or the wave profile according to the water depth variations induced by the waves themselves.

The technique involves extrapolating the wave spectrum to include the heights of the waves above the mean sea level, thereby ensuring that the forces exerted by these waves on structures are more accurately represented. Figure 2.6 represent the a overview of how the Wheeler Stretching theory applies for the ocean waves.

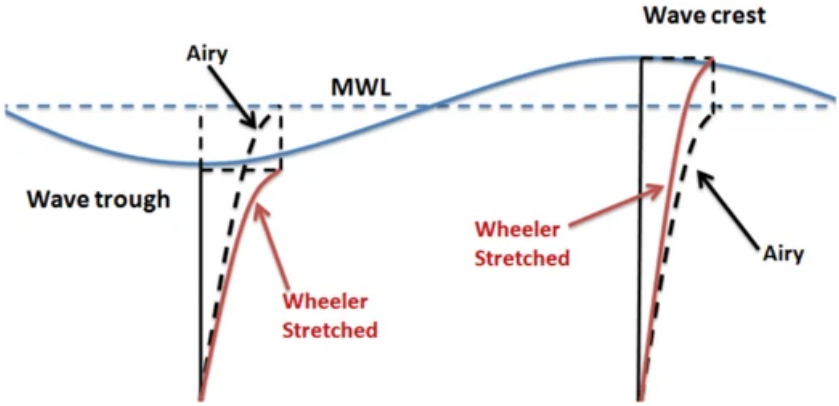

Figure 2.6: Wheeler Stretching Theory [39]

Equation 2.9 represents the equation applicable to extrapolate the mean sea level to the top side of the wave crest.

$$z' = d\frac{d+z}{d+\zeta} - d \tag{2.9}$$

Where z' is the new z-coordinate in the Wheeler stretching model, d is the water depth, z is the coordinate of the observation depth of the original coordinate system, ζ is the z-coordinate corresponding to the instantaneous water surface.

2.2. Thrust force on wind turbine

The wind loading consists two main components: the distributed wind loading on the wind turbine tower above sea level and the thrust force on the rotor blades. The contribution of the distributed wind load

on the tower is considered negligible. However, the thrust force is deemed significant. It acts as a lumped load exerting on the center of the nacelle.

To determine the thrust on various types of wind turbines, certain assumptions are made: the flow is a perfect fluid, steady, and incompressible, and the flow is uniform through the rotor blades. Figure 2.7 illustrates how the wind exerts the thrust force on the wind turbine.

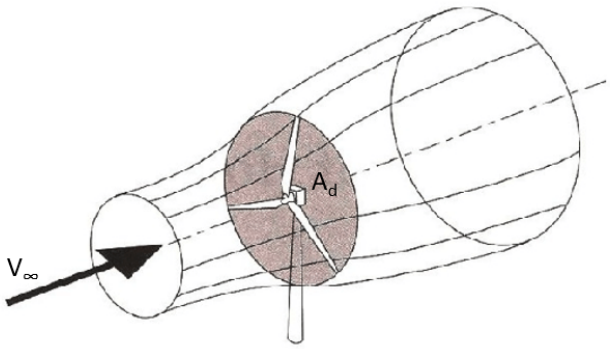

Figure 2.7: Thrust force, adapted from [40]

The thrust force on the wind turbine can be calculated with Equation 2.10 [41].

$$F_T = \frac{1}{2}\,\rho_a\,C_T\,A_d\,V_\infty^2 \tag{2.10}$$

Where T is the thrust force, ρ_a is the density of air, C_T is the thrust coefficient, A_d is the surface of the rotor blades and V_∞ is the free stream velocity. The thrust coefficient is a correction factor based on the how much the wind velocity has been affected by the surface of the rotor blades.

The formula for the thrust coefficient is represented in Equation 2.11, where C_T is the thrust coefficient and a is the axial induction factor

$$C_T = 4\,\alpha(1-\alpha) \tag{2.11}$$

The axial induction factor indicates how much the wind velocity is affected by the surface of the rotor blades. When a = 0.5, the thrust coefficient and so the thrust force is maximum. In the determination of the design loads, the maximum thrust force is considered.

2.3. Soil-structure interaction

This subsection provides an overview of soil-structure interaction, which constitutes the final stage of defining the structural model for monopile design. Here, the background of calculating the stiffness of the springs that represent soil resistance are outlined.

2.3.1. Beam on Nonlinear Winker Foundation

To simulate the stiffness of the soil acting on the foundation piles, a soil-spring stiffness model is created to simulate the stiffness of the soil at various depths. The model consists of three different types of springs: lateral springs along the pile to determine the horizontal soil resistance, axial springs along the pile to determine the shaft friction of the pin piles, and one axial spring at the tip of the pin piles representing the tip bearing resistance of the pin piles. Figure 2.8 represents the model, which is better known as the Beams on Nonlinear Winkler Foundation [30].

In the Winkler method, the soil is depicted by a series of nonlinear springs. The number of lateral and axial springs varies along the pin pile shaft, as does the spacing between them. The nonlinear response of the soil resistance acting on the pin piles is simulated with p-y curves (lateral), t-z curves

(axial), and q-z curves (end-bearing). These curves represent the soil resistance over the deflection of the pile in a certain direction, and are numerical models based on empirical tests.

The curves are numerical models based on empirical test and the curve is unique for every spring type and depths the spring appears. In this research different p-y, t-z and q-z models are used based the type of soil. The curves are used to model the variation in stiffness along the depth of piles. These curves change based on soil properties such as unit weight, friction angle, cohesion, and layer depth.

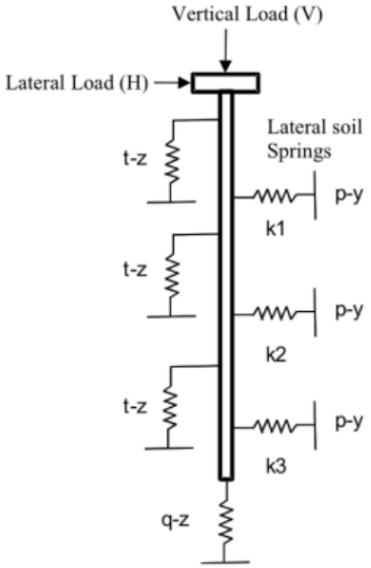

Figure 2.8: Soil-spring stiffness model [30]

2.3.2. P-y curves for sand

Terzaghi [42] conducted research in 1955 on the initial stiffness of stress-strain curves for sand as a function of confining pressure and shearing strain magnitude. These values, known as subgrade moduli, provided a basis for computational lateral pile responses. The first field experiences with the lateral loading of piles date back to 1974 and were conducted by Reese et al. [31], involving an embedded length of 21 meters and a diameter of 0.6 meters. Reese et al. established the first procedure for determining p-y curves in 1974 [31], which can be used for both static and cyclic loading. This method was widely adopted by the American Petroleum industry until research by Murchison and O'Neill in 1983 [43] suggested using a hyperbolic formula to substitute the formulation of Reese et al. This updated method and formula are still widely used in the industry.

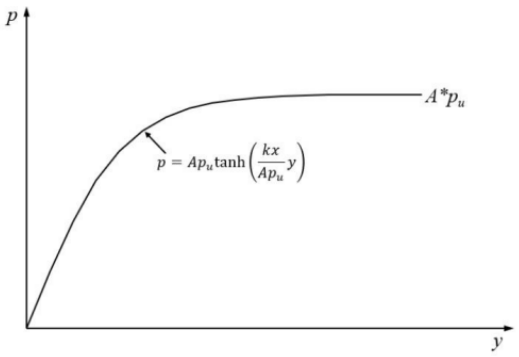

Figure 2.9: The API p-y curve for sand [44]

More recent research by Norris in 1986 [33] introduced a new model to predict soil stiffness for larger piles. However, this model overpredicts the soil stiffness of sand for large monopile diameters, resulting in insufficient penetration depth when designing structures. Therefore, the model is not recommended for use. As of now, a new method for determining p-y curves for sand has not been established. The method created by Reese et al. in 1974 and adapted by Murchison and O'Neill in 1983 is still used and is currently known as the API-sand method. It is recommended by ISO and DNV standards [34]. Figure 2.9 shows the API p-y curve for sand. The entire derivation of the p-y curve is outlined in the LPILE 2016 Technical Manual [44].

The resistance factor for sand is taken as the lesser value of the calculated p_{us} and p_{ud} for shallow and larger depths, respectively. Here, k is the initial modulus of subgrade reaction, x is the depth below the seabed, y is the lateral deflection of the pin pile, and b is the diameter of the pin piles.

2.3.3. P-y curves for clay

P-y curves for clay soils are derived from empirical tests conducted by Reese, Cox, and Welch [29]. Their research focused on stiff clay under conditions with free water. Research by Welch and Reese [32] explored clay behavior without free water, which is not applicable to offshore clay environments [45]. Matlock [46] also studied similar conditions in 1970, but emphasized soft clay. It's important to note that both studies used relatively small pin piles up to 0.61 meters in diameter, whereas modern pin piles are significantly larger.

Haiderali et al. [45] investigated the accuracy of these models under similar environmental conditions but with larger monopiles of 5 meters and 7.5 meters in diameter. Their findings indicated that Matlock's p-y curves underestimate soil resistance for larger diameters, potentially leading to overdesigned structures.

Industry standards still rely on pile theories based on Matlock and Reese, Cox, and Koop. To establish p-y curves for stiff clay with free water, following Reese and Welch's methodology, the process begins with determining key soil parameters such as undrained shear strength (c), effective unit weight (γ'), and pile diameter (b). The parameter ϵ_{50} is then derived from stress-strain curves extrapolated from Reese, Cox and Welch's empirical tests.

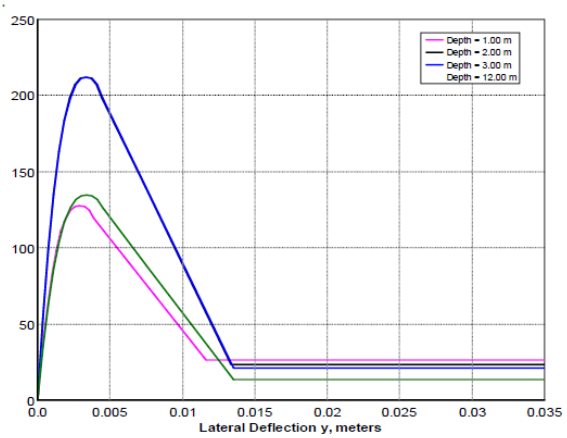

Figure 2.10: Example of a p-y curve in stiff clay with free water, adapted from [44]

In clay, undrained shear strength (S_u) and cohesion (c) are closely related. Cohesion allows clay particles to adhere, significantly contributing to shear strength. Moreover, clay's low permeability restricts water flow, particularly under rapid loading, resulting in undrained behavior where drainage is negligible. Under these conditions, cohesive properties primarily govern clay's shear strength, overlapping with undrained shear strength.

After establishing soil properties and calculating ϵ_{50}, soil resistance (P_u) is determined. Figure 2.10 illustrates an example of the p-y curve at various depths. The comprehensive derivation of p-y curves in stiff clay can be found in the LPILE 2016 technical manual [44].

2.3.4. T-z and q-z curves

The establishment of the first t-z and q-z curves dates back to 1966 following empirical research conducted by Coyle and Reese on axial loading of piles in clay, as documented in Coyle's 1966 study [47]. Subsequently, in 1967, Coyle and Sulaiman conducted similar empirical tests on piles in sand, leading to the first development of t-z curves [48]. Building upon this foundational work, Vijayvergiya in 1977 [49] and API in 1993 [50] provided general recommendations for estimating t-z and q-z curves.

Beyond empirical research, several researchers explored theoretical models related to the shear stiffness of soil surrounding piles. Kraft et al. in 1981 [51], Chow in 1986 [52], and Randolph in 1994 [53] contributed significantly to developing these theoretical approaches.

In 2006, Pando et al. [54] conducted a comparative study evaluating different models, concluding that the error margins of various approaches were comparable. Consequently, newer models did not demonstrate superior accuracy compared to the empirical models developed by Coyle and adapted by API.

Currently, the API method, based on Coyle's empirical models from 1967, remains widely used in the industry for cohesive and cohesionless soils due to its established accuracy. This method is particularly noted for its t-z and q-z curves, as depicted in Figure 2.11 and Figure 2.12, which illustrate the nonlinear behavior of soil resistance under axial loading. Both clay and sand exhibit a similar nonlinear pattern with respect to maximum vertical soil resistance. Following this peak, clay shows a decrease in soil resistance, whereas sand maintains its maximum resistance level. These curves are derived from empirical tests conducted by the American Petroleum Institute and are scaled based on the pile diameter requirements.

For sand, the relative density is critical in determining shaft friction and tip bearing capacity, while for clay, undrained shear strength is the primary factor influencing soil stiffness at different depths.

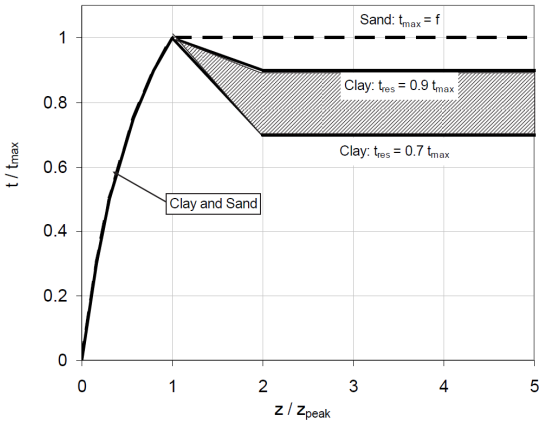

Figure 2.11: T-z curve for sand and clay according to API RP 2GEO [50]

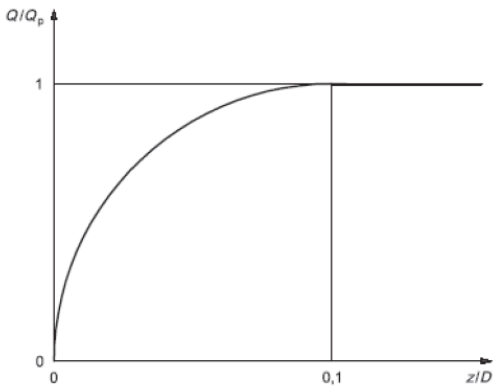

Figure 2.12: Q-z curve for sand and clay according to API RP 2GEO [50]

2.4. Dynamic amplification factor

The dynamic amplification factor for a single-degree of freedom (SDOF) mass-spring-damping system is used to determine the excitation of a system when the frequency of a load approximates with the natural frequency of the structure itself. Figure 2.13 shows the mass-spring-damping system with one degree of freedom. below a short summary is given of how the derivation of the formula of the dynamic amplification factor is established.

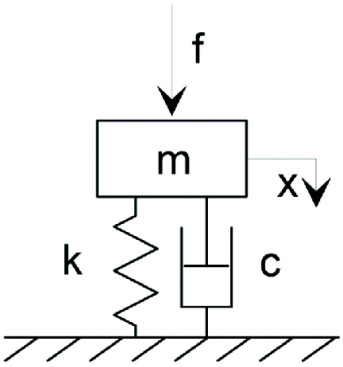

Figure 2.13: Mass-spring-damping SDOF system [55]

Equation 2.12 represents the equation of motion (EOM) of the mass-spring-damping system. The equation of motion consist of a second order differential equation.

$$m\ddot{x} + c\dot{x} + kx = F_{ext} \tag{2.12}$$

The response x(t) consists of two different solution; the homogeneous solution (where no external force is there) and the particular solution (the steady state solution). The primary interest is the forced response due to dynamic loading. Therefore the focus is on the particular solution which addresses the system's response to these loads. The influence of the homogeneous solution will be neglected in this case.

The assumed solution is represents Equation 2.13

$$x = \hat{X}cos(\omega_n t - \phi) \tag{2.13}$$

Where

$$\dot{x} = -\hat{X}\,\omega_n\, sin(\omega_n t - \phi)$$
$$\ddot{x} = -\hat{X}\,\omega_n^2\, cos(\omega_n t - \phi)$$

Substituting these solution in Equation 2.12 and solving the obtained equation gives the results that is represented in Equation 2.14

$$\hat{X} = \frac{F_{ext}}{(\sqrt{k - m\omega_n^2)^2 + (c\omega_n^2)}} \tag{2.14}$$

Substituting Equation 2.14 in Equation 2.13 and rewrite the equation a bit Equation 2.15 is obtained.

$$x(t) = \underbrace{\frac{\delta_{\mathrm{ST}}}{\sqrt{\left[1 - \left(\frac{\omega_w}{\omega_n}\right)^2\right]^2 + \left[2\zeta\frac{\omega_w}{\omega_n}\right]^2}}}_{\text{Amplitude } \hat{X}} \cos(\omega t - \phi) \tag{2.15}$$

$$\frac{F_0}{k} = \delta_{\mathrm{ST}}, \qquad \frac{m}{k} = \frac{1}{\omega_n^2}, \qquad \frac{c\omega_w}{k} = 2\zeta\frac{\omega_w}{\omega_n}$$

Now it can be seen that the amplitude of the response is given by Equation 2.16, which simultaneously is the solution of the derivation of the mass-spring-damping system.

$$\frac{\hat{X}}{\delta_{\mathrm{ST}}} = \frac{1}{\sqrt{\left[1 - \left(\frac{\omega_w}{\omega_n}\right)^2\right]^2 + \left[2\zeta\frac{\omega_w}{\omega_n}\right]^2}} \tag{2.16}$$

where:

$\frac{\hat{X}}{\delta_{\mathrm{ST}}} = \mathrm{DAF}$

ω_W = frequency of the wave spectrum

ω_n = natural frequency of the structure

2.5. Pile group factor

The pile group effect is a crucial consideration in the design and analysis of pile foundations, particularly when piles are installed in close proximity to each other. This effect arises due to the interactions between individual piles within the group, leading to significant differences compared to the behavior of a single, isolated pile.

Soil-structure interaction plays a vital role, as the presence of piles alters the stress distribution in the surrounding soil. This change impacts how load is transferred from the piles to the soil, often reducing the effective load-bearing capacity of each pile due to overlapping stress zones. The shadowing effect further intensifies this by causing piles to shield each other from the soil, thereby reducing the effective contact area. This leads to a reduction in the overall load-bearing capacity of the group.

One of the most significant impacts of the pile group effect is on settlement behavior. The settlement of a pile group can be substantially greater than that of a single pile due to the combined compression zones of the piles. If these interaction effects are neglected, the resulting design may underestimate the settlement, leading to significant settlement that affects the structure's serviceability.

Neglecting the pile group effect in foundation design can have several consequences. It can lead to an overestimation of the group's load-bearing capacity, resulting in foundations that may not support the applied loads, causing a risk of structural failure or significant settlement. .

O'Neill conducted research in 1983 [28] on the effects of pile group efficiencies in different types of soils with varying numbers of piles in the group. The study used pile diameters of 0.6 meters and 1 meter, and lengths of 30 meters. The results of this research are depicted in Figure 2.14 and Figure 2.15.

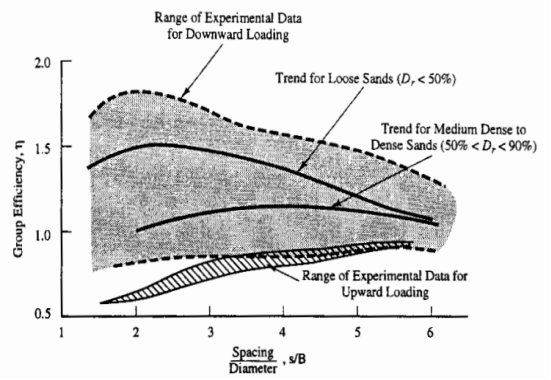

Figure 2.14: Group efficiencies from tests of model pile groups in cohesionless soils subjected to axial loading [28]

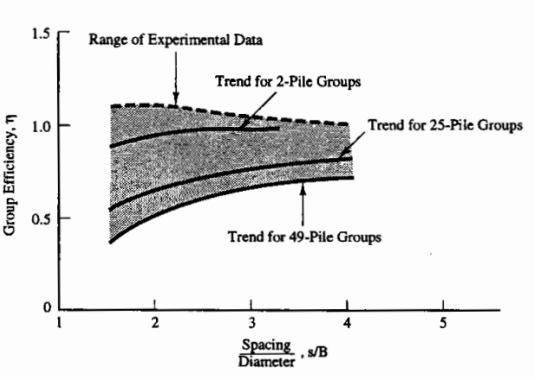

Figure 2.15: Group efficiencies from tests of model pile groups in cohesive soils subjected to axial loading [28]

The high group efficiency for cohesionless soils is primarily due to the radial consolidation that occurs during driving, resulting in an increase in lateral stress and, consequently, an increase in shaft friction per pile. However, group efficiency is lower in cases where the soil's relative density is high. Additionally, group efficiency for upwards loading is significantly lower compared to cases where downward force is applied. Lastly, the greater the spacing between the piles, the more the resulting group efficiency converges to 1, indicating minimal influence of the group effect on bearing capacity .

Zhang et al. researched in 2022 [56] the pile group factor for offshore pin piles in clay, considering different numbers of piles, configurations, and loading angles. They concluded that the loading angle has a higher influence compared to the number of piles or spacing. The situation that most closely mimics the Hybrid Monopile is depicted in Figure 2.16 and Figure 2.17. The influence of the pile group factor reduces with increased spacing between the pin piles.

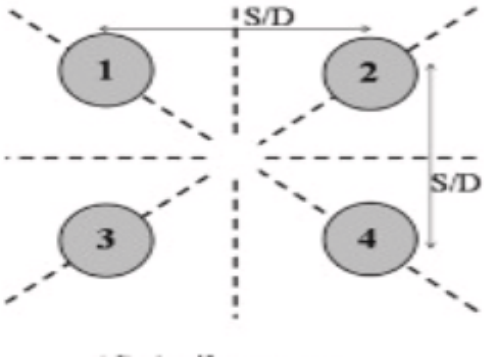

Figure 2.16: Pile configuration for offshore piles subjected to lateral loading [56]

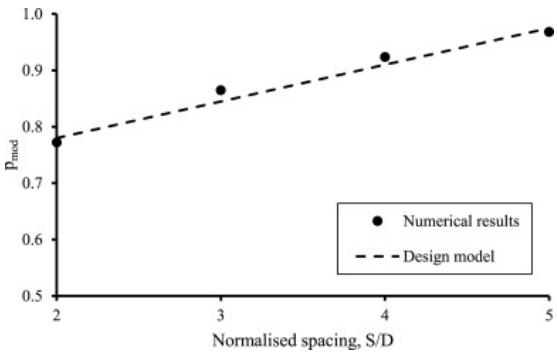

Figure 2.17: Group efficiencies from tests of model pile groups in cohesive soils subjected to lateral loading [56]

2.6. Limitation factors

In this research various limitation factors are identified over a broad range. A monopile with a diameter of 20+ meter can be designed and structurally be approved. However, the technical readiness level of the industry should be taken into account. The installation of the offshore foundation should be possible when comparing the foundation methods with each other. When the offshore wind foundation is simply not able to install due to weight, size or installation regulations, it is taken into account. This section dives deeper into the limitations factors of the installation of offshore wind foundations.

2.6.1. Noise and vibration pollution

In the last couple of years more and more factors are considered during the installation of monopiles or pin piles for other offshore foundation structures. Hammering of these piles causes a lot of noise

pollution which affects the quality of marine life.

Multiple countries across the world introduced regulations for the noise pollution during offshore constructions works. Figure 2.18 represents the a overview of the regulations established by six different countries. Germany, The Netherlands and Taiwan introduced the most restricted measurements to protect the quality of marine life. The USA even restricted any activities where noise pollution is created during certain seasons where protected mammals are migrating.

Country	Piling sound limit
Germany	Max. unweighted $SEL_{ss,5\%}$ ($L_{E,5\%}$) at 750 m = 160 dB re 1 µPa²s Max. $L_{p,pk}$ at 750 m = 190 dB re 1 µPa
Denmark	Max. unweighted SEL_{cum} for fleeing animals = 190 dB re 1 µPa²s
Belgium	Max. $L_{p,pk}$ at 750 m = 185 dB re 1 µPa
Netherlands	Max. unweighted SEL_{ss} ($L_{E,max}$) at 750 m = 159-172 dB re 1 µPa²s, depending on season and number of piles. After 2023: Max. unweighted SEL_{ss} ($L_{E,max}$) at 750 m = 168 dB re 1 µPa²s
Taiwan	Max. unweighted SEL_{ss} ($L_{E,max}$) at 750 m = 160 dB re 1 µPa²s
USA	Max. frequency weighted SEL_{cum} exposure per species group (NMFS, 2018)

Figure 2.18: SEL regulations established by various countries [57]

Researchers from the University of Hamburg [36] conducted research to identify the influence of different parameters like pile diameter, ram weight, strike energy and water depth. Various models are created to mimic the sound exposure level (SEL) during the installation of piles, by performing a sensitivity study, they investigated the extend of how the SEL is affected by these parameters. It appears that with exception of ram weight, the SEL increases by increase the pile diameter, water depth and strike energy. Besides, they investigated the SEL at twenty one different offshore wind projects, it appears that without and noise mitigation strategy none of these projects were allowed to be executed in these countries.

Moreover, this research showed that projects where pile are installed of 8 meter, at a water depth of 39 meter, the SEL reached 182 dB at 750 meter of the installation site. In the future, assuming the deployment of monopiles at larger water depths which goes align with increasing diameters are installed, the SEL is going to exceed the established limits.

Multiple noise mitigation measurements are introduced to reduce the SEL offshore. Research conducted by the The Federal Maritime and Hydrographic Agency [35] shows that a Big Bubble Curtain BBC is the most effective measurement to mitigate noise vibrations. According to the utilized models, the sound exposure level can be reduced by approximately 15 to 17 dB in water depth of around 25 to 40 meters. The influence of the characteristics (e.g. size of the bubbles, pressure inside the bubble curtain) of the BBC are insufficiently known on the SEL. For the employment of piles into deeper water no accurate answer can be provided.

Besides hammering the piles, a vibrohammer can be used. In past projects it is proven that the vibrohammer can install monopiles of over 30 meter in diameter [58]. Vibrating the piles into the subsurface reduces noise significantly. Nevertheless, vibrohammers are on average more expensive to use and the soil conditions can be a limitations factor for the utilization of the vibrohammer. The vibrohammer cannot provide enough energy to drive piles into the subsurface, specifically in stiff soils the vibrohammer is not able to provide sufficient energy.

Based on the information obtained from research mentioned above on the noise pollution, certain limitation factors are identified. For this research the installation of piles larger than 9 meter in diameter and deployment in water depth larger than 40 meter is considered unfeasible assuming the use of BBC only. This can be extended to around 50 meters by using specific project measurements for noise mitigation, as implemented by HMC in the He Dreight project [59]

2.6.2. Lift capacity

The lift capacity and maximum hook height of the installation vessels are important to keep in mind. The installation of wind turbines becomes difficult when the installation height of the nacelle extends the hook height or the structure becomes to heavy to install. To assign a limitation to this, the largest SSCV is considered to be a absolute limit to this.

The Sleipnir is the largest installation vessel in the world and has a crane capacity of 2 x 10.000 metric tons, and has hook height above deck of 135 meter. Note for the SSCV more vessels are available from different companies, however the Sleipnir is considered to be the absolute limit regarding offshore installation vessels, as soon as the working range or crane capacity is exceeded, the offshore substructure is considered to be unfeasible to install in this research.

2.6.3. Manufacturing

The Titan Group has recently announced plans to construct a new production factory for XXXL monopiles in northern Germany. This factory is expected to produce monopiles with a diameter of 14 meters, a length of 140 meters, and a total weight of 3500 mt [37]. This facility is set to become the largest monopile factory currently in operation.

3

Research Methodology

In this chapter, the research methodology is explained to formulate an accurate answer to the main research question. Initially, a framework is created to represent the overall approach of this research. Subsequently, the structural model, installation model, and cost model are outlined within this framework. These frameworks identify the steps conducted to achieve specific outcomes, which are essential for answering the subquestions and, ultimately, the main research question.

3.1. Overall feasibility framework

Several models are developed to explore the technical and economic feasibility of the Hybrid Monopile compared to traditional monopiles and jacket structures. The research divides these aspects into three main categories: the design of each foundation type, their installation processes, and a cost evaluation based on both design and installation factors. A clear framework is necessary since the output of certain models is taken as an input for the following model. Figure 3.1 illustrates the framework of how technical and economic feasibility are evaluated through structural design, installation assessments, and economic evaluations.

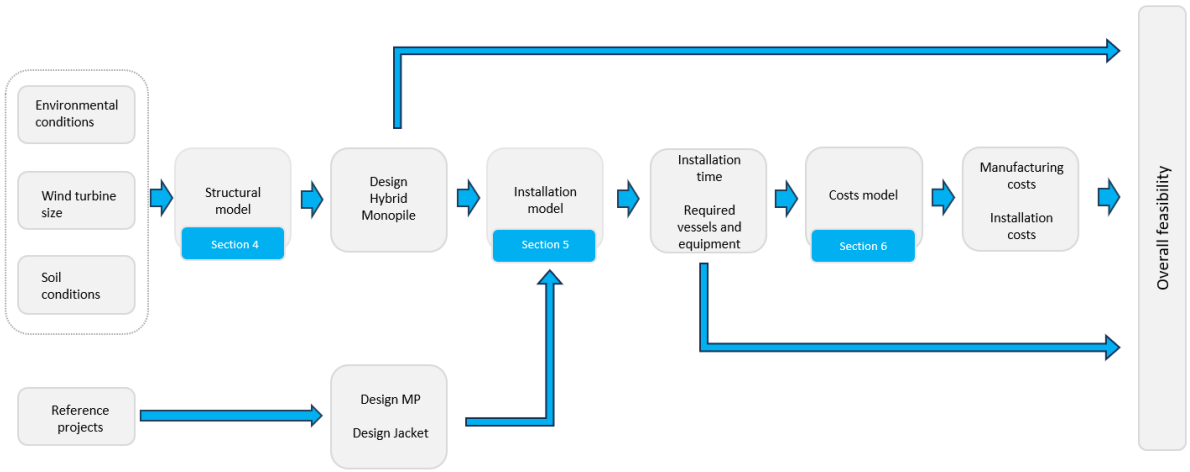

Figure 3.1: Overview of overall feasiblity of the Hybrid Monopile compared to traditional monopile and jacket structure

3.2. Software

This report includes the provided software, code, and notebooks developed during the project.

3.2.1. Abaqus

Abaqus is a software suite for finite element analysis FEA and computer-aided engineering (CEA). Developed by Dassault Systèmes, it is widely used for simulating the behavior of products and materials under various physical conditions. Abaqus offers a comprehensive range of tools for analyzing linear and nonlinear problems, structural mechanics and fluid dynamics.

3.3. Framework models

In this section the framework of the structural model, installation model and costs model are outlined.

3.3.1. Structural model

The first model created in this research is the structural model used to obtain the design of the Hybrid Monopile. Figure 3.2 provides the framework of how the design process for the Hybrid Monopile is set up.

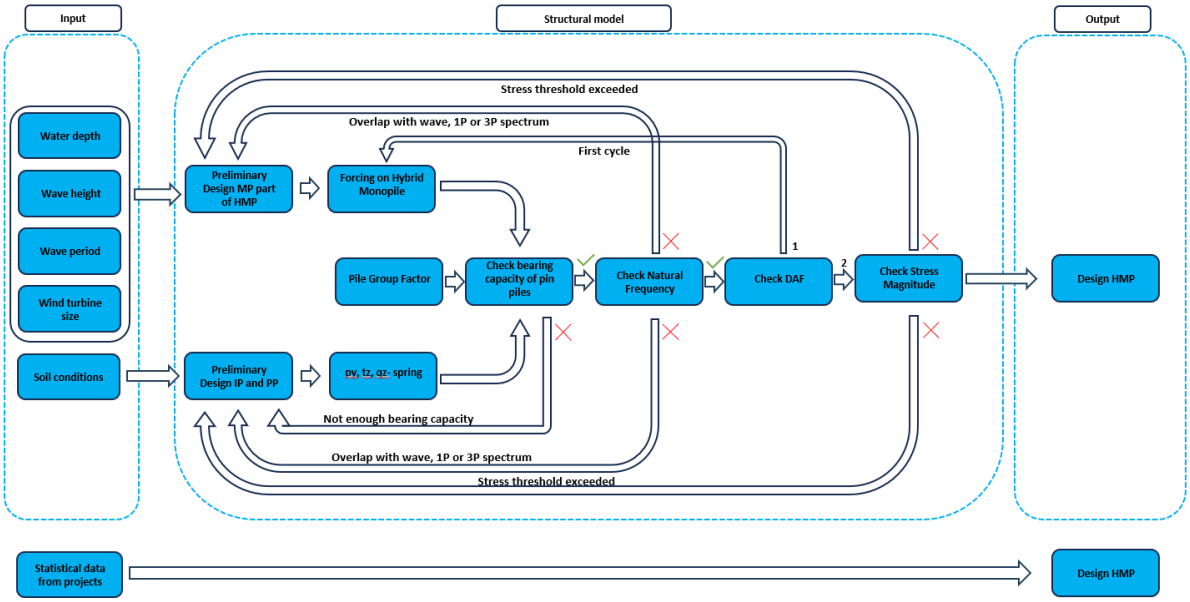

Figure 3.2: Structural model

The initial model developed in this research focuses on the structural design of the Hybrid Monopile, as depicted in Figure 3.2. This model begins with inputs such as environmental conditions, soil characteristics, and specifications of the wind turbines. Using these inputs, the model initially determines the diameter of the monopile of the Hybrid Monopile based on statistical data from previous monopile projects. The design of the interface piece and pin piles follows through iterative adjustments.

Once the preliminary design is established, the model calculates the forces acting on the structure, which are specified by the user depending on factors like monopile diameter, turbine specifications, and environmental conditions. Similarly, the soil-structure interaction of the pin piles is defined based on input soil conditions, determining the dimensions and stiffness of the soil springs applied to the structure.

The model conducts several critical checks during the design process. First, it verifies the bearing capacity of the structure and pin piles against the applied forces. If forces exceed the capacity, adjustments are made to the pin pile dimensions and corresponding soil stiffness. Second, the model assesses the natural frequency of the structure to ensure it does not overlap with critical 1P, 3P and wave frequencies, requiring iterative design adaptions in case these the model of the Hybrid Monopile does pass these checks.

Next, the Dynamic Amplification Factor (DAF) is computed to account for dynamic forces due to wave

action. The DAF depends on the natural frequency of the structure relative to wave frequencies, with adjustments made if necessary to maintain structural integrity under dynamic loading conditions.

Finally, stress levels within the structure are evaluated against Ultimate Limit State (ULS) thresholds. If stresses exceed allowable limits, design adjustments are made to ensure structural reliability.

This iterative design process aims to design the Hybrid Monopile's structural configuration. The output of the model, the design of the Hybrid Monopile, is used as an input for the installation model and costs model.

Lastly, Figure 3.2 shows outside of the model the design of the traditional monopile and jacket structure. The design (dimensions and weights) of these structures are based on reference projects where wind turbines are installed on these type of foundations in the North Sea.

3.3.2. Installation model

The second model that is developed is the installation model. This model determines the installation strategy for the Hybrid Monopile, traditional monopile and jacket structure. Figure 3.3 represents the framework for the installation model.

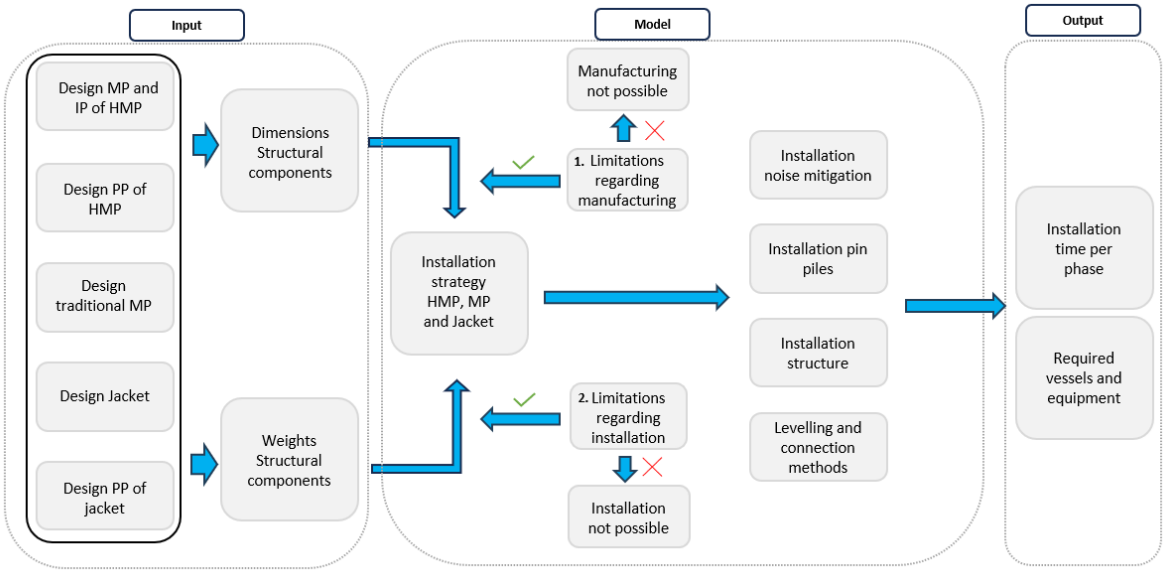

Figure 3.3: Installation model

The installation model takes as input values the design of the three different installation methods considered in this research. For the Hybrid Monopile and jacket structure it subdivides the part of the main structure above water level and the pin piles. Based on these designs the weights and dimensions of the various structures are determined.

Before determining the installation strategy, the model decides whether the manufacturing and installation is possible. In case the diameter of the monopile are becoming too big, the manufacturing monopile is currently not possible. Similar for the installation, in case the structures are becoming too big, that hammering is not possible due to underwater noise pollution or crane capacity limitations, it is not possible to install a specific structure in specific water depths.

The model subdivides the installation of the structures in various phases. The first one is the installation of noise mitigation, the second phase is the installation of the pin piles (this one does not apply for the installation of the traditional monopile), the installation of the structure, and the last one is the levelling and connection methods.

The output of the model is the installation time per phase, since various vessels could be used for different phases. Besides, the model also provides the type of vessel and equipment required for the

installation for a certain type of structure.

3.3.3. Costs model

The third model developed in this research is the costs model, depicted in Figure 3.4, which evaluates the economic feasibility of the Hybrid Monopile compared to the traditional monopile and jacket structure. This model takes inputs derived from the outputs of the structural and installation models, including dimensions, weights, required vessels and equipment, and installation times for each foundation type.

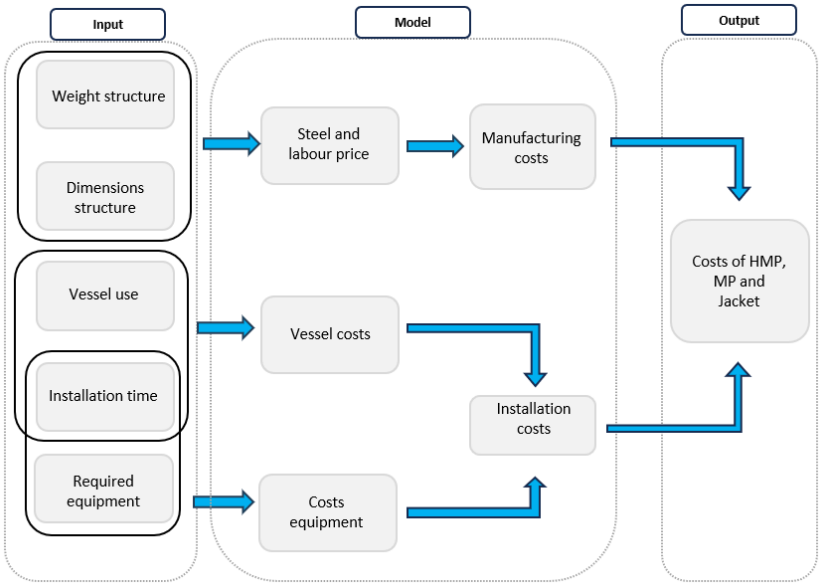

Figure 3.4: Costs model

The cost model calculates the manufacturing costs based on the dimensions and weight of each structure type, with costs per kilogram of steel accounting for labor-intensive processes such as welding, particularly significant for jacket structures compared to monopiles.

Additionally, the model considers the type of vessels required for installation phases (noise mitigation, pin piles, main structure), factoring in vessel dayrates and required equipment. By combining manufacturing and installation costs, the total costs for each foundation type (Hybrid Monopile, traditional monopile, jacket structure) are determined, enabling a comparative analysis of their economic feasibility.

3.4. Verification and validation

Ensuring the validity of the Hybrid Monopile research requires a keen understanding of the potential pitfalls and challenges in validating results. In structural, installation, and cost engineering, validation can be achieved through several methods: application, comparison, statistical analysis, or simulation. Choosing the right validation method is essential for accurate results.

The structural model is constructed using the software Abaqus, which is recognized for its reliability in determining the natural frequency and stresses for structures. To ensure the model's accuracy, a sensitivity analysis is conducted, and the modal shapes of the structure are checked to verify they match the expected shapes for the first, second, and third modes. The model is tested under various loading conditions to assess its sensitivity and to ensure that the stress concentrations occur at expected locations. However, exact verification and validation are challenging because the model cannot be compared to reference projects where Hybrid Monopiles are used as foundations for offshore wind turbines.

Not all outcomes lend themselves to straightforward validation. For example, assessing the correct installation of an offshore structure often relies on human interpretation rather than direct measurement.

This subjectivity makes it difficult to validate qualitative outcomes with quantitative methods, such as statistical analysis or comparison, potentially leading to flawed decisions.

A similar situation arises with cost comparisons. While cost estimates are based on existing literature and sources, they cannot be exactly verified due to the lack of public data on reference projects for offshore wind turbines. This limitation hinders the ability to ensure that the established costs accurately reflect current conditions.

By acknowledging these challenges and carefully selecting appropriate validation methods, the Hybrid Monopile research aims to produce reliable and credible results, ensuring that the proposed designs and strategies are both technically and economically viable.

4

Structural analysis

4.1. Load combinations

The load combinations adhere to the standards outlined in IEC 61400-3 and Eurocode 0. As this research includes various locations, the values are presented parametrically. Environmental loads are provided based on their return period, while load factors are determined according to the ultimate limit state.

The environmental conditions considered in this research are based on DLC 1.6 and are presented in Table 4.1

Table 4.1: Environmental conditions corresponding to DLC1.6

Parameter	Value
Wind speed	Rated wind speed
Wave height	50 year return period
Current	50 year return period
Wave period	Corresponding to wave height

The rated wind speed for the turbine ranges between 9-12 meters per second, depending on the reference turbine type considered for each situation. For the given design conditions, it is assumed that the wind turbine operates at the rated wind speed, thus experiencing maximum thrust force.

Environmental conditions were derived from data downloaded from Copernicus [60]. Using hourly data over the past 10 years, an extreme value analysis was performed to obtain the 50-year return value for significant wave height and mean wave period. These return values were used to create a 20-minute time series. This duration is sufficiently long to provide reliable estimates (t≥15 minutes) yet short enough to maintain stationary wave conditions (t≤30 minutes) [61]. The values from this analysis are used as inputs for the maximum wave height and wave period.

Table 4.2 presents the combination factors for the various types of loading based on the regulation in the DNV-OS-C101 [62].

Table 4.2: Load combination factors according to DNV standards

Load	Permanent load (G)	Variable Load (Q)	Environmental Load (E)
a)	1.2	1.2	0.7
b)	1	1	1.15

4.2. Design conditions

To access the technical and economic feasibility of the Hybrid Monopile, the design across diverse site conditions are established. This analyses is conducted on variables including water depth with corresponding significant wave height and mean wave period representative to the North Sea, soil conditions and the size of the wind turbine installed atop the foundation.

six different water depths are considered for the investigation of the design for the Hybrid Monopile, traditional monopile and the jacket structure. The following water depth are considered: 30, 40, 50, 60, 70 and 80 meters. The reason to start from 30 is that the installation of large wind turbines required large diameters of monopiles. Large diameter of monopiles installed in shallow water falls outside of the spectrum where the Morison equation is valid. Therefore the analysis start from 30 meter water depth. Figure 4.1 provides an overview of all variables considered for the design conditions of the Hybrid Monopile.

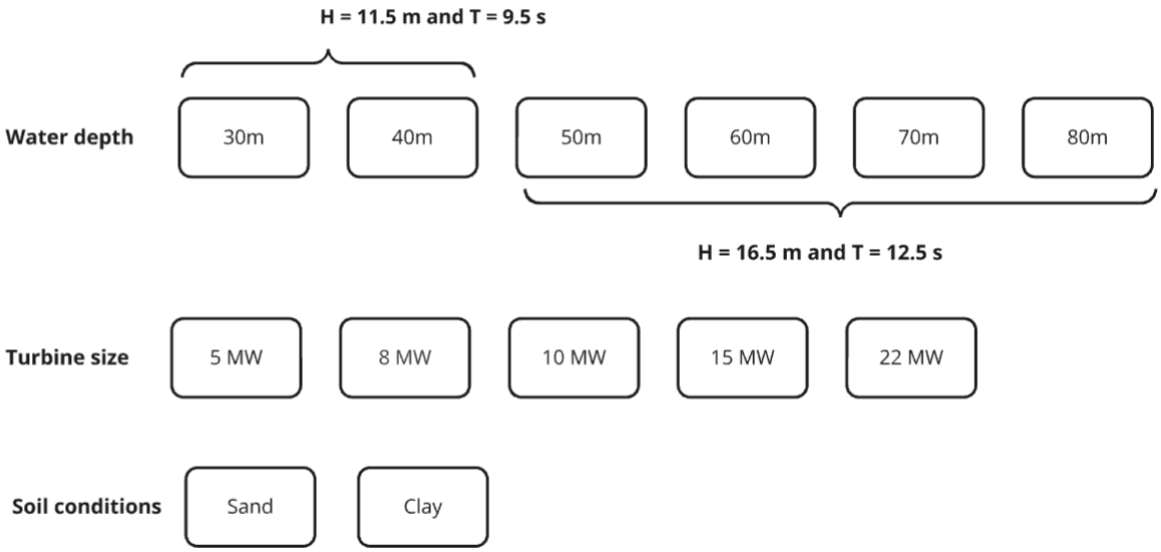

Figure 4.1: Overview of various variables for the site conditions

4.2.1. Environmental conditions

In designing the Hybrid Monopile, the environmental conditions shown in the figure above are considered. The maximum wave height is derived from a significant wave height and peak wave period of 6.1 meters and 16.8 seconds, respectively, for water depths of 30 to 40 meters, and 9.6 meters and 20.8 seconds for water depths of 50 to 80 meters. Additionally, a constant current velocity of 0.3 m/s is assumed.

For the resulting wind speed it is assumed that the rated wind speed for the various wind turbine sizes occurs at the site. At these wind speed the thrust force is at maximum.

4.2.2. Soil conditions

The response of the piles heavily depends on the soil conditions where the foundation is installed, in this research two different types of soil are investigated, sand and clay. These two soil types are considered to be the most common in offshore environments. Both sand and clay contains various soil characteristics, in Table 4.3 the characteristics of both the considered sand and clay are represented. These soils will later on be used for the determination of the p-y, t-z and q-z curves for the Hybrid Monopile.

The soil will be primary homogeneous, this means that the entire subsurface consist of sand and clay with similar characteristics, It provides valuable insights to see how to the structure should be designed in cases where the subsurface mostly consists or either sand or clay. Thus, for sand the subsurface

will be entirely homogeneous and has the characteristics as mentioned in Table 4.3. This is similar for clay, however, this undrained shear strength will increase along with the increasing depth.

Table 4.3: Considered soil conditions for the designs

	Sand	**Clay**
Unit weight (γ)	21 (kN/m^3)	16 (kN/m^3)
Friction angle (φ)	32 °	20 °
Cohesion (c)	0 kPa	15 kPa [0 - 4m] 100 kPa [4 - 20m] 200 kPa [20 - 40m] 300 kPa [40 - 60m] 400 kPa [60m +]

In this table it can be seen that the cohesion for sand is 0 and that the cohesion of clay varies along the depth. The deeper the clay layer, which is relative to the seabed, the higher the cohesion of the clay layer.

4.2.3. Reference wind turbines

In order to assess the feasibility of the Hybrid Monopile compared to the traditional monopile and jacket structure different scenarios are created to analyze components of both horizontal and vertical loading on its foundation. These scenarios consider factors such as the size of the wind turbine's rotor, which directly influences the thrust force exerted on the turbine. In the table the maximum thrust force at rated wind speeds are assumed. Additionally, the weight of the tower, including the Rotor Nacelle Assembly (RNA), is taken from the reference turbines. These wind turbines are categorized into five types, and the preliminary design of the monopile part of the Hybrid Monopile is developed based partly on these classifications.

Table 4.4: Overview reference turbines

Type	**Source**	**Rotor diameter (m)**	**Tower length (m)**	**Tower mass (t)**	**RNA & blade mass (t)**	**Thrust force (kN)**
5 MW	NREL	126	90	347	314	779
8 MW	LW	164	110	558	410	1320
10 MW	DTU	178	119	605	715	1560
15 MW	IEA Wind	240	150	860	1082	2827
22 MW	IEA Wind	284	170	1574	1023	3959

4.3. Hybrid Monopile

This section provides an outline of the structural model for the Hybrid Monopile, including the input for the installation and cost assessment. Initially, a preliminary design is determined. Based on this preliminary design, the forces acting on the Hybrid Monopile under different site conditions are calculated. The input for the Abaqus model is then explained. Using the FEM model, the natural frequency and stresses are calculated. Finally, the dynamic amplification factor is outlined, including the trends for different types of structures. All design checks and results are obtain for installations in both sand and clay. From these design checks, the final design of the Hybrid Monopile is derived.

4.3.1. Overview and assumptions

The structural analysis is conducted using Abaqus. Figure 4.2 provides an overview of the parametric model setup. The model uses various colors to highlight different parts that can be adapted in the input file. The main structural components include the monopile, the interface piece, and the pin piles.

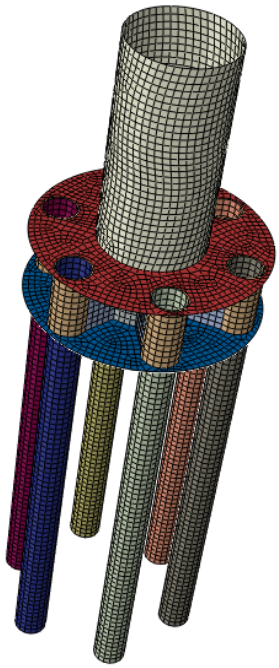

Figure 4.2: Overview of structural model HMP in Abaqus

Given the numerous input parameters, certain assumptions have been made to fix specific parameters, ensuring a clear analysis of the influence of variable parameters. The fixed parameters are as follows:

- The number of pin piles for the Hybrid Monopile is fixed at six.
- The height of the interface piece, i.e., the distance between the top and bottom flange, is fixed at 5 meters for all cases.
- The design layout is fixed, with only the dimensions of the parameters being adaptable.
- The maximum distance between the sleeve of the monopile and the sleeves of the pin piles is limited to 1 meter.
- The thicknesses of the structural elements of the interface piece, including the upper and lower flanges, the monopile sleeve, the pin pile sleeves, and the supporting shims between the flanges, are uniform.

The variable parameters in the Abaqus model include:

- Diameter and thickness of the monopile.
- Diameter and thickness of the interface piece.
- Diameter, thickness, and length of the pin piles.

4.3.2. Preliminary design of the Hybrid Monopile

To estimate the forces acting on the Hybrid Monopile supporting offshore wind turbines, a preliminary design is established. This design involves replacing the lower part of a regular monopile with an interface piece and several pin piles, with the design depending on the force magnitude and soil properties. The force magnitude on the Hybrid Monopile is determined by the hydrodynamic loading and the reference turbine installed on top of the structure. Estimating the hydrodynamic loading requires determining the diameter of the monopile.

Data from 100 offshore wind turbine projects in or around the North Sea, where sea conditions are assumed to be similar, were extracted from a Spinergie database [63]. This dataset includes projects that are either completed, under development, or currently being assessed. This data includes information

on monopile diameters, water depths at the project sites, and the sizes of the installed wind turbines. To obtain the preliminary diameters of the monopiles, the water depth is plotted against the diameter, and wind turbine sizes are categorized into five groups.

Table 4.5: Five groups to determine preliminary design based on turbine size

Group	Boundaries
1.	3 MW < WTG ≤ 5 MW
2.	5 MW < WTG ≤ 8 MW
3.	8 MW < WTG ≤ 10 MW
4.	10 MW < WTG ≤ 15 MW
5.	15 MW < WTG ≤ 22 MW

All data points were plotted, and a curve fitting is applied to derive a trend line. This graph enables the estimation of a monopile's diameter based on the water depth and the installed wind turbine size.

The curve fitting involved comparing the first, second and third order polynomial. The least squares error for each trend line is calculated to determine the best fit. The least square error of each trend line can be calculated with Equation 4.1.

$$S = \sum_{i=1}^{n} (y_i - f(x_i, \phi))^2 \tag{4.1}$$

Where S is the sum of the squared residuals of each line, y_i is the y-value of the data points, $f(x_i, \boldsymbol{\phi})$ is the model function where $\boldsymbol{\phi}$ is a vector with the best fitted parameter for the function. The model function for the first, second and third order are represented below:

- First order: $f(x, \phi) = \phi_0 x + \phi_1$
- Second order: $f(x, \phi) = \phi_0 x^2 + \phi_1 x + \phi_2$
- Third order: $f(x, \phi) = \phi_0 x^3 + \phi_1 x^2 + \phi_2 x + \phi_3$

The analysis shows that the error difference between the first and second order is in 3 of the 6 cases is 0%, see plots in Appendix A, the other three cases has error differences of 0.57 %, 3.43 % and 7.9 %. It is assumed that every group of wind turbine sizes follow the first order curve fit. For the case where the error difference is 7.9 could be chosen to take the second order curve fit. However, this should assume that preliminary design of monopiles for 5-8 MW wind turbines has a higher diameter compared to 8-10 MW, which is highly unlikely, therefore also in the 5-8 MW case the first order curve fit is assumed to be most representable. Figure 4.3 represents the overview of all first order trends of the diameter of the monopile based on the water depth where they are installed and the wind turbine installed on the foundation.

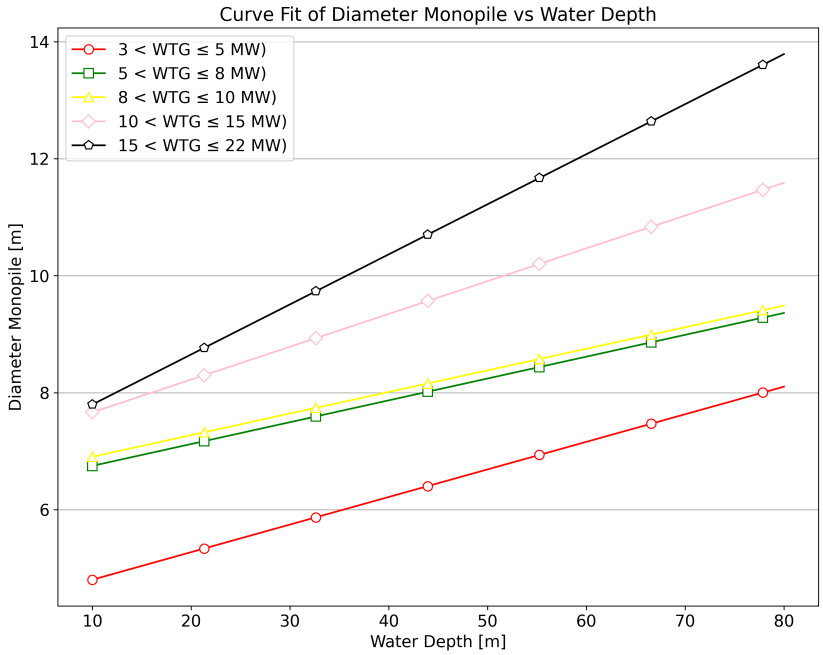

Figure 4.3: First-order trend line for initial diameter of MP for the HMP

In the plot, it is evident that as the size of the wind turbines increases, the linear trend becomes steeper. This observation can be attributed to the fact that larger wind turbines require larger supporting structures. Consequently, the diameter of the monopile, which supports the turbine, also increases. The forces acting on the monopile grow exponentially with the increase in diameter, as these forces are proportional to the square of the diameter. Therefore, as the diameter increases, the design of the monopile increases relatively more compared to smaller diameters, leading to a steeper trend line in the plot.

To ensure that the linear assumption is representative, the Pearson correlation coefficient is determined between the diameter and the depth of the monopiles. Two different coefficients: the correlation and the strength of the interpretation are determined in this case.

The Pearson correlation coefficient is calculated according to Equation 4.2.

$$r = \frac{n\left(\sum xy\right) - \left(\sum x\right)\left(\sum y\right)}{\sqrt{\left[n\sum x^2 - \left(\sum x\right)^2\right]\left[n\Sigma y^2 - \left(\sum y\right)^2\right]}} \tag{4.2}$$

Where, r is the Pearson correlation coefficient, n is the amount of observations, x is the diameter of the observation, y is the water depth of observation.

Calculating the Pearson correlation coefficient gives a value of 0.7 and the p-value = 0. According to the literature, this means a positive correlation which is moderately strong. A p-value of 0 (or very close to 0) indicates that the observed result is extremely unlikely under the null hypothesis, which is that there is no correlation between diameter and water depth. This typically means that the correlation is statistically significant, and there's strong evidence against the null hypothesis of no correlation [64].

4.3.3. Forcing on Hybrid Monopile

The forcing on the Hybrid Monopile consists of the hydrodynamic loading, the wind loading (only the thrust force is taken into account) and the vertical loading, which consists of the weight of the RNA, tower and monopile itself. Figure 4.4 represents an overview of the loading on the Hybrid Monopile including wind turbine.

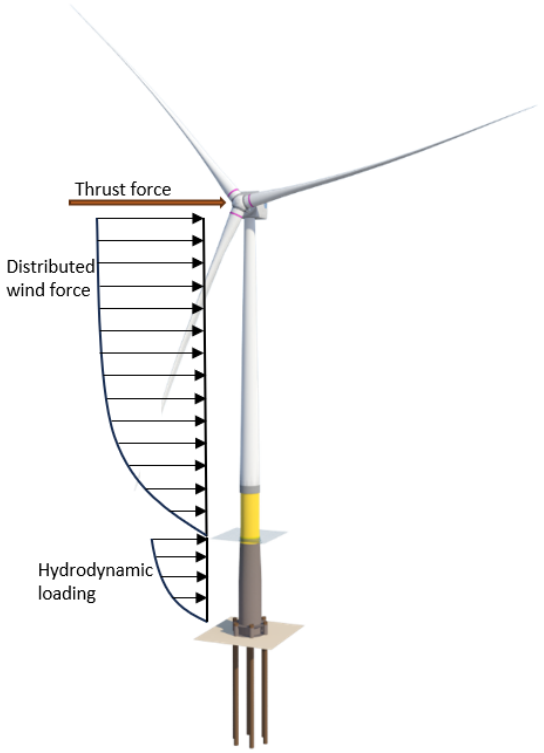

Figure 4.4: Wind and hydrodynamic loading on Hybrid Monopile [7]

The monopile is cut-off a few meters above the interface piece. From this point the replaced foundation for the monopile is placed. Based on the linear/Airy wave theory and Wheeler stretching the velocity and acceleration of the propagating waves are calculated. With Wheeler stretching the force on three places on the monopile are determined, since especially in deeper waters, the forcing of the waves does not go until the seabed. The determination of the forces on top, the lowest point where the waves reach and the location in the exact middle of these two forces. This is done by calculating the wave velocity and acceleration at the calculated depths, using the new coordinates of the wheeler stretching model. These parameters can be plugged into the Morison equation to determine the forces at these three locations. By using Simpson's rule to determine the base shear from the hydrodynamic loading. Simpson's rule represents a simplified integral based the quadratic integration of the hydrodynamic loading. Figure 4.5 represents an overview of the three calculated forces, this is an example, for deeper waters, the F_{lower} does not reach until the bottom.

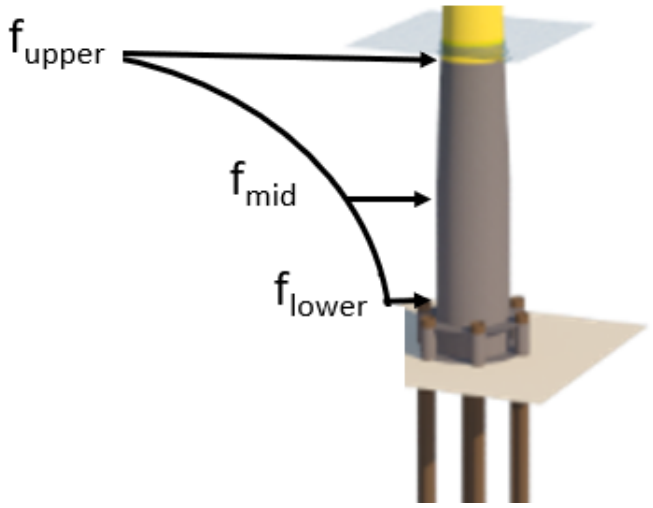

Figure 4.5: Three calculated hydrodynamic forces based on wave characteristics and Morison equation

The base shear and overturning moment are calculated according to Equation 4.3

$$F_b = \frac{Z_{upper} - Z_{lower}}{6}(f_{upper} + 4f_{mid} + f_{lower}) + F_{thrust} \tag{4.3}$$

Here, F_b represents the base shear force. Z_{upper} is the z-coordinate of the highest point where the waves exert a force, and Z_{lower} is the z-coordinate of the lowest point where the wave forces extend. f_{upper} denotes the force at the highest point where the waves exert a force, while f_{lower} indicates the force at the lowest point where the waves exert a force. f_{mid} is the force at the midpoint between the upper and lower points. Additionally, F_{thrust} is the thrust force from the wind turbines.

The vertical loading of the structure consists of the weight of the tower, including the RNA and the weight of the monopile. The weight of the monopile is based on the dimensions of the preliminary design consequently, consisting on the density of steel, the diameter, the wall thickness and the length of the monopile, which is based on the depth. For the submerged parts there needs to be accounted for the buoyancy. It is assumed that the entire monopile is submerged and the tower including RNA not. Therefore the vertical forcing depends on the weight of the structure minus the buoyancy of the monopile self

The overturning moment depends on two loading components. The first is the hydrodynamic loading, assumed to be quadratic and centered at two-thirds of the distance from the seabed. This component of the overturning moment is calculated by multiplying the horizontal loading (base shear) by two-thirds of the length of the monopile measured from the seabed. The second component is the thrust force exerted at the center of the wind turbine blades. This thrust force is multiplied by the total length of the structure above the seabed, which includes the length of the monopile and the tower of the reference turbine.

$$M = \frac{2}{3} Z_{upper} F_b + F_{thrust} L_{MP+tower} \tag{4.4}$$

These three force components are applied to the top side of the foundation of the Hybrid Monopile. Figure 4.6 represents how the forces on the model are applied. The forces that are caused by the environmental loading is multiplied by partial safety factor to account for the ULS situation.

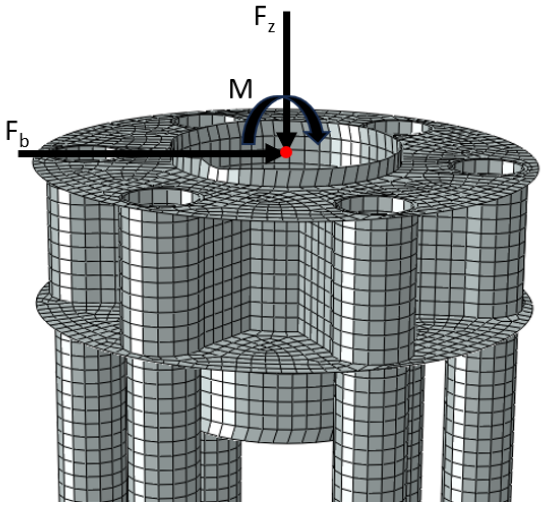

Figure 4.6: Forces on Hybrid Monopile model Abaqus

The horizontal loading, vertical loading and overturning moment are determined according the method described above, the three forces exerting on the model for all the different site conditions are represented in Figure 4.7 until Figure 4.9.

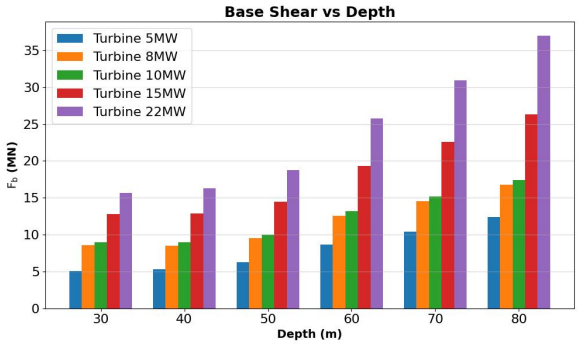

Figure 4.7: Base shear on the reference point per water depth and wind turbine size

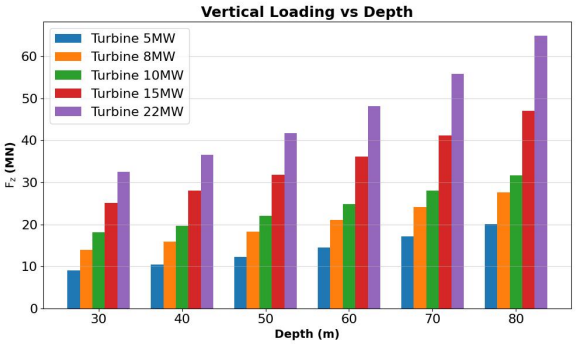

Figure 4.8: Vertical loading on the reference point per water depth and wind turbine size

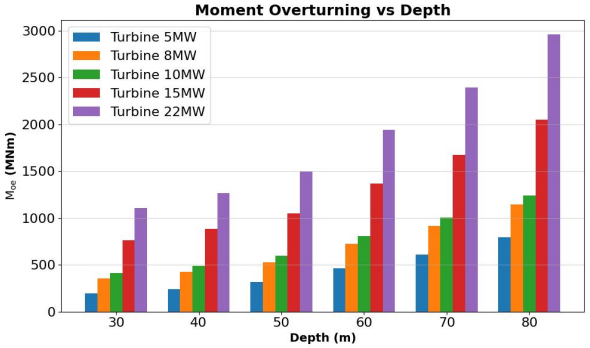

Figure 4.9: Overturning moment on the reference point per water depth and wind turbine size

As shown in the forcing bar plots, the forcing grows exponentially. When shifting to deeper water

while maintaining the same wave height and wave period, the wave velocity and acceleration decrease slightly. However, the preliminary diameter increases with deeper water. In the inertia component of the Morison equation, the diameter is squared, resulting in an exponential growth of forces as depth increases. The diameter's influence in the inertia component is more significant than the wave velocity's influence in the drag component, where velocity is also squared.

4.3.4. Frequency spectrum

To check the design of the Hybrid Monopile for the various design cases, the natural frequency of the Hybrid Monopile is checked to prevent overlapping of the wave spectrum, 1P and 3P spectrum with the natural frequency of the structure. In cases where the input design occurs resonance in the frequency spectrum, the design of the Hybrid Monopile is adapted so no chance on resonance will occur.

The wave spectrum is derived from the JONSWAP spectrum, generated using time-series data where significant wave height and peak wave period are input variables defined by site conditions at various water depths. Figure 4.10 and Figure 4.11 present the wave spectrum for two different scenarios: one for water depths of 30 and 40 meters, and the other for water depths ranging from 50 to 80 meters. It is observed that the wave spectra in deeper water are relatively lower compared to shallower water due to the larger wave period in deeper waters.

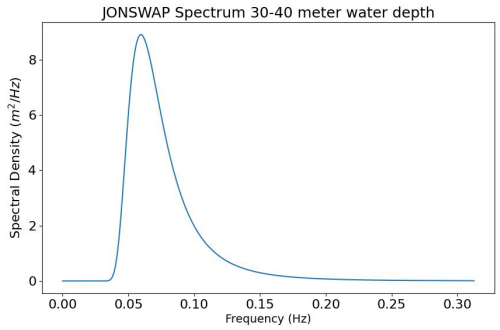

Figure 4.10: JONSWAP Spectrum 30-40 meter WD

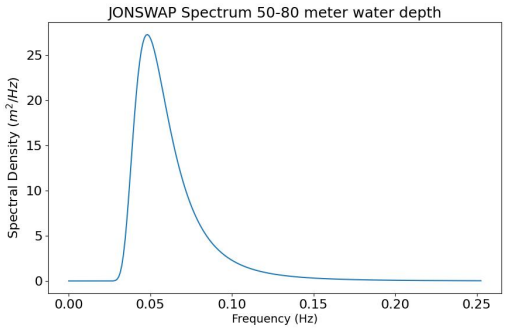

Figure 4.11: JONSWAP Spectrum 50-80 meter WD

The 1P frequency of the turbine depends on the time that all three blades passed a certain reference point, in this case the mast. The 1P frequency is determined based on the parameters of the reference turbines mentioned earlier in this report. The frequency depends on the rotor speed, which can be converted to Hertz. Equation 4.5 shows the equation from which the 1P frequency for different turbines can be determined.

$$f_{1P} = \frac{RPM}{60} \tag{4.5}$$

The 3P frequency is the frequency every time a blade passes the mast, the calculation looks similar to the one for the 1P frequency, only it should be multiplied with three, Equation 4.6 shows the equation for the 3P frequency.

$$f_{3P} = \frac{RPM}{60} * 3 \tag{4.6}$$

Table 4.6: 1P and 3P frequency of various reference turbines

Wind turbine	RPM (r/min)	1P (Hz)	3P (Hz)
3 MW	18.45	0.30	0.90
5 MW	12.10	0.20	0.60
8 MW	10.40	0.17	0.52
10 MW	9.61	0.16	0.48
15 MW	7.56	0.13	0.39
22 MW	7.02	0.12	0.36

The table illustrates that as turbine size increases, the frequencies of 1P and 3P decrease. Combining all frequencies into a single plot alongside the natural frequencies from the Abaqus model allows to check whether the structure's natural frequencies align with wave, 1P, or 3P frequencies. As depicted in Figure 4.12, for a 10 MW turbine at a water depth of 40 meters, the natural frequency of the HMP overlaps with the 1P spectrum. To mitigate this, adjustments are made to increase the structure's natural frequency. Options include enlarging the monopile's diameter or thickness, increasing the pin piles' dimensions, or modifying the interface piece's size. Figure 4.12 exemplifies the natural frequency including the results of such adjustments. For detailed frequency spectra across all scenarios, see Appendix C.

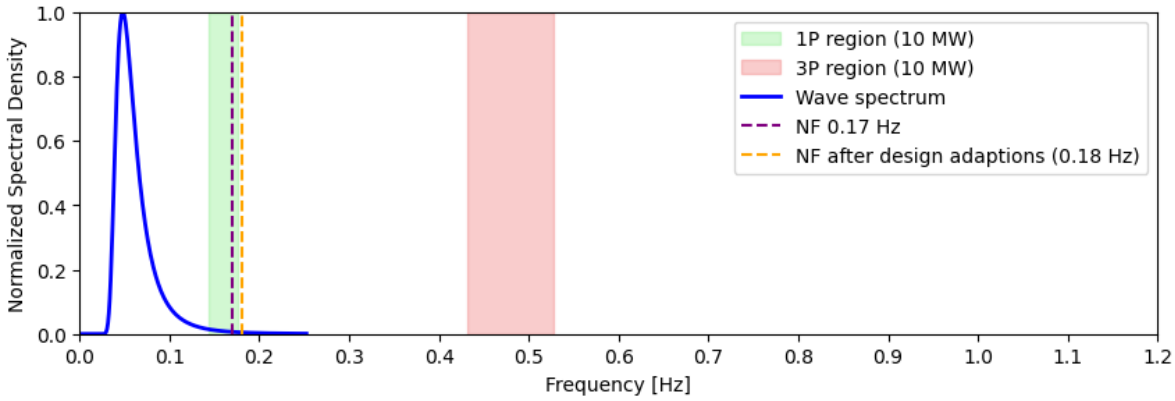

Figure 4.12: Frequency spectrum of the waves, 1P and 3P, including first natural frequency of the structure, example is 40 meter water depth and 10 MW wind turbine in sand

To examine how water depth influences the natural frequency of the Hybrid Monopile, all verified natural frequencies against the respective water depths are plotted. As depicted in Figure 4.13, a general trend emerges where larger water depths correspond to higher natural frequencies for the structure. This trend occurs because deeper water requires larger dimensions for the Hybrid Monopile. As the structural dimensions increase, the stiffness of the structure grows more rapidly than its weight. Consequently, the natural frequencies of the structure increase with increasing water depths.

However, this trend does not hold for the 10 MW turbine. Initially, during the preliminary design phase, the natural frequency overlaps with the 1P frequency of the wind turbine. Consequently, adjustments were made to the parameters of the Hybrid Monopile to shift its natural frequency outside of this spectrum.

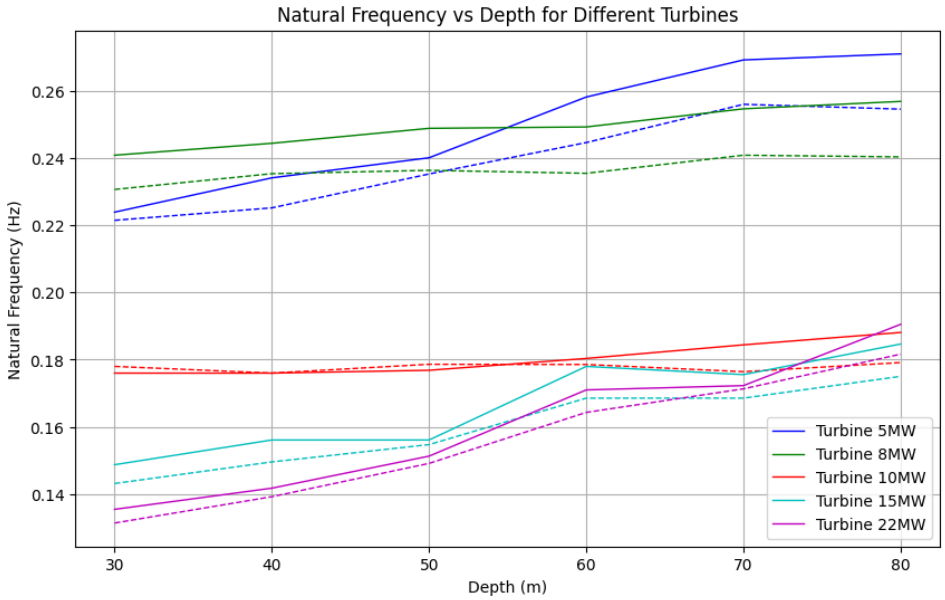

Figure 4.13: Natural frequency of the HMP against the water depths, dashed line is in clay, solid line is in sand

Furthermore, the influence of various parameters on the natural frequency of the Hybrid Monopile is examined. As detailed earlier in this chapter, some parameters are taken as variables while others are kept constant. Analyzing the impact of these five parameters on the natural frequency using the 10 MW turbine installed at a water depth of 40 meters, with preliminary design values serving as the baseline. The parameters investigated include the diameter and thickness of the monopile, the thickness of the interface piece, and the diameter and thickness of the pin piles.

Figure 4.14 illustrates how the natural frequency varies with changes in these design parameters.

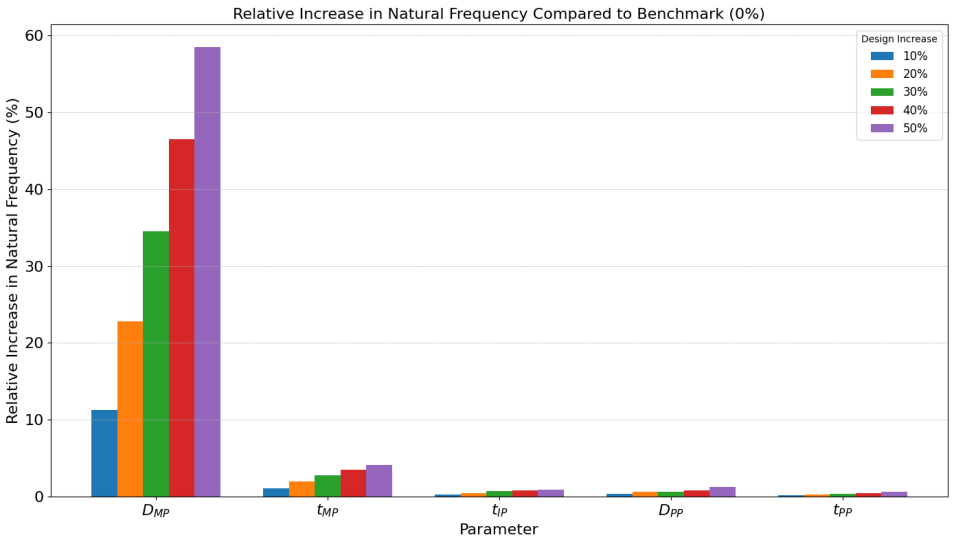

Figure 4.14: Sensitivity of the natural frequency of the HMP with varying design parameters

From Figure 4.14, it is apparent that the diameter of the monopile has the most significant influence on the natural frequency. This is due to the larger diameter of the monopiles compared to the pin piles, which greatly affects the overall stiffness. A 10% increase in the diameter of a 10-meter monopile has a much more substantial impact than the same percentage increase applied six times to 2.5-meter pin piles, this is due to the fact that the diameter goes to the power four on the formula of the moment of

inertia. Conversely, changes in the parameters of the pin piles and the interface piece have minimal impact on the natural frequency of the structure. Although the thickness of the monopile also affects the natural frequency, its influence is comparatively minor compared to variations in diameter.

4.3.5. Dynamic amplification factor

The dynamic amplification factor (DAF) is not directly calculated within the Abaqus model. Instead, a Python script is used to determine the DAF for various cases. The DAF depends on two input parameters: the frequency of the wave spectrum, which is influenced by site conditions, and the natural frequency of the structure. For this analysis, two different JONSWAP wave spectra are considered: one for water depths of 30 to 40 meters and another for water depths of 50 to 80 meters.

Figure 4.15 and Figure 4.16 show the dynamic amplification factor based on the natural frequency of the Hybrid Monopile deployed in water depths of 30-40 meters and 50-80 meters, respectively. The wave spectra are based on the data presented in subsection 4.3.4. The y-axis represents the dynamic amplification factor, while the x-axis illustrates the natural frequency of the structure. The DAF for a specific case is determined based on the structure's natural frequency. When the wave spectrum frequency and the natural frequency of the structure are very close, the dynamic amplification factor tends to infinity. For steel structures in water, a damping ratio of 2% is used [65].

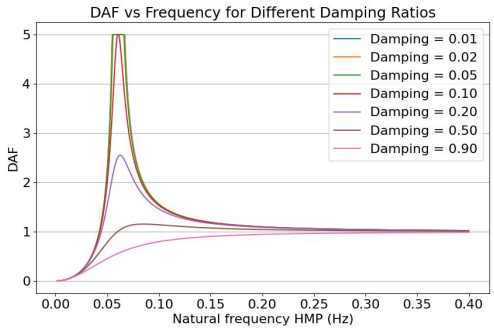

Figure 4.15: Dynamic amplification factor against natural frequency of the Hybrid Monopile, based HMP design in water depths of 30 and 40 meter

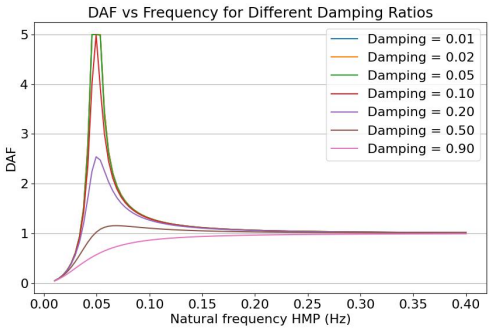

Figure 4.16: Dynamic amplification factor against natural frequency of the Hybrid Monopile, based HMP design in water depths of 50 till 80 meter

The plots appear almost identical; however, the wave frequency for the 30-40 meter water depth is slightly higher compared to that for the 50-80 meter water depth. This difference arises because the significant wave height and mean wave period for deeper waters are greater, resulting in a lower wave frequency. Consequently, the DAF varies for different natural frequencies of the structure.

To investigate the trend of the dynamic amplification factor, it is plotted against the water depth. It is observed that smaller wind turbines, and consequently smaller hybrid monopiles, tend to have smaller DAFs because their natural frequencies are significantly higher compared to larger structures.

As water depth increases, the DAF decreases for every wind turbine size. This is because, in each case, the natural frequency increases with the size of the structure. An interesting observation is that the DAF remains constant for the 10-megawatt wind turbine. This occurs because for the initial case the natural frequency overlaps with the 1P frequency of the wind turbine. In the 30 and 40 meter depths, the design is adjusted so it falls just outside this spectrum. Thus, both depths have the same natural frequency, resulting in an equal DAF.

Figure 4.17 illustrates the trend of the DAF for various wind turbines at different water depths. After the first run, the DAF is determined for every structure, the occurring base shear and overturning moment is done times the corresponding dynamic amplification factor. The design cycle start after this again to check how the design responds to the increasing forces.

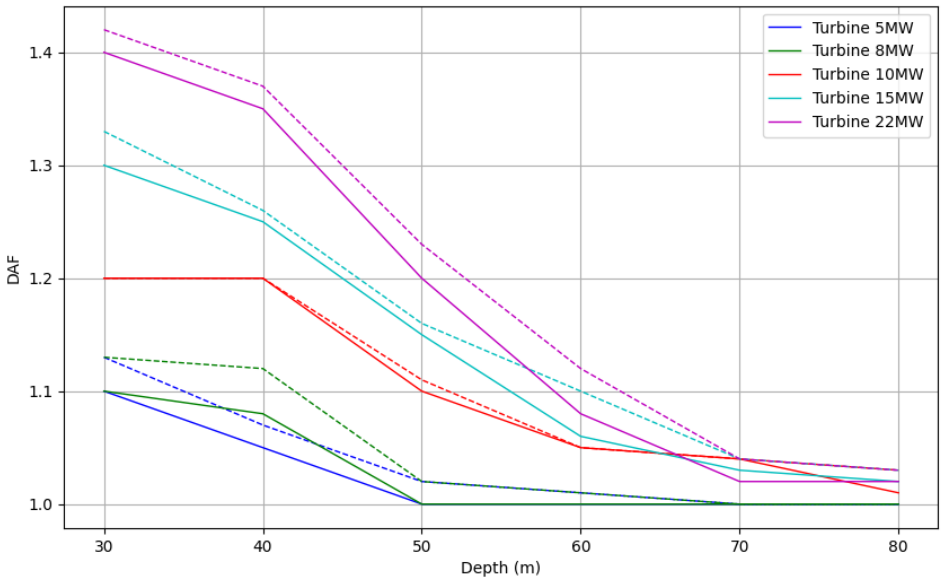

Figure 4.17: Dynamic amplification factor for various wind turbines against the installation depth in sand. Solid line = sand, dashed line = clay

4.3.6. Pile group effect

The pile group effect is crucial to consider, as discussed in chapter 2. However, no research precisely simulates the exact conditions representative of the Hybrid Monopile. Therefore, assumptions are drawn based on existing literature.

According to literature, for lateral forces on the Hybrid Monopile with a pin pile spacing of 5 meters, the pile group factor is 0.95. For the smallest structure in this study (3-5 megawatt wind turbine in 30-meter water depth), the spacing is already 4.87 meters. Hence, the assumption is that a spacing up to 6 meters results in a pile group factor of 0.95, while beyond 6 meters, the pile group effect for lateral loading is considered negligible.

For axial loading, a similar approach can be applied based on available research. Although no exact matches exist for the Hybrid Monopile, reliable assumptions can be made. In dense sand conditions, the pile group factor for downward loading is typically around 1. Since the Hybrid Monopile also experiences upward loading, an average value is considered, which is approximately 0.8 for dense sand with spacing around 5 meters and above.

For clay soils, similar values can be used. A pile group factor of 0.8 is assumed for clay, based on spacing of around 5 meters and higher.

4.3.7. Design Hybrid Monopile

The final stage of the structural analysis involves stress checks based on the Ultimate Limit State (ULS) threshold. Stresses in the structure are computed considering its geometry and applied forces. After applying safety factors described in the design conditions, these stresses are compared against the maximum allowable stress for the chosen steel type, S355, as defined by Equation 4.7.

$$\frac{\sigma_{N_{Ed}} \times SF}{\sigma_{N_{Rd}}} + \frac{\sigma_{M_{Ed}} \times SF}{\sigma_{M_{Rd}}} < 1 \tag{4.7}$$

Here, $\sigma_{N_{Ed}}$, $\sigma_{M_{Ed}}$, and represent the occurring normal and bending stresses in the structure, respectively. These are scaled by the safety factor and compared to the corresponding design resistances $\sigma_{N_{Rd}}$, $\sigma_{M_{Rd,}}$, for the maximum allowable stress in the structure, a safety factor of 1.5 is considered, while a factor of 1.15 is applied on the exerting environmental forces.

An illustration of such occurring stresses is depicted in Figure 4.18, which exemplifies the situation for a 10-megawatt wind turbine at 40-meter water depth. These stress checks are conducted for every structure type to ensure that every Hybrid Monopile structures matches with the safety and design criteria.

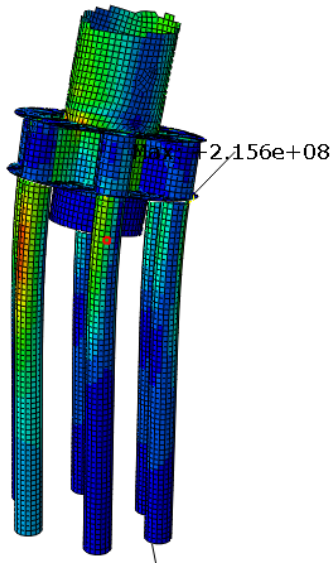

Figure 4.18: Example of occurring stress in a Hybrid Monopile for a 10-megawatt wind turbine at 40-meter water depth

Pin piles

The first part of design consist of the pin piles of the Hybrid Monopile. The pin piles are the piles driven into the subsurface. Table 4.7 shows the dimensions of the Hybrid Monopile at the final design at various water depth and wind turbine sizes. All the occuring stresses in the structures are relatively close to the ULS threshold. It can be seen that at increasing water depth and wind turbine sizes, the pin piles are also increasing in diameter, thickness and length. The dimensions of the pin piles also ensures that the bearing capacity of the foundation is enough to maintain during severe environmental conditions.

Table 4.7: Dimensions pin piles for sand at various water depths and turbine sizes

	5 MW			**8 MW**			**10 MW**			**15 MW**			**22 MW**		
	L	D	t	L	D	t	L	D	t	L	D	t	L	D	t
WD 30	26	2	0.04	31	2	0.06	30	2.5	0.06	44	3	0.06	52	3.5	0.07
WD 40	28	2	0.04	34	2	0.07	37	2.5	0.06	51	3	0.06	54	3.5	0.07
WD 50	34	2	0.04	37	2.5	0.06	41	2.5	0.06	53	3	0.06	56	3.5	0.08
WD 60	44	2	0.05	51	2.5	0.06	56	2.5	0.07	59	3	0.07	61	3.5	0.08
WD 70	41	2.5	0.05	51	2.5	0.07	56	3	0.06	66	3	0.07	69	3.5	0.08
WD 80	54	2.5	0.06	51	2.5	0.08	58	3	0.07	61	3.5	0.08	71	4	0.1

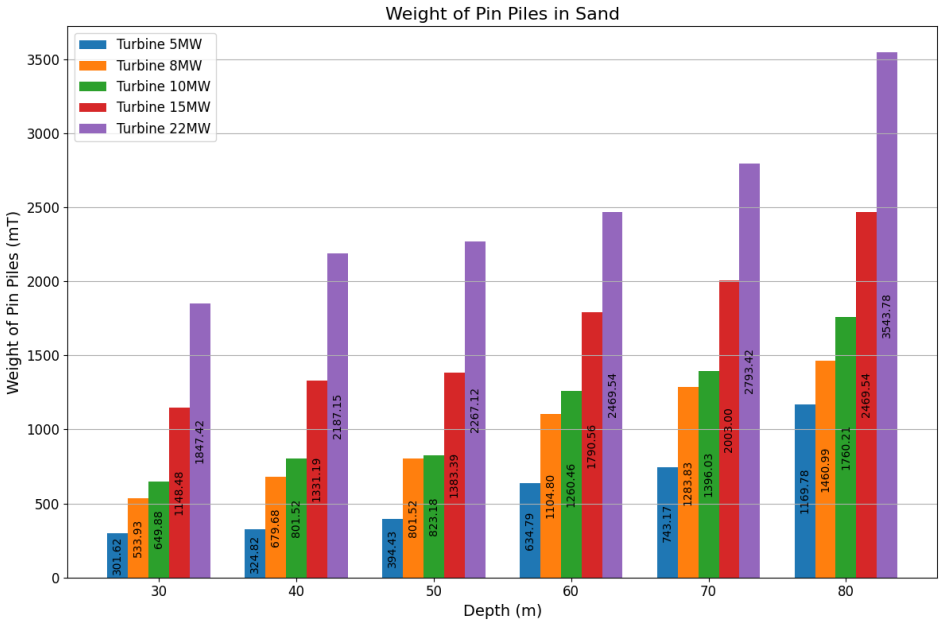

Figure 4.19: Weight of the pin piles of the HMP in sand

The total weight of the pin piles, including all six piles together, is illustrated in Figure 4.19. It can be observed that the weights do not increase linearly. This non-linear trend arises because the dynamic amplification factor for shallower water depths is significantly larger compared to deeper waters. Consequently, the design of the pin piles in shallower waters tends to be relatively heavier than those in deeper waters.

Table 4.8 and Figure 4.20 depict the dimensions and weights of the pin piles for the Hybrid Monopile when installed in clay. It is evident that the pin piles in clay are slightly larger. This increase is attributed to the less favorable soil characteristics of clay compared to sand. Particularly, the upper layers of clay are relatively soft compared to deeper layers. Therefore, for smaller wind turbines and shallower water depths, the pin piles need to be installed deeper to penetrate through these softer layers of clay to achieve sufficient bearing capacity for the structure.

Table 4.8: Weight of the pin piles of the HMP in clay

	5 MW			**8 MW**			**10 MW**			**15 MW**			**22 MW**		
	L	D	t	L	D	t	L	D	t	L	D	t	L	D	t
WD 30	40	2	0.05	53	2	0.07	53	2.5	0.06	60	3	0.05	65	3.5	0.07
WD 40	44	2	0.05	58	2	0.07	55	2.5	0.06	63	3	0.06	68	3.5	0.07
WD 50	50	2	0.05	59	2.5	0.06	65	2.5	0.06	68	3	0.06	74	3.5	0.07
WD 60	59	2	0.05	60	2.5	0.06	60	3	0.06	77	3	0.07	80	3.5	0.08
WD 70	60	2.5	0.05	65	2.5	0.07	65	3	0.06	73	3.5	0.06	77	4	0.08
WD 80	65	2.5	0.05	63	3	0.06	75	3	0.07	78	3.5	0.07	83	4	0.09

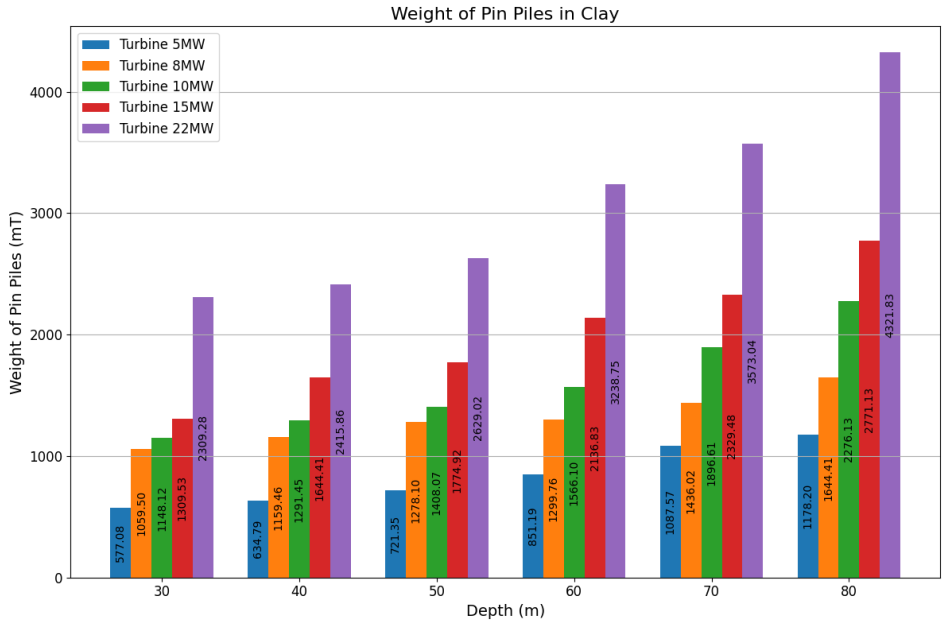

Figure 4.20: Weight of the pin piles of the HMP in clay

Interface piece

This subsection describes the design of the interface piece, which is a crucial component of the Hybrid Monopile, connecting the pin piles to the monopile. The interface piece includes an upper and lower flange, a large central sleeve for the monopile, six smaller sleeves for the pin piles, and internal shims for reinforcement. The shims are welded between the pin pile sleeves and the central monopile sleeve.

Table 4.9 and Figure 4.21 present the dimensions and weight of the interface piece for the Hybrid Monopile installed in sand. As expected, these findings indicate that the dimensions and weight of the interface piece increase with both the water depth and the size of the wind turbine.

Table 4.9: Dimensions of the interface piece at various water depths and wind turbine sizes in sand, values in meters

	5 MW		**8 MW**		**10 MW**		**15 MW**		**22 MW**	
	D	t	D	t	D	t	D	t	D	t
WD 30	12.74	0.05	14.48	0.06	17	0.06	17.5	0.09	19	0.13
WD 40	13.22	0.05	14.86	0.06	18	0.07	18.5	0.09	22	0.12
WD 50	13.68	0.06	16	0.07	18	0.08	19	0.08	22	0.13
WD 60	14.16	0.06	16.5	0.08	18.5	0.08	21	0.12	23	0.14
WD 70	16.5	0.07	17	0.08	18.5	0.1	21.5	0.11	24	0.13
WD 80	16	0.08	18	0.09	19.5	0.11	22	0.14	26	0.17

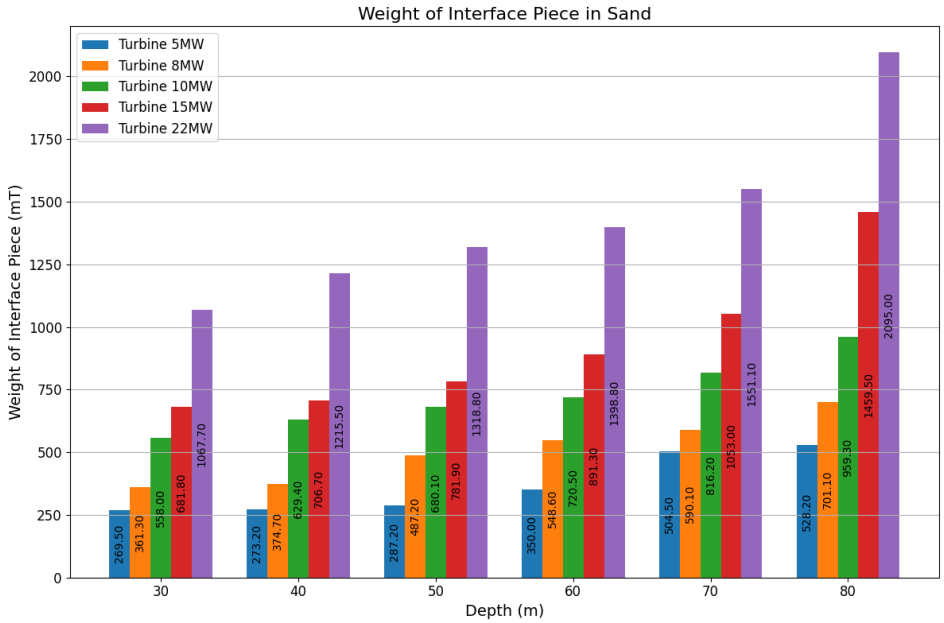

Figure 4.21: Weights of the interface piece part of the Hybrid Monopile ,in sand

Table 4.10 and Figure 4.22 present the dimensions and weight of the interface piece for the Hybrid Monopile installed in clay.

Table 4.10: Dimensions of the interface piece at various water depths and wind turbine sizes in clay, values in meters

	5 MW		**8 MW**		**10 MW**		**15 MW**		**22 MW**	
	D	t	D	t	D	t	D	t	D	t
WD 30	12.74	0.05	14.48	0.06	16	0.08	18	0.09	19	0.13
WD 40	13.22	0.05	14.86	0.06	16.1	0.08	18.5	0.09	22	0.13
WD 50	13.68	0.06	16	0.07	16.4	0.08	19.3	0.09	22	0.12
WD 60	14.16	0.06	16.5	0.08	17.5	0.09	21	0.13	21.5	0.18
WD 70	16.5	0.07	17	0.08	18.5	0.09	21.5	0.14	24	0.17
WD 80	16	0.08	18	0.09	18	0.11	22	0.15	26	0.17

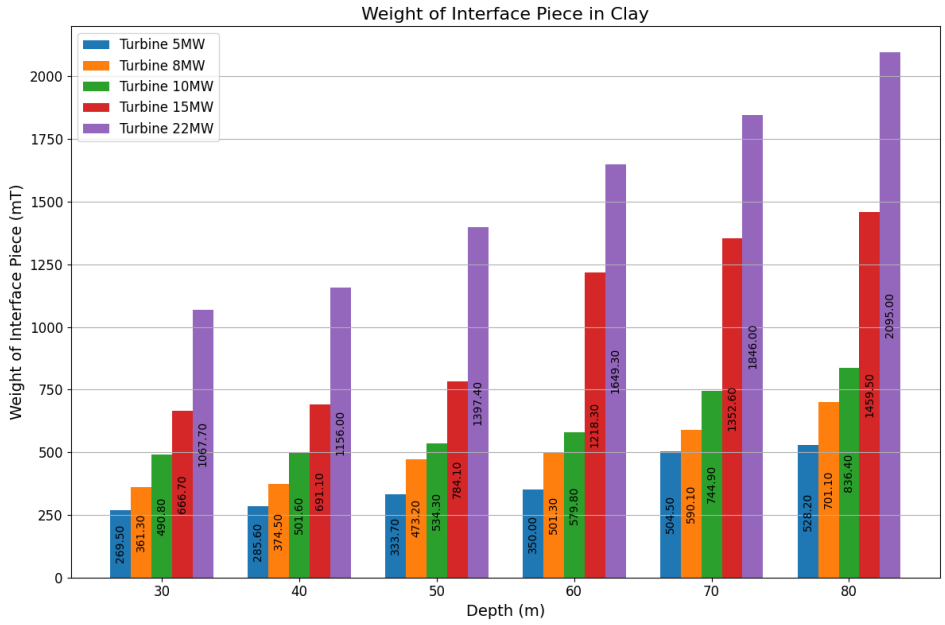

Figure 4.22: Weights of the interface piece part of the Hybrid Monopile, in clay

The design of the interface piece is closely related to the design of the pin piles. A stiffer interface piece transfers more forces to the pin piles, making it an iterative process. Conversely, a less stiff interface piece transfers fewer forces to the pin piles. For pin piles in 80-meter water depths, there is a significant change in design requirements. Since the pin piles need to be larger, the interface must be adapted accordingly.

Monopile

The design of the monopile part of the Hybrid Monopile is based on the preliminary design values obtained from the project data for the traditional monopile. As indicated before, the influence of the diameter of the monopile has the biggest influence on the natural frequency of the entire structure, including the reference towers installed on top of the Hybrid Monopile. In the case of the 10 MW wind turbine, the first natural frequency of the wind turbine falls into the 1P spectrum. In this case the diameter of the monopile is slightly increased to ensure the first natural frequency falls outside of the 1P spectrum. Increasing the diameter also increased the environmental loading on the structure and increase the weight of the structure itself. Besides this case, all the values of the monopiles are kept similar to what is determined in the subsection of the preliminary design of the monopile part of the Hybrid Monopile.

Table 4.11 and Figure 4.23 show the dimensions and weights of the monopile in various situations. The length of the monopile consists of the following elements: the assumed 4 meters self-penetration depth, the water depth where it is installed and extra for clearance.

The thickness of the monopile depends on the diameter. The thickness is calculated according to Equation 4.8 [66].

$$t = 0.00635 + \frac{D}{100} \tag{4.8}$$

Table 4.11: Dimensions of the monopile in sand and clay over various water depths and wind turbine sizes

		5 MW		8 MW		10 MW		15 MW		22 MW	
	L	D	t	D	t	D	t	D	t	D	t
WD 30	47	5.74	0.064	7.49	0.081	7.64	0.083	8.78	0.094	9.51	0.101
WD 40	57	6.22	0.069	7.87	0.085	8.01	0.086	9.34	0.100	10.36	0.110
WD 50	72	6.69	0.073	8.24	0.089	8.37	0.090	9.91	0.105	11.22	0.119
WD 60	82	7.16	0.078	8.61	0.092	8.74	0.094	10.47	0.111	12.07	0.127
WD 70	92	7.63	0.083	8.99	0.096	9.12	0.098	11.03	0.117	12.93	0.136
WD 80	102	8.1	0.087	9.36	0.100	9.49	0.101	11.59	0.122	13.79	0.144

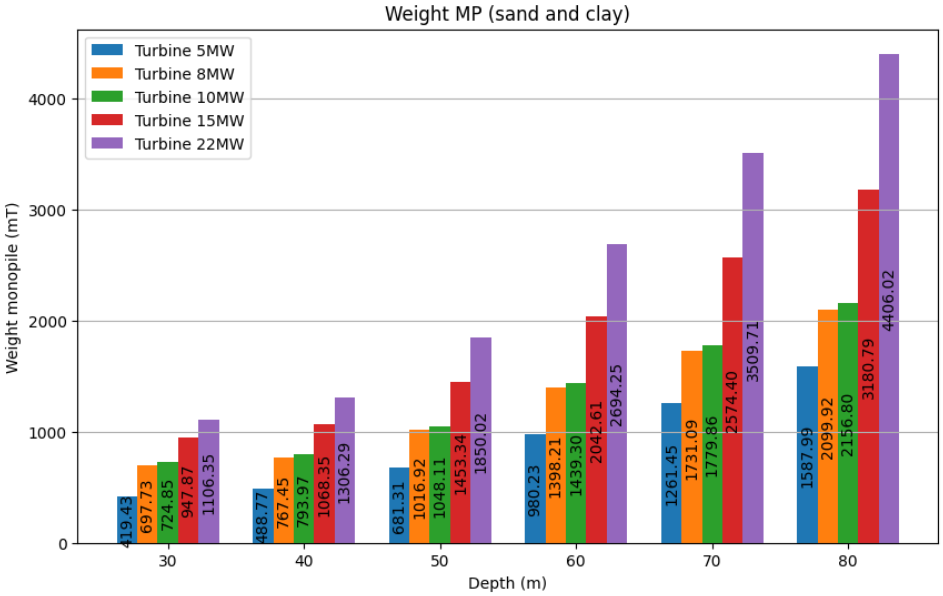

Figure 4.23: weight of the monopile part for the HMP

The weight of the monopile does not increase linearly, and the trend shifts notably between 40 and 50 meters of water depth. This change is attributed to varying environmental conditions. For instance, the monopile designed for 50-meter water depth must deal with higher maximum wave heights. Consequently, the pile itself needs to be slightly longer to accommodate these conditions, which explains why the monopile is heavier in this scenario.

The contribution of the total weight of the Hybrid Monopile is calculated and represented in a pie chart. Figure 4.24 and Figure 4.25 show the weight ratios of the pin piles, monopile, and interface piece of the Hybrid Monopile.

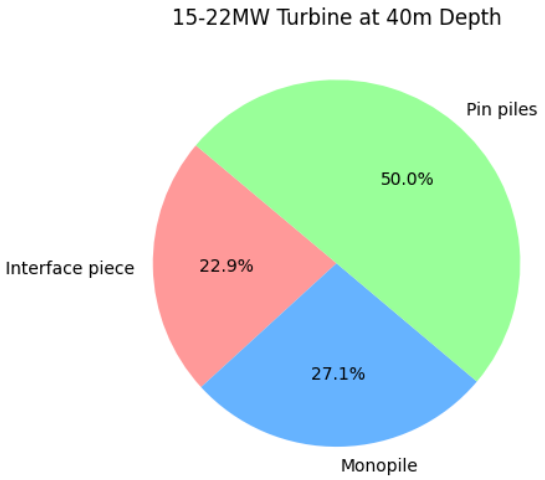

Figure 4.24: Ratio of weight per structural component at 40m depth

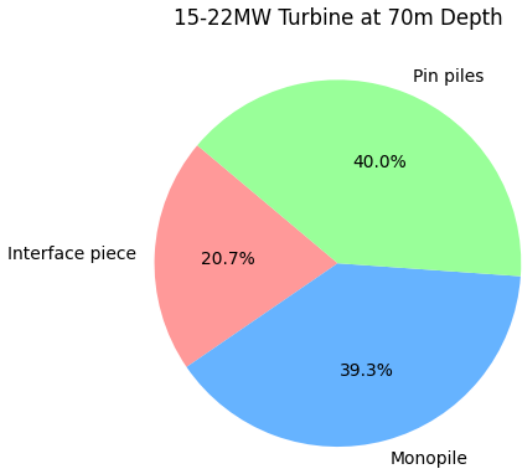

Figure 4.25: Ratio of weight per structural component at 70m depth

It can be observed that the pin piles contribute the most to the weight of the entire structure in both cases. However, in deeper waters, the contribution of the pin piles decreases by around 10%. This decrease is due to the increased resistance provided by the soil as the pin piles penetrate deeper into the subsurface. The deeper the pin piles go, the more resistance they encounter per unit depth. The interface piece consistently accounts for approximately 20% of the total weight in both scenarios. The contribution of the monopile increases with increasing water depth, which is because the weight of the monopile grows exponentially. This exponential growth is due to the diameter of the monopile being squared in the Morison equation, which is used to determine the forces on the structure.

4.3.8. Design improvement

After running the simulations, several problems were identified for each situation. These issues are illustrated in Figure 4.26, which indicates their locations on the Hybrid Monopile.

1. The stress right above the interface is particularly problematic in scenarios with water depths greater than 50 meters and wind turbines of 10 MW or larger. To address this, a thicker steel plate was incorporated in this part of the models.
2. The stress magnitude in the steel section between the monopile sleeve and the pin pile sleeves also orovides issues.

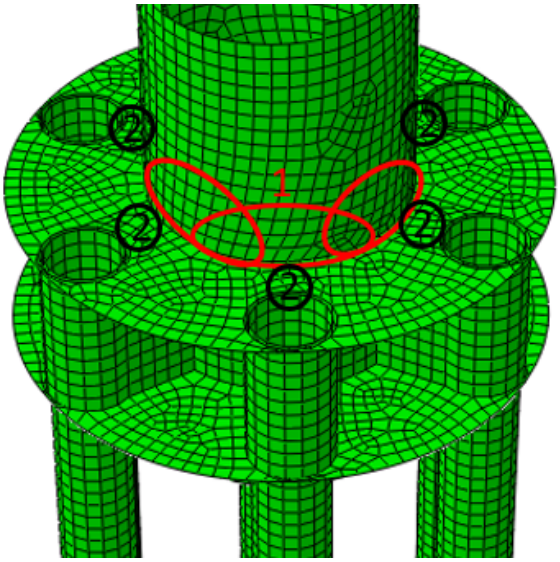

Figure 4.26: Design bottlenecks in the Hybrid Monopile

The issues could be mitigated by adding extra shims at critical stress points for additional support. For the steel section between these points, it could be eliminated, allowing the sleeves to be directly welded together. This modification would result in higher moments in the pin piles due to the reduced distance. Consequently, the thickness of the sleeves or the dimensions of the pin piles would need to be increased to compensate.

In addition to identifying problems, the simulations also highlighted areas where the design could be improved. Certain parts of the design do not contribute significantly to the structural integrity of the Hybrid Monopile, as shown in Figure 4.27.

1. The top and bottom flanges between the pin piles experience negligible stress compared to other parts. These flanges could be removed to reduce the weight of the interface piece.
2. The pin piles currently have a uniform diameter and thickness. However, the highest stress magnitudes occur on the top side, near the interface piece. This suggests that the dimensions of the lower part of the pin piles could be reduced.

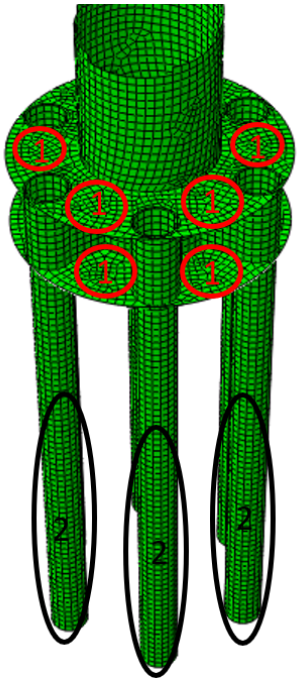

Figure 4.27: Possible design improvements

An adaptation of the design can lead to a different load distribution within the structure. Therefore, it is necessary to emphasize that the entire design loop should be redone to verify whether the proposed improvement actually enhances the design.

4.4. Traditional monopile

To estimate the dimensions and weight of traditional monopiles, curve fit lines were drawn based on project data from wind farms in the North Sea. As a form of validation, some public domain projects were plotted on these lines. Figure 4.28 illustrates the trend lines depicting monopile heights against water depths.

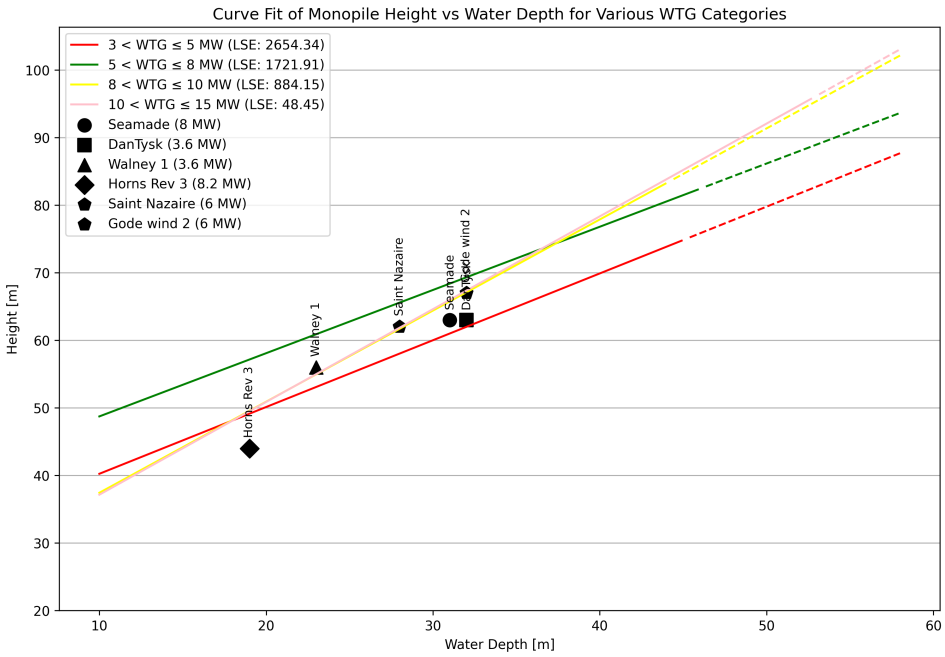

Figure 4.28: Heights of the monopile, based on project data from wind farms in the North Sea

Unfortunately, no project data or assessments are available for projects involving wind turbines between 15 and 22 megawatts. However, the four categories of wind turbines plotted exhibit an interesting trend. The plots for 8-10 MW and 10-15 MW wind turbines overlap and are steeper compared to those for 3-5 MW and 5-8 MW turbines. This difference might be attributed to older wind projects in the North Sea being designed less efficiently than current projects and assessments due to the limited knowledge at the time.

When considering the total heights of the monopiles, which include the length driven into the subsurface, the heights do not vary significantly compared to the diameters of the monopiles at different water depths. For water depths between 30 and 40 meters, which are considered feasible in this study, the height difference between turbine sizes is around 10%. This suggests that most of the strength and stability is achieved by increasing the diameter rather than the length.

For simplification, the maximum values from the trend lines are considered governing for this case, including for 15-22 MW wind turbines. The diameters and thicknesses of the monopiles are assumed to be similar to those from the preliminary design of the Hybrid Monopile, as this data originates from monopile projects themselves.

According to research conducted by Sánchez et al. [67], the penetration depth of monopiles in sand and clay is considered to be similar. This suggests that the behavior of monopiles in both soil types does not significantly differ from each other. Therefore, for both of the situation the same monopile size is considered.

Table 4.12 and Figure 4.29 present the dimensions and weights of the traditional monopile considered in this research, based on the curve fit data of the projects.

Table 4.12: Dimensions of the traditional monopile based on trend line of former wind projects

		5 MW		**8 MW**		**10 MW**		**15 MW**		**22 MW**	
	L	D	t	D	t	D	t	D	t	D	t
WD 30	67	5.74	0.064	7.49	0.081	7.64	0.083	8.78	0.094	9.51	0.101
WD 40	77	6.22	0.069	7.87	0.085	8.01	0.086	9.34	0.100	10.36	0.110

Figure 4.29: weight of the traditional monopile

4.5. Jacket structure

To determine the weight of the jacket structure based on the size of the wind turbine that needs to be placed on top of it and the various water depths, a method similar to the estimation of the monopile height is used. Curve fit lines are drawn based on projects conducted in the North Sea. It's noticeable that for the 3-5 MW wind turbine size range, no project data is available, and hence, no curve fit is drawn for this group of wind turbines. Given that wind turbines are becoming increasingly larger, it is highly unlikely that 3-5 MW wind turbines will be installed on a jacket structure in the North Sea in the near future. Therefore, this group is neglected in the jacket structure analysis.

There was also insufficient information for the 10-15 MW range; thus, the lines between the 8-10 MW and 15-22 MW ranges are extrapolated to obtain a reliable estimation for this group. No wind turbines larger than 15 MW have been installed yet in the North Sea, so these data points rely on assessments of jacket structures for certain water depths and wind turbine sizes.

It is assumed that the curve fit follows a linear trend. The second-order and third-order polynomials for the various wind turbine groups can be found in Appendix A.

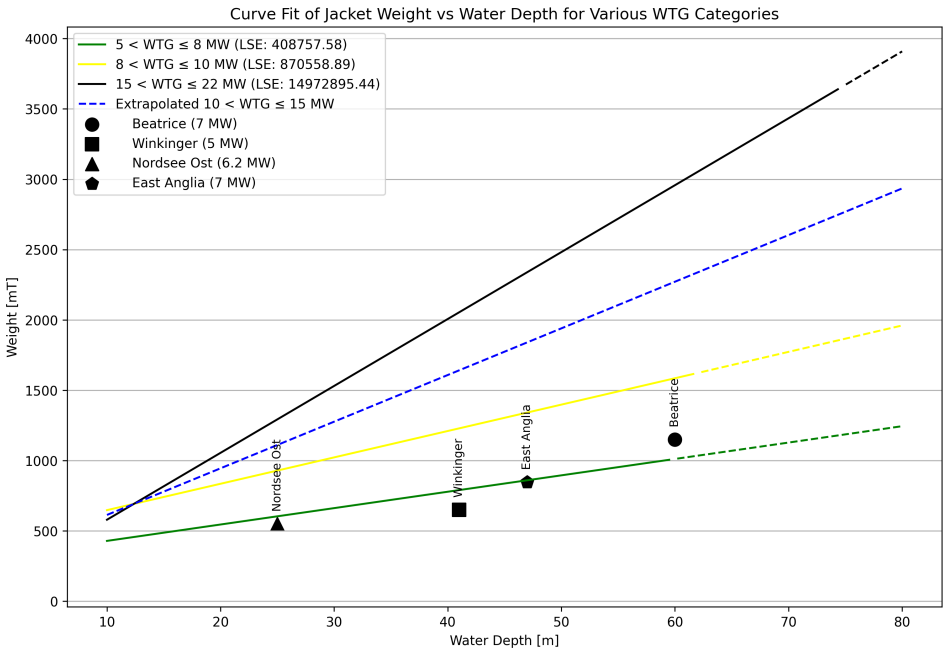

Figure 4.30: Weight of the jacket structure for various wind turbine sizes and water depths

Figure 4.30 shows the weight of the jacket structure. These weights exclude the weight of the pin piles required for the jacket's foundation. It is assumed that each jacket needs four pin piles and that the size of the pin piles is similar to those for a Hybrid Monopile. Figure 4.31 and Figure 4.32 show the weight of the jacket and pin piles in sand and clay, respectively. The size of the jacket structure is considered similar in both situations since the environmental loading for sand and clay will be similar. However, the size of the pin piles differs because the bearing capacity of clay is less than that of sand, requiring larger pin piles in clay.

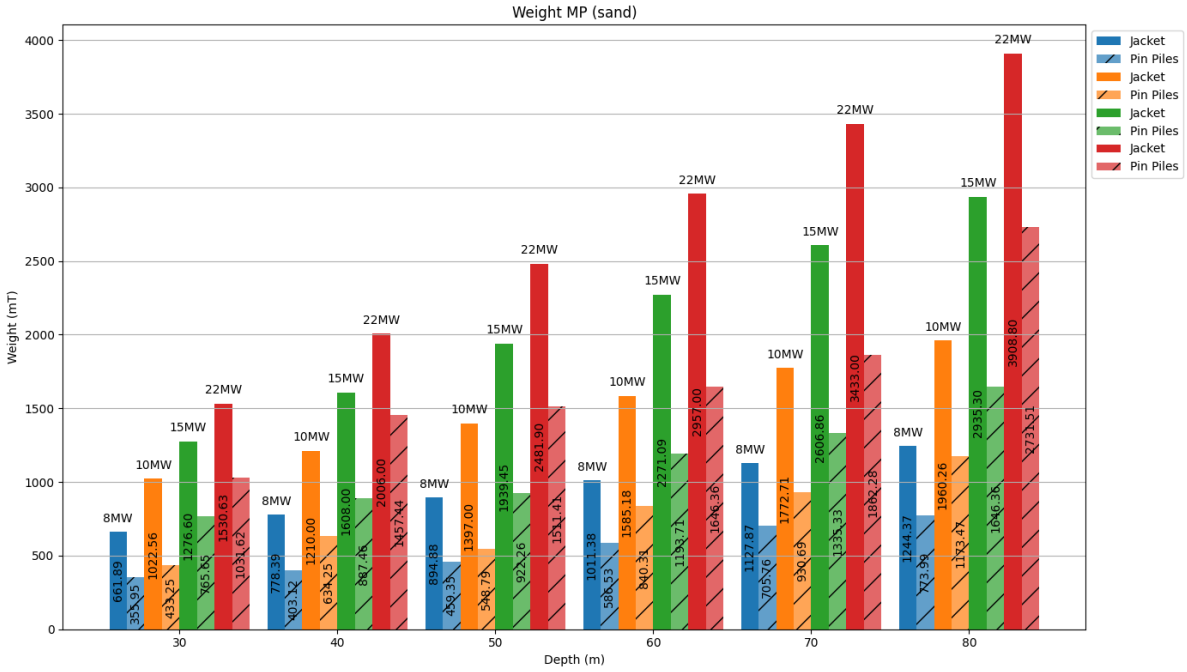

Figure 4.31: Weight of jacket and pin piles in sand

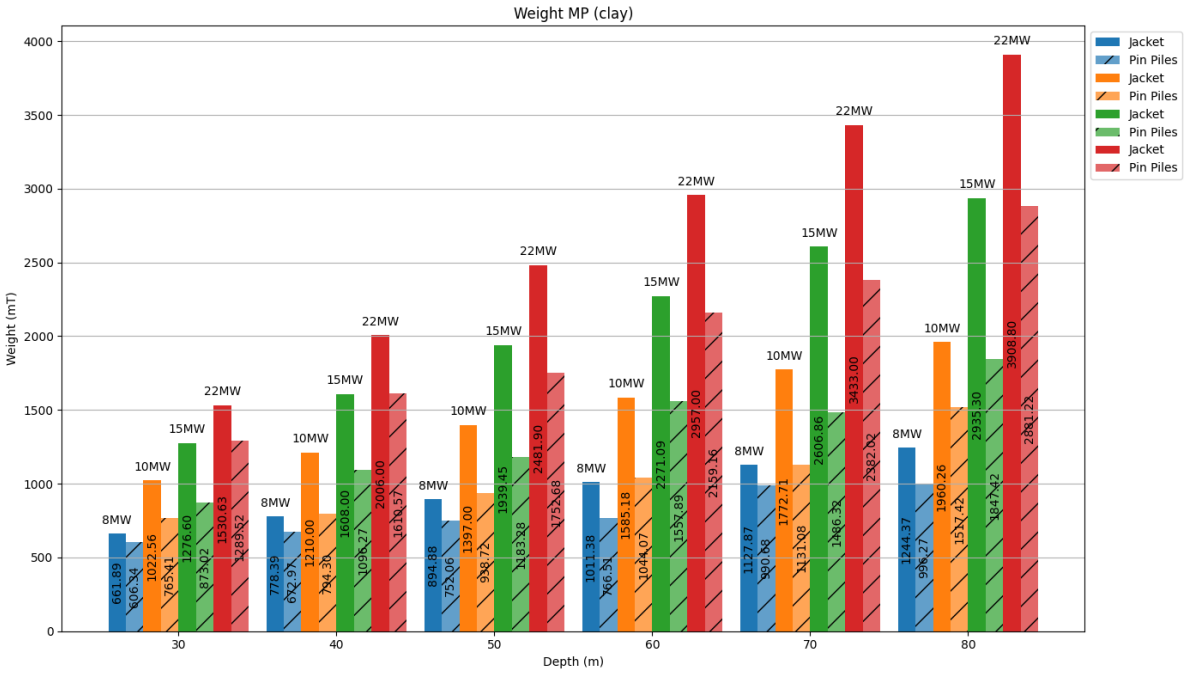

Figure 4.32: Weight of jacket and pin piles in clay

To provide a clear comparison of the Hybrid Monopile's weight relative to the jacket structure, four separate plots are presented, each corresponding to a different wind turbine size. These plots offer insights into whether the Hybrid Monopile's weight is heavier, lighter, or comparable to that of the jacket structure in similar scenarios (see Figure 4.33 - Figure 4.36).

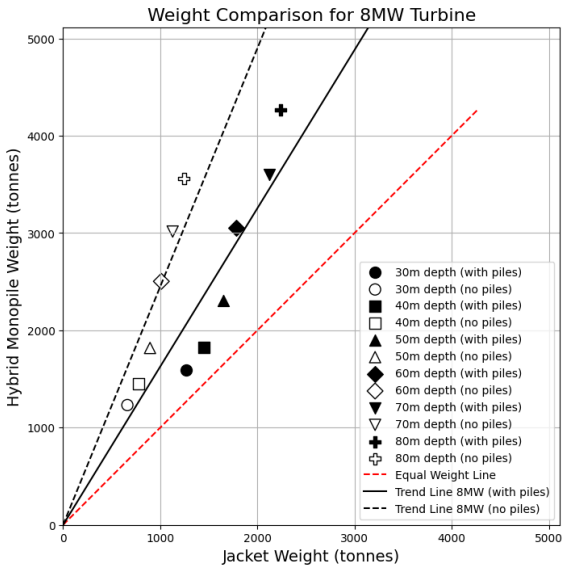

Figure 4.33: Weight HMP vs Jacket for 8 MW

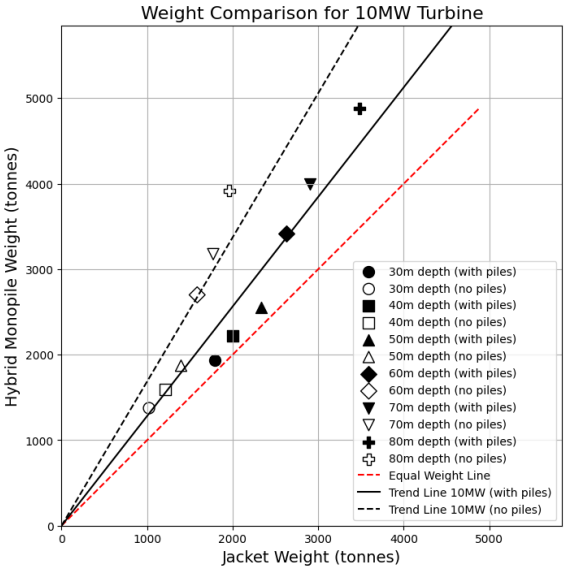

Figure 4.34: Weight HMP vs Jacket for 10 MW

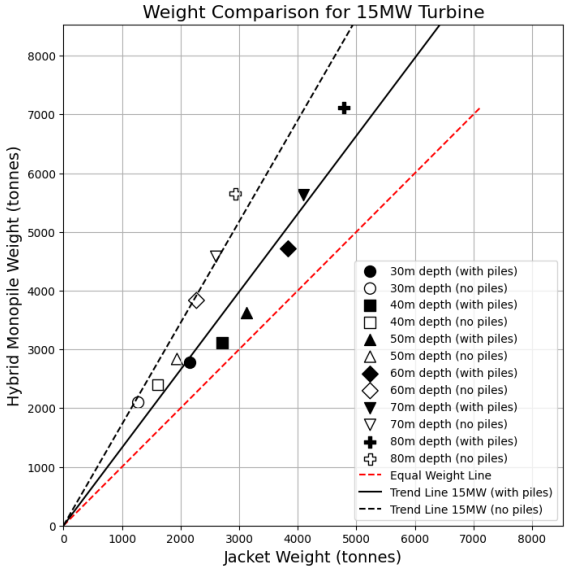

Figure 4.35: Weight HMP vs Jacket for 15 MW

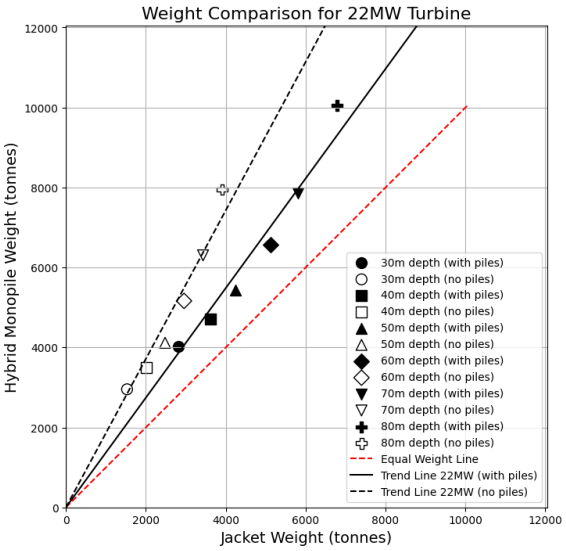

Figure 4.36: Weight HMP vs Jacket for 22 MW

The plots reveal that, in all cases, the weight of the Hybrid Monopile is greater than that of the jacket structure. The trend lines are steeper for smaller wind turbines, such as the 8 MW and 10 MW models. As the turbine size increases, the angle of the trend line decreases. This trend suggests that the Hybrid Monopile may be over-designed for smaller turbines, as it might not require the full complement of six pin piles for these lower-capacity wind turbines.

5

Installation assessment

This chapter provides an evaluation of the installation procedures for the Hybrid Monopile, traditional monopile and jacket structure. It details the essential installation steps, including average time estimates and necessary equipment. While the installation methods for traditional monopiles and jacket structures are well-established and straightforward, the installation of hybrid monopiles is a novel area of exploration. This chapter delves into different installation strategies for Hybrid Monopiles, discussing their advantages and disadvantages. Time estimates for specific installations are sourced from constructability studies and publicly available reports [68], [69].

5.1. Assumptions

For the installation of the Hybrid Monopile, traditional monopile and the jacket structure, some assumptions are made for the installation of it.

- It is assumed that the jacket will be installed with pre-installed pin piles, and then positioned atop these pin piles, rather than having the pin piles installed through the legs of the jacket.
- It is assumed that the grouting vessel works highly efficient and never has to wait for the installation vessel before start grouting
- The installation of the pin piles of the next location doesn't influence the hardening process of the grouting of the former installed pin piles
- It is assumed that the tip of the monopile penetrates the subsurface due to the self weight of the Hybrid Monopile
- It is assumed that the site is suitable for immediate installation of the foundation structure. No preparation is needed.
- For the installation of the traditional monopile a double bubble curtain is required, while pin pile installation only requires one bubble curtain as noise mitigation.
- The Hybrid Monopile is transported vertically. The interface piece is considered to be too big for overhang on the barge. Overhang can cause wave slamming on the structure, especially since the interface piece is relatively large

5.2. Hybrid Monopile

This section outlines the installation assessment of the Hybrid Monopile, which consists of four phases: installing the pin piles, lifting and positioning the structure, leveling the monopile and connecting the Hybrid Monopile to the pin piles.

5.2.1. Installation pin piles and Hybrid Monopile

In the first phase, the installation process of the pin piles and the Hybrid Monopile is outlined. The first installation strategy is described below:

Strategy 1

1. Installation pin piles using a template

The first method for the installation of the pin piles involves using a template, the spacing of the template is made identically compared to the interface piece, to ensure that the Hybrid Monopile including interface piece fits over the pin piles. Figure 5.1, Figure 5.2 & Figure 5.3 illustrates the installation of the pin piles by using the template.

The installation vessel can sail to the installation site. The installation can be done in combination with barges, positioned against the heavy crane vessel. The barges are responsible for the supply of the pin piles during the installation. This mean that the heavy-crane vessel does not have to go to the yard to retrieve the pin piles itself. When the installation of the template is done, the pin piles can be hammered or vibrated into the subsurface by the installation vessel. As soon as all the pin piles are installed, the template is removed and the vessel sails to the next site to repeat this.

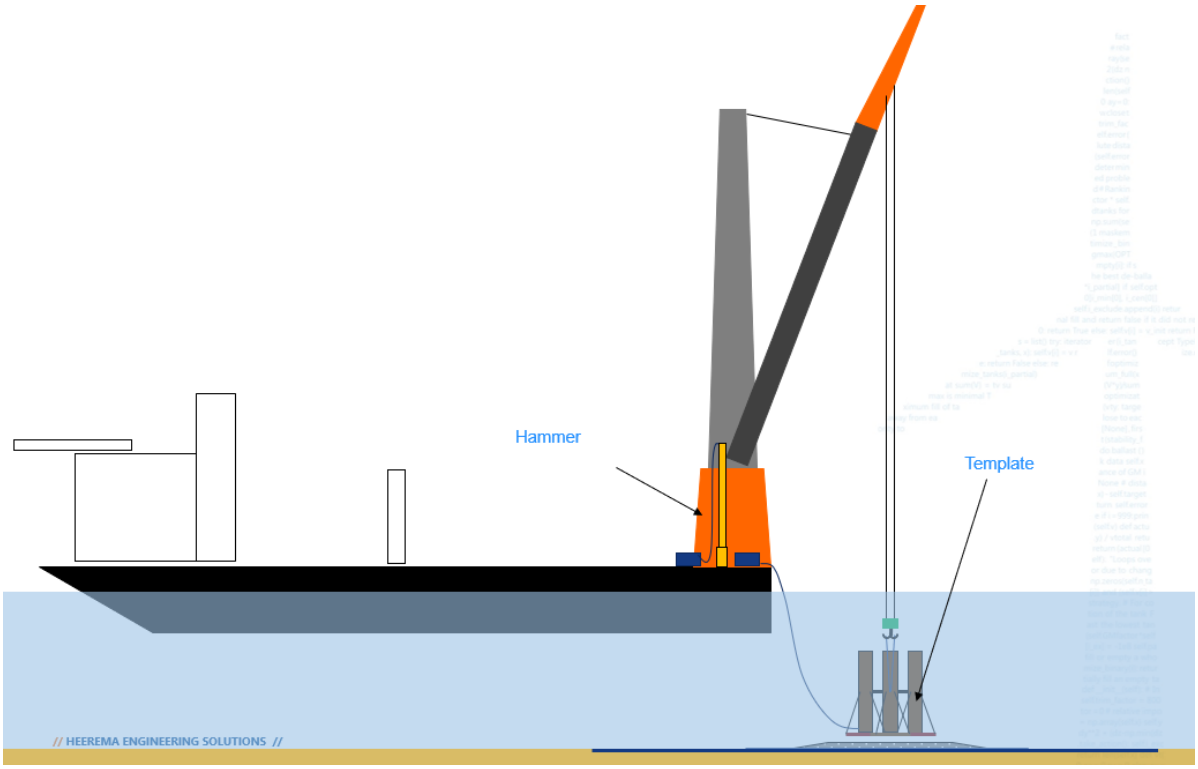

Figure 5.1: Installation of the template for the pin piles (HMP)

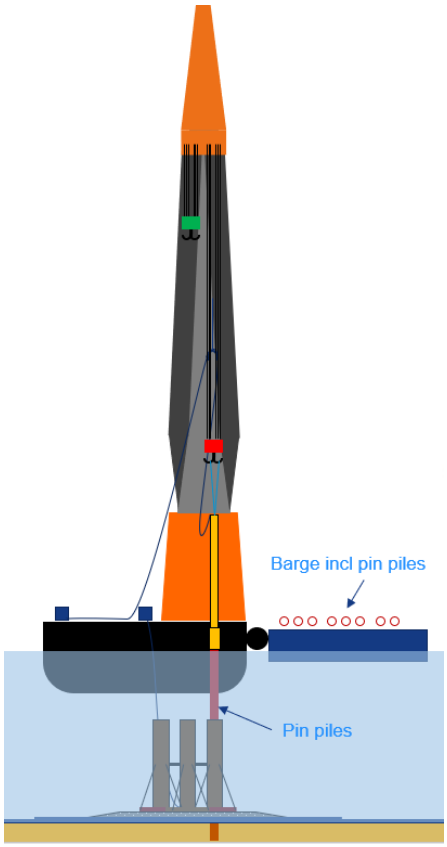

Figure 5.2: Installation of the pin piles.

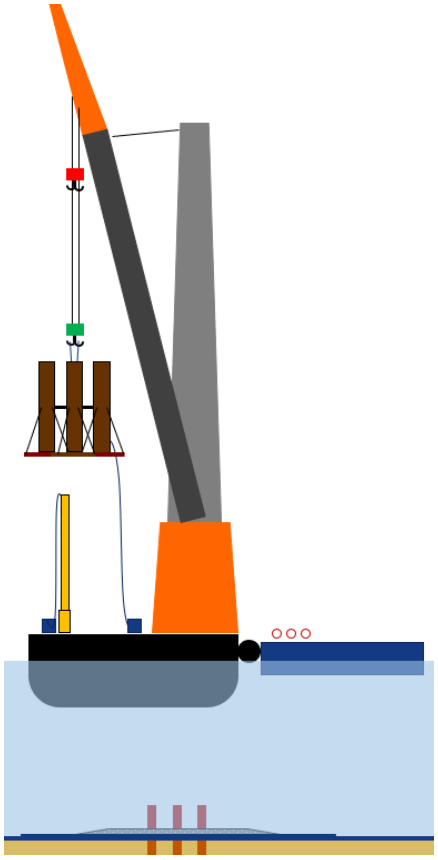

Figure 5.3: Remove template after installation all pin piles.

2. Lifting and positioning of the Hybrid Monopile

Now the lifting and the positioning of the Hybrid Monopile can be executed. The hybrid Monopiles are supplied by a barge. It is assumed that the Hybrid Monopile is transported vertically. Two different steps can be taken to install the Hybrid Monopile.

- Case 1: The interface piece and the transition piece can be assembled to the monopile onshore. In this case the HMP is installed together. (see Figure 5.4)
- Case 2: The interface piece can be assembled offshore. In this case the transition piece is installed afterward on top of the monopile. This involves one extra step which needs to be executed offshore. (see Figure 5.5)

In case that the interface piece and the transition piece are already assembled to the monopile onshore saves an extra step of installation offshore, consequently saving time and money during the installation. However, in case the Hybrid Monopile becomes to heavy and certain crane vessels are not suitable for the installation, it could be more advantageous to install the transition piece separately, as is illustrated in the second case. In both situation the sleeves of the HMP are guided over the pin piles. This process is quite dependent on the environmental circumstances. During severe environmental situations, this event can be hard to execute. The tip of the HMP is expected to push through the subsurface based on self penetration due to the weight of the HMP. The positioning of the sleeves above the pin piles are accompanied by an ROV to monitor the situation.

The benefit of strategy 1 is that the cycle can be subdivided into different phases, where first the pin piles and secondly the Hybrid Monopile is lifted and positioned on top of the pin piles. The separation of installation allows for more flexibility during the installation.

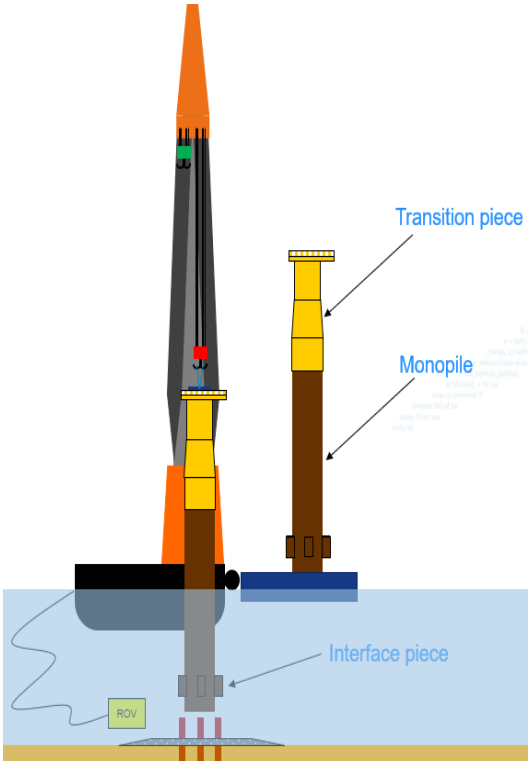

Figure 5.4: Case 1: Installation HMP including TP and IP

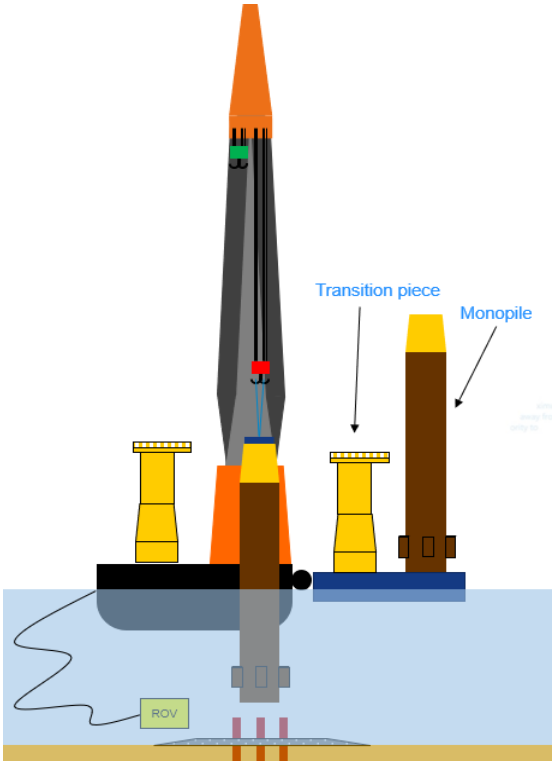

Figure 5.5: Case 2: installation HMP including IP

Strategy 2

1. Installation of the pin piles using the interface piece

The second strategy for installing pin piles involves utilizing the interface piece. Unlike the first option, this approach eliminates the need to transport the template to each new location. Instead, the interface piece is positioned on the subsurface, facilitating the installation of the pin piles. However, using the interface piece as a template introduces additional risks. Piling templates often incorporate advanced tools to ensure straight and secure pin pile installation, including mechanisms for easy decoupling [70]. When using the interface piece as a template, each interface piece must be equipped with these tools, which includes significant costs. Neglecting to equip the interface piece with necessary tools introduces risks, such as potential damage to sleeves and pin piles during the installation process. This could result in the components becoming fixed together, enabling the interface piece of being leveled.

Assuming the pin pile installation is executed correctly. The interface piece should be connected to the pin piles to ensure that it is fixed. There are multiple ways of connecting the interface piece to the pin piles, in the coming paragraphs various assembling methods are outlined.

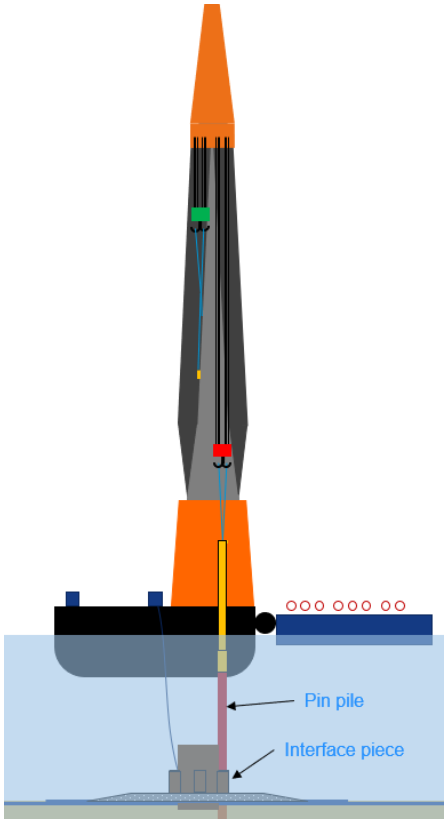

Figure 5.6: Position IP on the filter layer and install pin piles

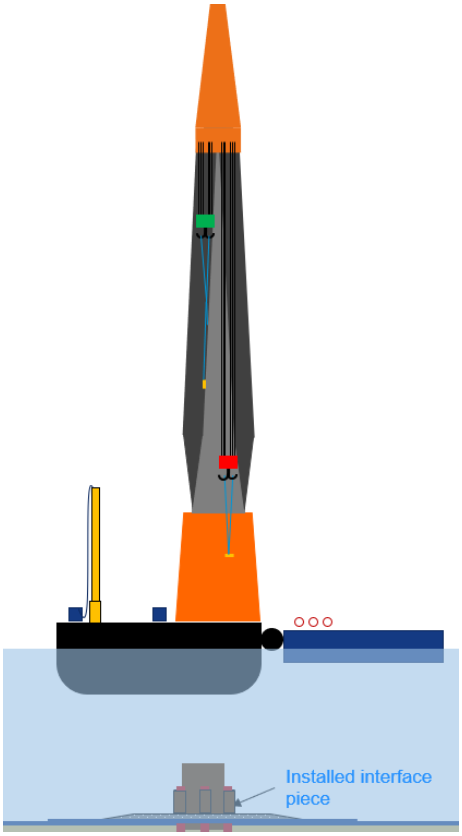

Figure 5.7: Install all the pin piles and keep the IP on the filter layer

2. Upend the monopile and position on top of the interface piece

Two different installation steps are identified to upend and install the monopile, dependent on the weight and height of the monopile including transition piece, note that this installation methods are similar to the situation where the pin piles are installed with the use of a template.

- Case 1: The transition piece can be assembled to the monopile onshore. In this case the HMP is installed together with the transition piece. (see Figure 5.4)
- Case 2: The transition piece can be assembled offshore. In this case the transition piece is installed afterwards on top of the monopile. This involves one extra step which needs to be executed offshore. (see Figure 5.5)

In case the interface is pre-installed, the the monopile should be placed into the interface piece. A barge supplies the monopiles. The crane vessels can take the monopiles from the barge. The monopile needs to be positioned above the interface piece. The same difficulties pops up with this method. The upending and positioning of the monopile is dependent on the environmental conditions. Severe environmental conditions effects the installation time, if it is even possible to install the monopile in the interface piece. The installation of the monopile is being monitored by a ROV to correct unexpected movements. When the monopile is at position it is leveled and assembled to the interface piece.

The benefits of strategy 2 is similar to strategy 1, where the installation cycle is split up in two different stages. This allows for more flexibility in the installation scheme. The disadvantageous of this method is that the interface piece should be equipped with advanced tools for the installation of the pin piles. Besides, strategy 2 requires two times a levelling and connection method, since first the interface should be connected to the pin piles, and secondly, the monopile should be connected to the interface piece. Also, the monopile needs to be kept in place during the grouting phase which leads to extra costs.

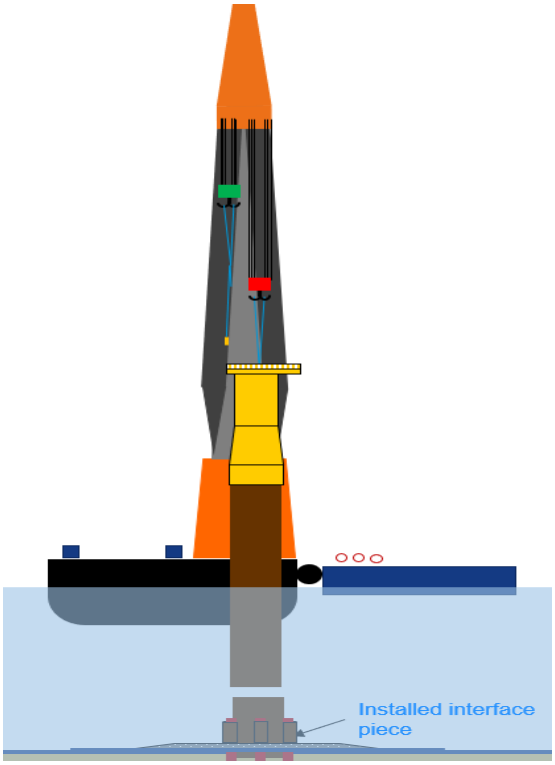

Figure 5.8: Case 1: Installation HMP including TP

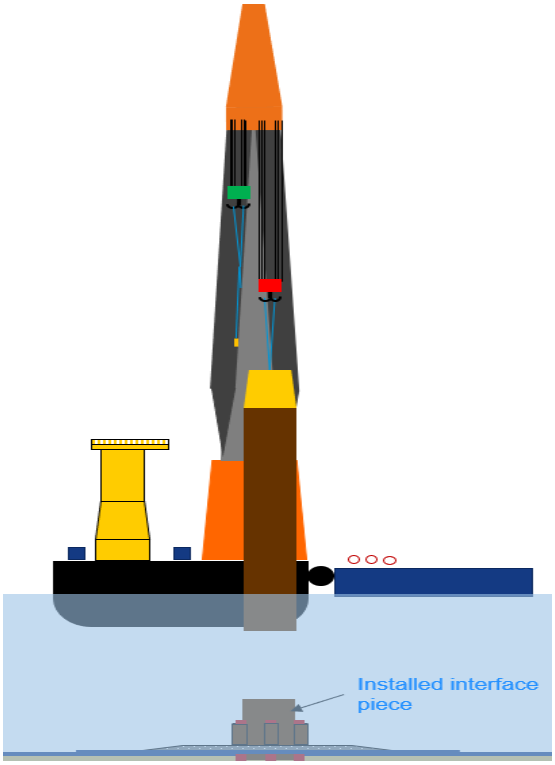

Figure 5.9: Case 2: installation HMP without TP

Strategy 3

Installation of the Hybrid Monopile prior to the installation of the pin piles

The third method involves installing the entire Hybrid Monopile before the pin piles. Hybrid monopiles are delivered by barges, and the installation vessel lifts and positions the Hybrid Monopile into the water. The interface piece is assembled onshore at the yard, along with the transition piece if possible. The Hybrid Monopile is then positioned on the subsurface and placed into a gripper to keep it vertically stable. The crane can then hammer the pin piles into the soil. This method simplifies the positioning of the monopile, as it does not need to fit over pre-installed pin piles. However, the interface piece must meet advanced requirements to prevent damage during installation of the pin piles.

The downside of this strategy is that installing the pin piles can be challenging, especially if the interface pieces are large. If the vessel is positioned above the interface piece, multiple pin piles cannot be installed simultaneously. This requires the use of multiple installation vessels or repositioning of the installation vessel to complete the installation of the remaining pin piles, which is time-consuming. Besides, this entire installation cycle should be conducted in once, therefore a relative long weather window is required for the installation of the Hybrid Monopile and pin piles.

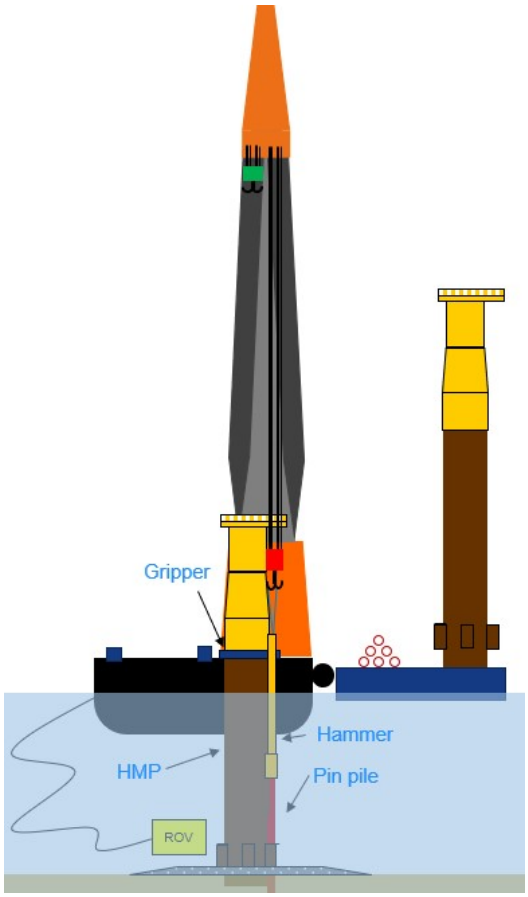

Figure 5.10: Installation of the HMP prior to the installation of the pin piles

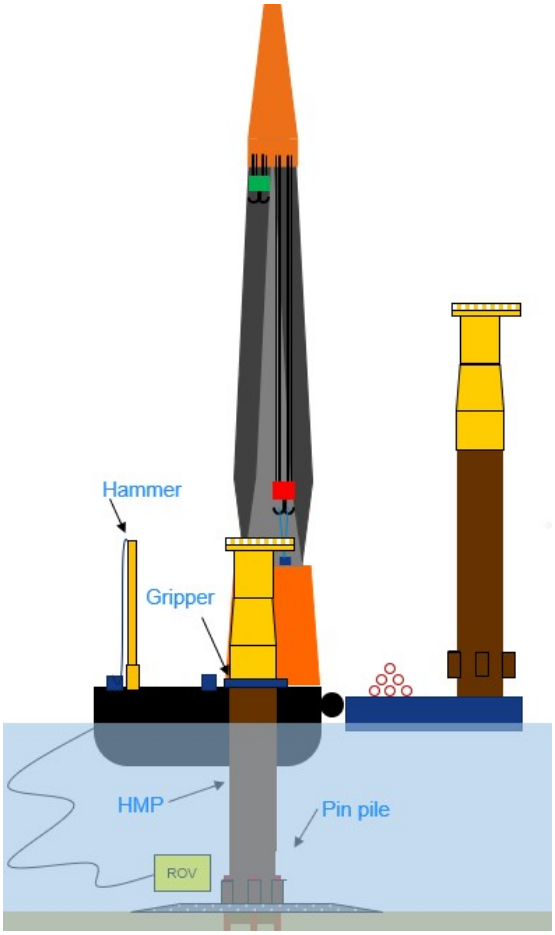

Figure 5.11: Case 2: installation HMP without TP

5.2.2. Levelling

For the levelling of the Hybrid Monopile, four different levelling methods are identified and considered interesting during the installation of the Hybrid Monopile. The methods are outlined below including the advantages and disadvantage of the method:

1. Levelling tool

The the first method involves employing a levelling tool invented by OilStates, an instrument utilized by the industry for the accurate alignment of jacket structures onto pre-installed pin piles. This method is mainly supported by the swaging connection technique, which will be elaborated on later in this chapter.

Following the positioning of the Hybrid Monopile, the levelling tool is positioned atop of the sleeves, which are equipped with a Lotch ring. The levelling tool secures itself onto the sleeves, using the built-in centralizers for alignment. Once horizontally aligned atop the pin piles,The leveling tool can adjust itself vertically because it is clamped in the sleeves and can leverage against the pin pile, which is vertically anchored in the subsurface [71]. Once the Hybrid Monopile is levelled according to this procedure, the connection process can proceed to assemble the Hybrid Monopile to the pin piles.
The advantages of the levelling tool is that the levelling of the Hybrid Monopile can be executed at the location and the technology is proven since it is already used multiple times by the oil and gas industry.
The disadvantages of the levelling tool is that offshore operation and hydraulic power is required.

Figure 5.12: Levelling tool [72]

2. Levelling by crane

The second method to level the Hybrid Monopile, is to use the crane of the vessel. The cabels of the crane are attached to the upper side of the Hybrid Monopile and level the Hybrid Monopile to its right position. This approach offers the benefit of having connections situated above the sea level, making them relatively simple to observe and secure. However, a difficulty from the vessel's motion caused by environmental factors, requiring dynamic compensation to properly align the Hybrid Monopile. Additionally, multiple lift points must be installed atop the Hybrid Monopile to prevent major disturbances.

3. Shims

The third levelling option is to add shims in the sleeves of the interface piece. This method is not applicable for the installation methods where the interface piece is used as a template to install the pin piles. The shims are installed prior to the installation of the Hybrid Monopile. The installation of the pin piles are measured after installation. Based on the elevation of the pin piles, a plan is made to determine at what height the shims are installed in the sleeves. The assembling of the shims is executed in the yard.

The advantages of shims is that the preparation can be done onshore and no offshore tool is required for the levelling of the Hybrid Monopile. The disadvantage is that it is difficult to adjust the positioning offshore.

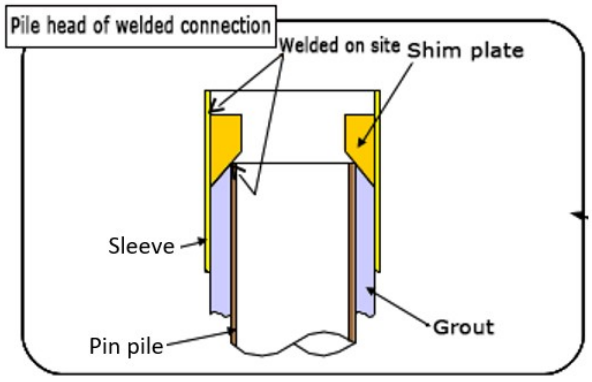

Figure 5.13: Shims welded inside the sleeve of the Hybrid Monopile [73]

4. Gripper

After positioning the Hybrid Monopile on top of the pin piles, the gripper is used to center the Hybrid Monopile horizontally and vertically.

The advantage of the gripper is that the Hybrid Monopile can be levelled on the site. The disadvantage is that the gripper requires a significant amount of space on the installation vessel and it is an external tool.

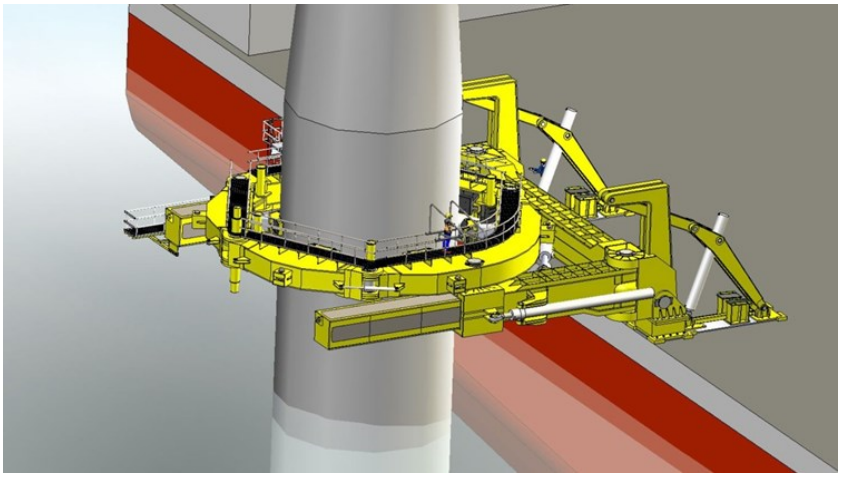

Figure 5.14: Gripper tool attached to a vessel [74]

5. Hydraulic gripper

The hydraulic gripper is a ring which can be installed on top of the sleeves of the Hybrid Monopile. After lifting and positioning of the Hybrid Monopile, the hydraulic grippers clamps around the pin pile. The hydraulic gripper allows for live levelling during offshore operation.

The advantages of the hydraulic gripper is that it can be assembled on the sleeve onshore in the yard, it allows for live levelling during offshore operation and it is proven technology.

The disadvantage is that the hydraulic gripper can only be used once, which makes the use quite expensive since multiple pin piles are installed per Hybrid Monopile. Besides, multiple tools are required, for example a ROV needs to be used to monitor and check whether the operation is going correctly.

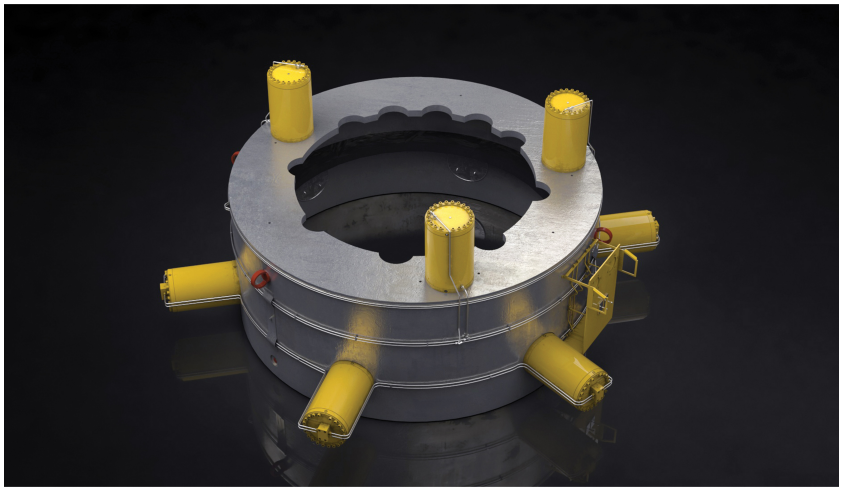

Figure 5.15: Hydraulic grippers [75]

5.2.3. Connection methods

The connection method are responsible for the assembling of the interface piece to the pin piles, and in some cases, for the assembling of the monopile into the interface piece. Multiple potential connection methods are identified for the assembling, they are outlined below:

1. Grouting

The most common method for assembling connections involves the use of grout, a fluid-like material similar to cement. Grouting typically consists of a mixture of cement and water and is primarily used to fill gaps and spaces to enhance load-bearing capacity [76]. Once the entire Hybrid Monopile is positioned or assembled into the interface piece, grout hoses are installed. The grout is then injected into the connection to fill the gaps and create a stable connection. It is assumed that the Hybrid Monopile remains stable during the grouting process due to its geometry, which typically lasts around 12 hours. Although the grout achieves its final strength after approximately 28 days.
One advantage of grouting is its widespread use in the industry. However, it requires considerable equipment for grout injection and is relatively expensive. Additionally, the waiting time for successful hardening can be a significant operational bottleneck, often requires a long period of mild weather conditions for optimal curing.

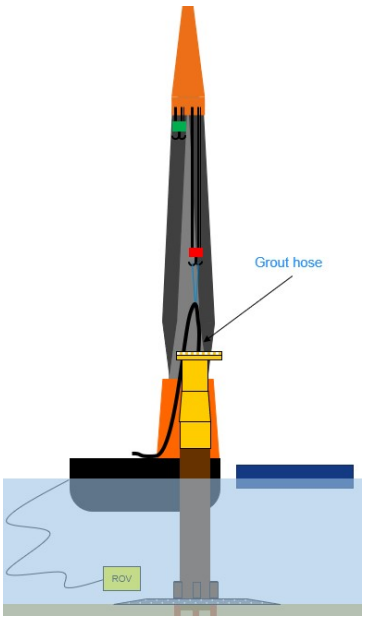

Figure 5.16: Grouting of the connections, adapted from [7]

2. Swaging

Swaging is a connection method that involves the plastic deformation of steel material. It can be employed alongside a levelling tool in the assembly process of Hybrid Monopile. First, the levelling tool ensures the Hybrid Monopile is leveled. Once horizontally and vertically aligned, the swaging tool is inserted into the pin pile. As pressure increases inside the tool, it causes the material of the pin pile to deform. This deformed material is pushed into pre-fabricated rings within the sleeves until the pin pile material is completely plastically deformed into the rings. This process fixes the connection, which can then be repeated for subsequent connections. One advantage of the swaging method is its relatively fast operation compared to grouting. However, each swaging tool can typically be used around 50 times before requiring maintenance. Additionally, it is an expensive tool to use, especially when multiple connections between pin piles and sleeves are needed simultaneously.

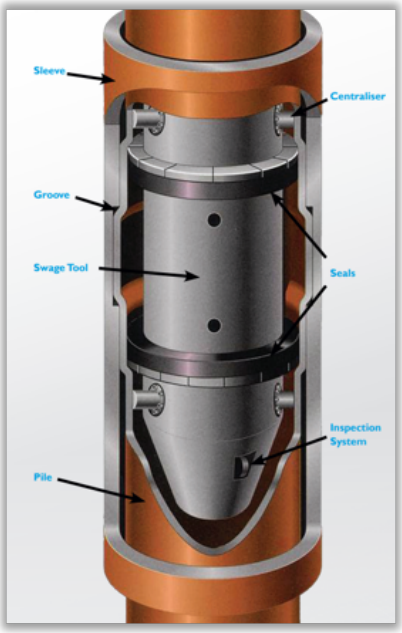

Figure 5.17: Illustration of the swaging tool [72]

5.2.4. Installation strategy selection

Based on the installation strategies for pin piles and Hybrid Monopile, as well as the leveling and connection methods, the preferred installation cycle for the Hybrid Monopile has been established.

The first decision involves choosing the installation strategy for the pin piles and the Hybrid Monopile itself. Strategy 1 is preferred for several reasons. It requires only one installation template, eliminating the need for every interface piece to be equipped with advanced tools, which significantly reduces costs. Additionally, Strategy 1 can be divided into different installation cycles, offering flexibility that minimizes the risk of major delays due to unpredicted circumstances. For instance, pin piles can be installed during the day when noise restrictions are not in effect, while the Hybrid Monopile can be installed at night. This approach also requires a smaller weather window, which is advantageous for the installation process.

In contrast, Strategy 2 requires two connections of the structural components, which increases time and costs. Furthermore, equipping interface pieces with advanced tools is assumed to be more expensive than lifting the piling template from the subsurface and moving it to the next location.

Strategy 3 is deemed unfeasible due to its requirement for a significantly longer weather window. Additionally, installing pin piles while holding the Hybrid Monopile in place is impractical. The vessel would need to be repositioned or supported by another installation vessel, substantially increasing time and costs.

For leveling, shims are assumed to be the best tool. Shims are a common, cost-effective industry technique that can be installed onshore, making them cheaper than offshore leveling. Offshore leveling tools are considered to be too expensive, especially since six pin piles are installed per Hybrid Monopile.

Grouting is identified as the best connection method. It is well-established in the offshore industry. Although it requires time to harden, it remains more practical than swaging. Swaging, while interesting, can only be used 50 times before maintenance is needed. Given that each Hybrid Monopile uses six pin piles, this limits the installation to only eight foundations before requiring an interruption for tool maintenance.

An additional component in the installation cycle is the implementation of noise mitigation measures.

For installing the pin piles, two different hammers can be used. Driving the pin piles into the subsurface requires noise mitigation, for which a bubble curtain is considered sufficient.

In summary, Strategy 1, using shims for leveling and grouting for connection, is the most efficient and cost-effective approach for the installation of the Hybrid Monopiles. Table 5.1 represents a overview of the installation times for the entire cycle of the Hybrid Monopile. The elaborate overview of all installation events are represented in Table 5.1.

Table 5.1: Installation times for the hybrid monopile including vessel type

Phase:	Events	Time indication (SSCV)	Time indication (OSV)
0	Installation bubble curtain	-	12 h
1	Pin piles installation	74 h	
2	Lifting and positioning HMP	7.5 h	
3/4	Grouting	-	21 h

5.3. Traditional monopile

The installation of traditional monopiles is a straightforward and well-known process in the industry. This subsection provides a brief summary of the transportation and installation of monopiles.

SSCVs are supplied by barges. The monopile is upended from a horizontal to a vertical position using cranes aboard the installation vessel, or an upend frame. Once vertical, the monopile is carefully lowered to the seabed at the location. Figure 5.18 and Figure 5.19 represents respectively the transportation and installation of the monopile.

Figure 5.18: Transportation of monopiles on a barge [77]

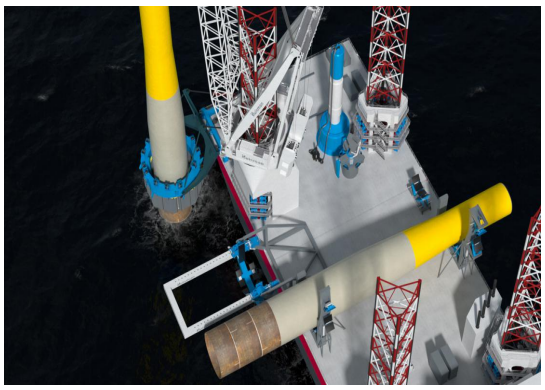

Figure 5.19: Installation equipment monopile [78]

With the monopile in position, the installation vessel uses a hydraulic gripper or temporary frame to hold it vertically stable. A hydraulic hammer then drives the monopile into the seabed, delivering powerful blows to the top of the monopile until the desired depth is reached. The process is closely monitored using sensors and GPS technology to ensure the correct depth and alignment. When using a hydraulic hammer, noise mitigation measures are required.

Once the monopile is driven into place, the transition piece is lifted and secured onto the top of the monopile. To ensure a robust connection, grout is often used to fill the annular space between the monopile and the transition piece. In some cases the transitions piece is already part of the monopile, avoiding the extra installation of the transition piece including grouting

Table 5.2 represents the installation cycle for a monopile. The phases are a total summary of the.

Table 5.2: Installation cycle of the monopile including vessel type

Phase:	Events	Time indication (SSCV)	Time indication (OSV)
0	Installation bubble curtain	-	24 h
1	Preparing, upending and installing monopile	12.5 h	

5.4. Jacket structure

Installing jacket structures is a well-established process in the industry, involving both transportation and installation phases. Typically, jackets are transported via barges, although fewer can be transported in once compared to monopiles due to their larger size.

There are two primary methods for jacket installation. The first method involves placing the jacket on the seabed and driving pin piles through its legs to secure it. Alternatively, a strategy comparable to the Hybrid Monopile installation involves pre-installing pin piles using a template before positioning the jacket. Installation of pin piles can utilize hydraulic or vibrohammers, with noise mitigation measures like a bubble curtain required depending on the hammer type used. Figure 5.20 and Figure 5.21 shows the transport and installation of the jacket structure.

Figure 5.20: Transportation of jacket structures on a barge [79]

Figure 5.21: Installing a jacket [80]

If feasible based on weight considerations, jackets can be lowered into the water with the transition piece already assembled onshore, which saves an extra lifting and installation action offshore.

Following pin pile installation, gaps between the pin piles and sleeves are filled with grout to ensure a solid connection. Similar to the Hybrid Monopile, the installation of jacket structures can be phased to provide flexibility in the installation process.

Table 5.3 shows the installation time of the entire cycle of the installation of the jacket structure.

Table 5.3: Installation time of the jacket structure

Phase:	Events	Time indication (SSCV)	Time indication (OSV)
0	Installation bubble curtain	-	12 h
1	Pin piles installation	52 h	
2	Jacket installation	7.5 h	
3/4	Grouting	-	21 h

6

Economic Evaluation

This chapter presents the economic evaluation of the Hybrid Monopile, traditional monopile, and jacket struture. The evaluation is based on manufacturing costs, which depend on structural design and labor intensity, as well as installation costs, which are influenced by vessel use and equipment. At the beginning of the chapter, an overview and assumptions are listed. Subsequently, the costs of the foundations are plotted. Finally, a sensitivity analysis is conducted to examine how certain parameter adjustments affect the results.

6.1. Overview and assumptions

To determine the costs associated with manufacturing and installation, certain assumptions are made due to scope limitations. The costs considered in this research are sourced from publicly available resources [81], [82].

- The cost of manufacturing the interface piece is considered to be 80% of the cost of a jacket per metric ton (mT). This assumption is based on the simpler design of the interface piece, making it easier to construct.
- Manufacturing costs include both the cost of steel and the labor required to construct the foundations.
- Installation costs are based on the installation cycle that an installation vessel needs to conduct.
- Potential yard and transport costs are not included in this analysis, as the study is not restricted to a specific location.

6.2. Manufacturing

The manufacturing of the Hybrid Monopile, traditional monopile and jacket structure consist of two different parameters: the steel price and the labor price to manufacture the structure.

The following prices regarding the manufacturing of the pin piles, monopile, jacket and interface piece are listed in Table 6.1. The prices are taken from a cost overview from the University of Strathclyde [81]. The costs originates from 2013, therefore the average Dutch inflation rate over the last 10 years is considered to update the costs to a more reliable nowadays estimation. This inflation rate is assumed to be 2.54% per year [83]. The costs includes the steel and labour price to produce the structure.

Table 6.1: Manufacturing costs various wind turbines

	Costs [€/mT]
Monopile	€ 2164
Jacket	€ 4551
Pin pile	€ 1525
Interface piece	€ 3551

The interface piece is a structure for which no cost data is currently available. By comparing its design to that of a jacket structure, it is assumed that the interface piece is relatively cheaper to produce. This is due to its lower overall height and simpler welds, which require less labor. Therefore, the cost of manufacturing the interface piece is assumed to be one thousand euros less per metric ton compared to a jacket.

Figure 6.1 till Figure 6.5 gives the manufacturing costs of the Hybrid Monopile, traditional monopile and jacket structure. The costs are based on the weight of the structures resulting from the chapter 4 and the costs for manufacturing the structures, depicted in Table 6.1.

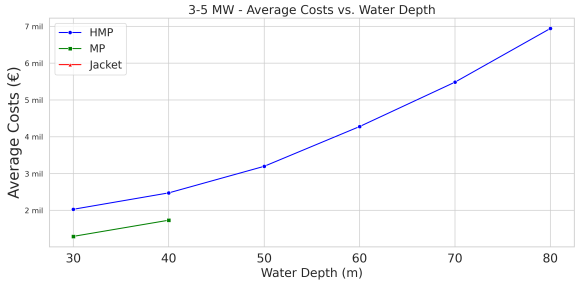

Figure 6.1: WTG Range 3-5 MW

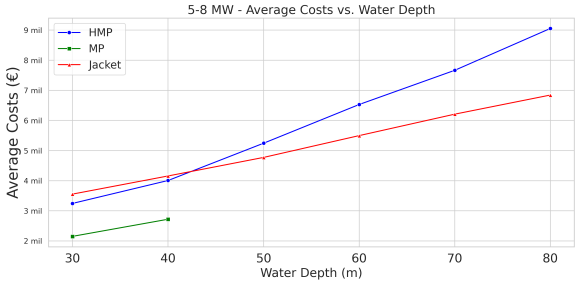

Figure 6.2: WTG Range 5-8 MW

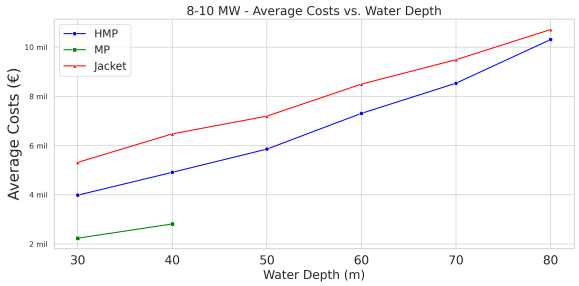

Figure 6.3: WTG Range 8-10 MW

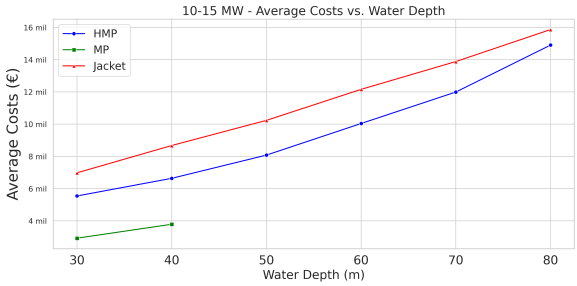

Figure 6.4: WTG Range 10-15 MW

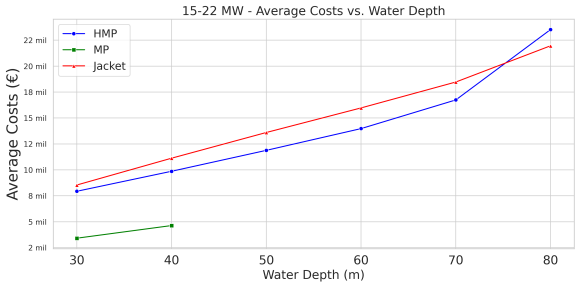

Figure 6.5: WTG Range 15-22 MW

Figure 6.6: Manufacturing Costs vs. Depth for Different WTG Ranges

This analysis reveals that manufacturing of monopiles is significantly cheaper across all scenarios, for

every wind turbine type, compared to both jacket structures and Hybrid Monopiles. The assumption that monopiles can be used in water depths up to 50 meters consistently makes them at least the most cost-effective option for water depths until 40 meter. Until 50 meter of water depth is in this research not assessed due to missing information regarding project specific noise measurements after 40 meter water depth.

For jackets, it's notable that no data is available for wind turbines in the 3-5 megawatt range. For the 5-8 megawatt range, the cost of jackets appears relatively linear when compared to hybrid monopiles. This linearity arises because the increase in size for jackets follows a linear trend, whereas the increase in size for hybrid monopiles, pin piles, and especially the interface piece, does not. For the 5-8 megawatt range, jacket structures are invariably cheaper than hybrid monopiles.

In the 8-10 megawatt and 10-15 megawatt ranges, hybrid monopiles are cheaper than jackets up to water depths of approximately 65 meters and 74 meters, respectively. Beyond these depths, jacket structures become the more cost-effective option.

For the very large turbines in the 15-22 megawatt range, the costs of hybrid monopiles and jacket structures are comparable up to a water depth of about 70 meters. Beyond this depth, the size and cost of the interface piece for hybrid monopiles increase significantly due to the higher forces, making jackets the cheaper option.

Figure 6.7 and Figure 6.8 show the cost ratios per structural component for the Hybrid Monopile.

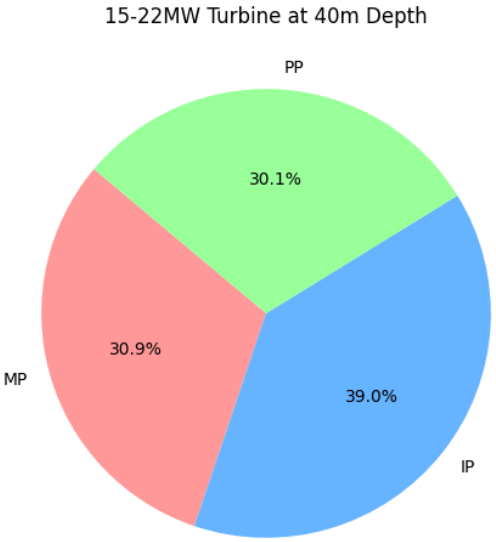

Figure 6.7: Costs ratio per structural component

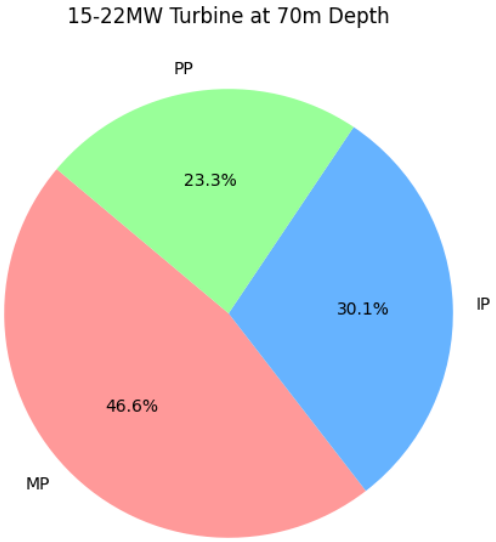

Figure 6.8: Costs ratio per structural component

At a water depth of 40 meters, the interface piece is the largest cost contributor, despite consisting only about 20% of the total weight of the structure. It accounts for approximately 40% of the total costs. For water depths of 70 meters, the contribution of the interface piece decreases to 30%, but it remains 10% higher than its weight contribution.

It is also noteworthy that the cost share of the pin piles ranges from 23-30%, while their weight contribution is around 50%, indicating significantly lower costs relative to their weight. Conversely, for larger structures, the monopile component is the largest cost contributor, reflecting its substantial impact on the overall costs for these deeper and larger installations.

6.3. Installation

The installation costs for hybrid monopiles, traditional monopiles, and jacket structures consist of two main components: the vessel dayrate, which covers the operation of the vessel including crew and fuel

costs, and the costs for the required equipment for the operation. The data required to determine these installation costs come from the structural analysis and the installation assessment.

Based on the results of the structural analysis, it can be determined whether the foundation can be installed based on the weight and dimensions of the structure. If a structure becomes too heavy for the assumed smaller installation vessel, a heavier vessel is required, leading to a higher rate for the installation of this type of foundation in certain water depths.

The installation assessment determines how long it takes for a specific type of vessel to complete an operation. The installation process is subdivided into different phases to ensure that large vessels are not used for installing smaller and lighter pin piles. For each phase, a certain type of vessel is determined, and the total time (in hours) needed to install these structural components is calculated. Table 6.2 represents the costs considered in this research. These costs come from a cost analysis by Strathclyde University [81], which is considered reliable since they were established in collaboration with the industry. However, these costs were established in 2013. To adjust these values to current levels, the average Dutch inflation rate of 2.54% over the past 10 years has been taken into account [83].

Table 6.2: Costs in dayrates for the different types of vessels

	Operating range [mT]	Costs [€/day]
OSV	-	€ 38,793
HLV (small)	0 - 3000	€ 239,111
HLV (medium)	3000 - 5000	€ 458,569
HLV (large)	5000 <	€ 694,709

The vessels are subdivided into three sizes: small vessels with lift capacities up to 3000 mT (e.g., Bokalift and Alfa Lift), medium vessels with lift capacities up to 5000 mT (e.g., Orion, Green Jade, Aegir, and Les Alizes), and large vessels with lift capacities above 5000 mT (e.g. Saipem, Thialf, and Sleipnir).

In addition to the use of vessels, suitable equipment is required for the installation of hybrid monopiles, traditional monopiles, and jacket structures. For example, the placement of a bubble curtain requires both an offshore support vessel and the equipment itself. The installation of pin piles and monopiles requires a hydraulic hammer, and for monopile lifting and stabilization, equipment is needed to hammer the pile vertically. Table 6.3 represents the costs of the equipment. These costs come from sources from Strathclyde University [81] and BVG Associates[82].

It should be noted that the costs are based on the average prices from different equipment suppliers. The price of the equipment is therefore vulnerable to market supply and demand fluctuations, especially for hydraulic hammers. Consequently, the prices can vary significantly. Figure 6.9 to Figure 6.13 illustrate the total installation costs for the Hybrid Monopile, traditional monopile, and jacket structure based on the assumed costs.

Table 6.3: Day rates of installation equipment

	Costs [€/day]
Bubble curtain	€ 29,637
Pile gripper	€ 11,855
Upending equipment	€ 11,855
Hydraulic hammer	€ 59,275

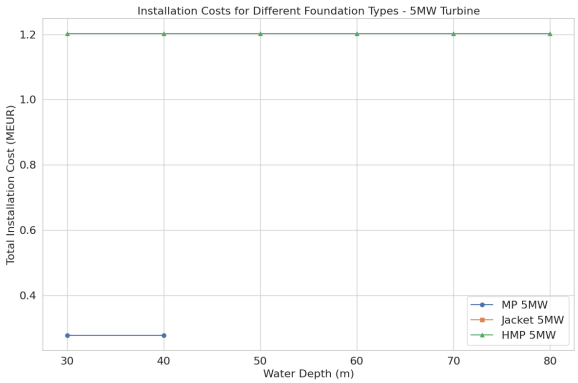

Figure 6.9: 5 MW Installation Costs

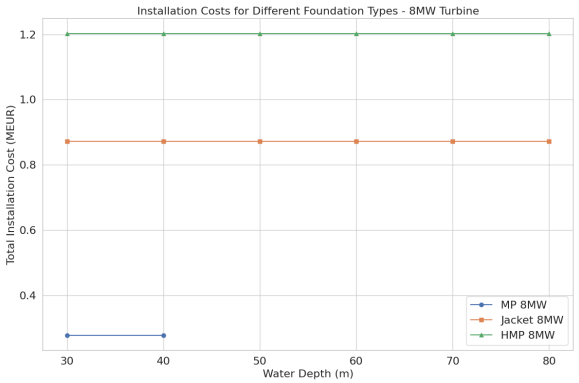

Figure 6.10: 8 MW Installation Costs

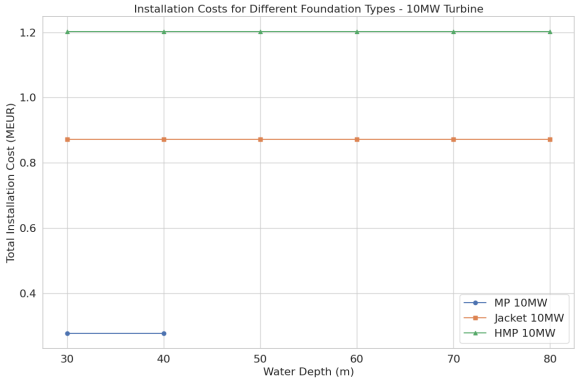

Figure 6.11: 10 MW Installation Costs

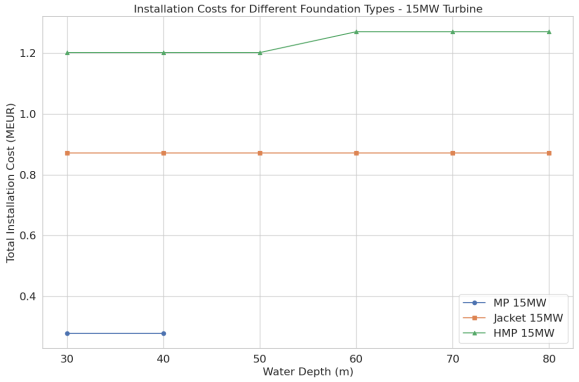

Figure 6.12: 15 MW Installation Costs

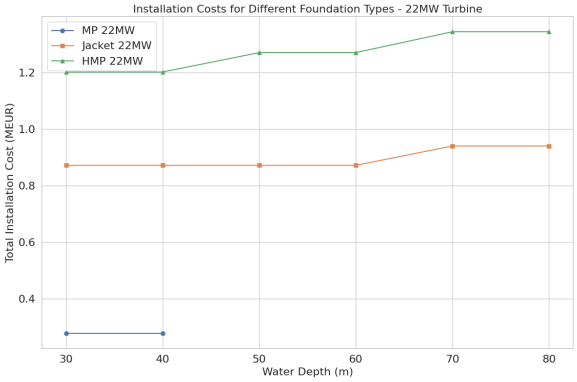

Figure 6.13: 22 MW Installation Costs

It can be observed that the installation costs generally follow a linear trend. This is because the costs of equipment and vessels remain constant within a certain range, regardless of the structure size. Structures below 3000 mT have similar installation costs since the same vessels are used for their installation. However, when a structure's components exceed 3000 mT (or 5000 mT), a larger vessel is required, leading to an increase in installation costs as shown in the plots. For traditional monopiles, the vessels used are consistent across different foundation types, irrespective of the wind turbine size installed. For hybrid monopiles and jacket structures, there are points where the costs increase due to deeper water depths and thus larger structures.

The reason the installation costs for monopiles are significantly lower is due to shorter installation

times. While the installation of the superstructure is faster for hybrid monopiles and jacket structures, the overall installation cycle for all pin piles results in a much longer installation time for the vessel itself.

6.4. Total costs comparison

In the last paragraph, the total costs including a 10% uncertainty margin is added over the total costs of the Hybrid Monopile, traditional monopile and jacket structure. The total costs consist of a sum of the manufacturing and installation costs.

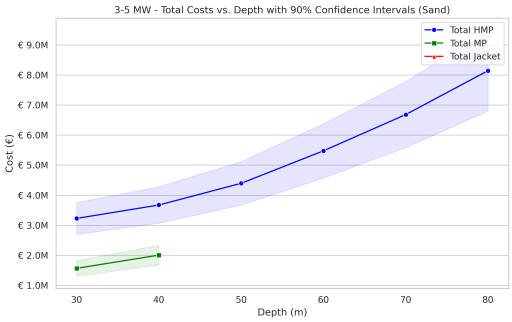

Figure 6.14: 3-5 MW Total Costs vs. Depth with CI (Sand)

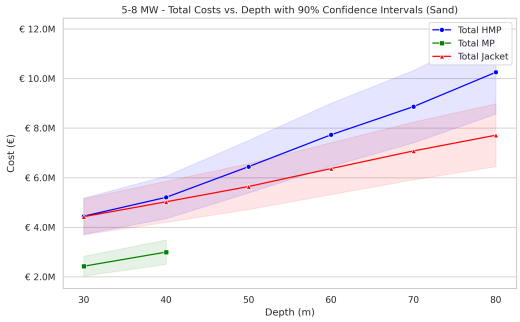

Figure 6.15: 5-8 MW Total Costs vs. Depth with CI (Sand)

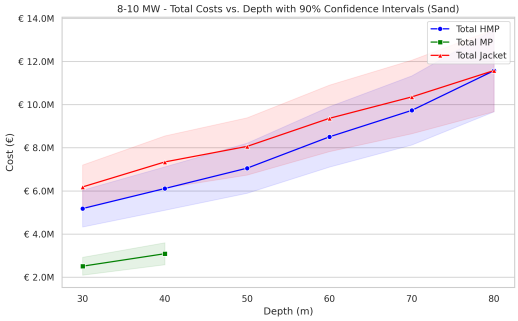

Figure 6.16: 8-10 MW Total Costs vs. Depth with CI (Sand)

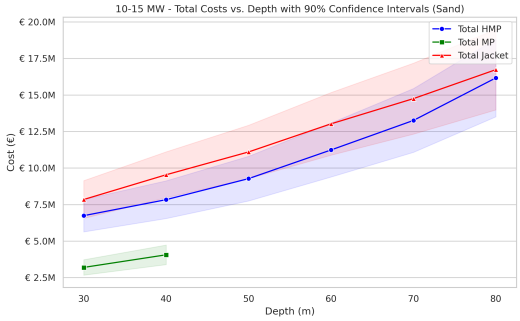

Figure 6.17: 10-15 MW Total Costs vs. Depth with CI (Sand)

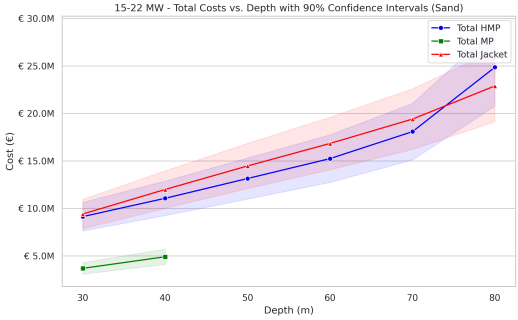

Figure 6.18: 15-22 MW Total Costs vs. Depth with CI (Sand)

The first important point to notice is that the traditional monopile, where feasible, is consistently the cheaper option. This is due to several factors. Firstly, the manufacturing of monopiles is relatively straightforward and cost-effective. When considering installation costs, the entire monopile can be installed much faster compared to jacket structures and hybrid monopiles. This is because the installation of jacket structures and hybrid monopiles requires driving pin piles into the subsurface, which is a time-consuming activity. The time required to install pin piles is almost equivalent to that needed to install a monopile itself. Therefore, the overall installation cost is significantly lower for monopiles. While lifting and installing the jacket and Hybrid Monopile onto the pin piles can be done more quickly than

installing a monopile, the extended preparation time for pin piles makes monopiles more cost-efficient.

When comparing hybrid monopiles to jacket structures, it becomes evident that jackets are more cost-effective for 5-8 MW turbines. This is due to two primary reasons. First, the manufacturing cost of jackets does not significantly increase with weight, as the weight-related cost trend is relatively flat. Additionally, the weight of the Hybrid Monopile components does not increase linearly. Furthermore, the assumed use of six pin piles can be a cost drawback, as the lighter design might not require such a number of pin piles. This assumption increases both manufacturing and installation costs.

For 8-10 MW and 10-15 MW turbines, the Hybrid Monopile becomes more cost-competitive compared to the jacket structure. Despite the relatively higher design costs of hybrid monopiles in shallower waters, jacket structures remain more expensive. The trend lines for the weights of jackets become steeper for larger wind turbines, although they remain linear. In contrast, the increase in weight for pin piles, interface pieces, and monopiles is not linear and becomes more pronounced in deeper waters, up to 80 meters. A similar trend is observed for 15-22 MW wind turbines. However, due to a significant weight increase for 15-22 MW turbines in 80-meter water depth, hybrid monopiles are only feasible up to around 70 meters.

The trends in clay are relatively similar to those in sand. However, in clay, the structure of the Hybrid Monopile becomes slightly heavier due to the lower bearing capacity of the soil compared to sand. This difference impacts the total costs for certain turbine capacities. Specifically, in the 8-10 MW and 10-15 MW situations, the total costs show a slight difference where the Hybrid Monopile is more cost-effective than the jacket structure. However, for the 15-22 MW situation, the Hybrid Monopile becomes more expensive compared to the jacket structure. The cost graphs for clay are detailed in Appendix D.

6.5. Sensitivity analysis

Given the vulnerability of costs to price fluctuations due to uncertainty in the manufacturing process of the interface piece, an analysis is conducted to assess the impact on the costs of the three foundation types considered. The cost of the interface piece, the most uncertain parameter, is initially assumed to be around 80% of the jacket structure cost due to its geometry. This analysis explores the scenario where the interface piece costs increase, potentially equaling or exceeding the costs of the jacket per metric ton (mT). The goal is to determine whether the total cost comparison remains consistent or if this change results in the Hybrid Monopile no longer being cost-effective in scenarios where it previously was. The focus of this analysis is primarily on larger wind turbines, as they are more likely to be installed in the future.

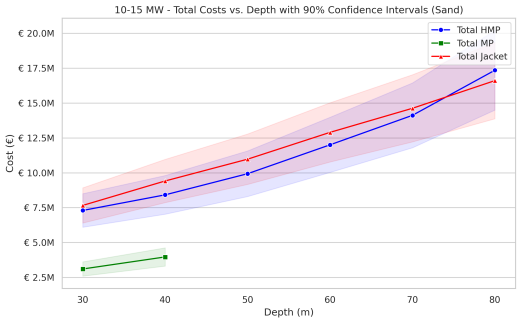

Figure 6.19: 8-10 MW Total Costs vs. Depth with CI for higher interface piece costs

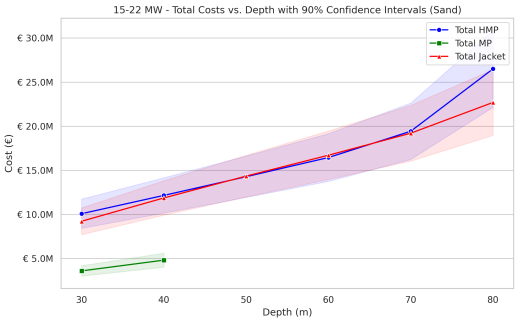

Figure 6.20: 15-22 MW Total Costs vs. Depth with CI for higher interface piece costs

Figure 6.19 illustrate the total costs when the interface piece are similar to the jacket regarding manufacturing costs. The design remains quite cost-effective up to approximately 75 meters of water depth. Figure 6.20 shows the total expenses for the 15-22 MW wind turbine. The total expenses are nearly equal when the manufacturing costs of the interface piece are relatively similar, but beyond 75 meters of water depth, the Hybrid Monopile becomes significantly more expensive.

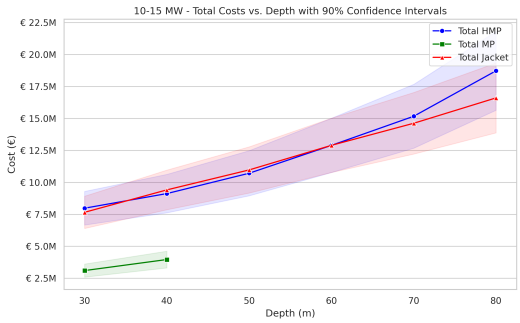

Figure 6.21: 10-15 MW Total Cost vs. Depth with CI for higher interface piece costs

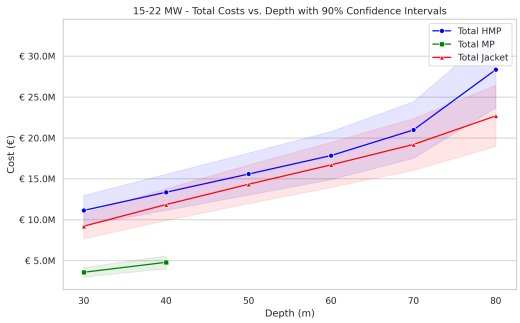

Figure 6.22: 15-22 MW Total Costs vs. Depth with CI for higher interface piece costs

Figure 6.21 and Figure 6.22 show the costs for the 10-15 MW and 15-22 MW configurations if the manufacturing costs of the interface increase by 1000 euros (21%) per metric ton. For the 10-15 MW range, the cost-effectiveness of the Hybrid Monopile decreases significantly, with costs being equal until around 60 meters of water depth and higher beyond that point, making it less effective than the jacket structure from 60 meters onward. For the 15-22 MW range, the costs for the Hybrid Monopile are higher in all scenarios. Therefore, if the manufacturing costs increase by 20%, the Hybrid Monopile's cost-effectiveness becomes negative in these cases.

It's important to note that installation costs cannot be directly compared here since reducing the number of pin piles may also influences the design dimensions, making such a comparison not viable.

The sensitivity of various parameters is evaluated to determine their impact on the total costs when certain costs increase by 10% or when no noise mitigation is required. Figure 6.23 and Figure 6.24 illustrate the increase in total costs due to changes in specific parameters.

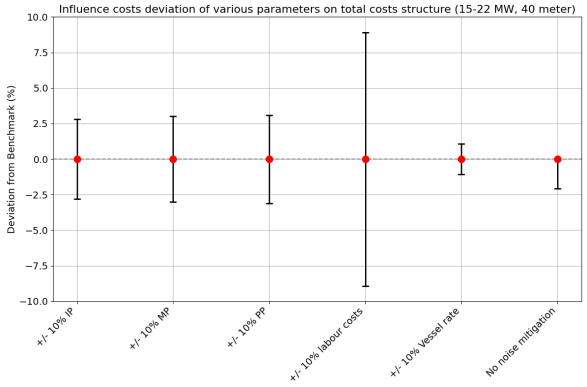

Figure 6.23: Influence of various parameters on total costs for 15-22 MW wind turbines at 40 meters water depth

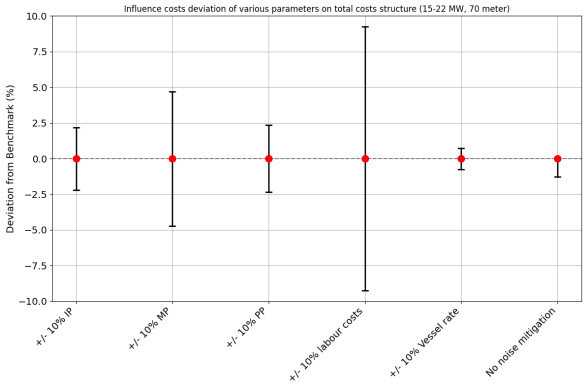

Figure 6.24: Influence of various parameters on total costs for 15-22 MW wind turbines at 70 meters water depth

From the figures, it is evident that in deeper waters, the contribution of the monopile part of the Hybrid Monopile becomes significantly larger. This is due to the exponential increase in the size of the monopile, as the diameter of the monopile is squared in the Morison equation. Additionally, it can be observed that the contribution of noise mitigation for the Hybrid Monopile is around 2-3%, based on the assumed costs for noise mitigation measures. If the costs for noise mitigation equipment increase, their contribution to the total costs will also become significantly larger. From these sensitivity plots it can be observed that improvements in design significantly contributes more to the total costs compared to the vessel rate. A 10% in manufacturing costs contributes more than a 10% increase in installation time.

7

Discussion and conclusion

This chapter includes the discussion, conclusions, and future recommendations. The discussion presents the interpretations, meanings, and limitations on the results obtained in this thesis. Following this, conclusions are provided on each subquestion, leading to the answer to the main question. Finally, opportunities and recommendations for future research are outlined.

7.1. Discussion

7.1.1. Structural analysis

The first part of the discussion addresses the limitations and interpretations of the methodology used for - and results obtained by the structural analysis of the Hybrid Monopile. One significant limitation concerns the forces acting on the Hybrid Monopile.

The initial limitation is the use of linear wave theory. This approach is used for convenience due to scope limitations but provides a reliable indication of the hydrodynamic loading that acts on the Hybrid Monopile. However, relying on linear wave theory can neglect the nonlinear effects of the waves, potentially underestimating wave steepness and wave height. Additionally, the wave velocity and acceleration might be underestimated, leading to larger wave forces than those accounted for. Using a linear wave theory does not yield results as accurate a using a higher order-wave theory

The forces on the structure are considered as quasi-static loading, resulting from hydrodynamic- and wind forces under worst-case scenarios. These forces are determined based on a 50-year return period, which exceeds the typical design life of an average offshore structure. However, quasi-static loading does not account for potential resonance of the Hybrid Monopile due to dynamic effects of the hydrodynamic loading. To incorporate dynamic effects, a dynamic amplification factor is calculated to account for the higher resulting displacements and stresses that could occur under dynamic loading, which is common in offshore situations. Nevertheless, using a dynamic amplification factor does not yield results as accurate as a full dynamic analysis would.

In this study, a single degree of freedom (SDOF) system is assumed to calculate and provide a preliminary estimate of dynamic amplification for the Hybrid Monopile in an offshore environment. However, the Hybrid Monopile is a complex offshore structure exposed to substantial dynamic loads from waves and wind. Given their complexity, a multiple degree of freedom (MDOF) approach is generally more accurate. Complex structures often exhibit multiple significant modes of vibration, stress propagation and failure modes, and the interactions between these modes can significantly influence dynamic responses. While an SDOF model offers a basic estimation, an MDOF model provides a more reliable and comprehensive results of the dynamic amplification, offering deeper insights into resultant forces and displacements.

Certain parameters are kept constant throughout the structural design research of the Hybrid Monopile, such as the number of pin piles and the height of the interface piece. It should be noted that the choice of six pin piles may not always be optimal. This quantity was selected for the feasibility study of the

Hybrid Monopile design. In scenarios where smaller wind turbines are installed in relatively shallow waters, fewer pin piles might be more advantageous. Conversely, situations involving larger wind turbines in deeper waters might benefit from more than six pin piles. Adjusting the number of pin piles has the potential to optimize the overall design of the Hybrid Monopile. However, for the purposes of the feasibility study, six pin piles are considered representative.

In addition to the pin piles considered in this study, the pile group factor is determined based on research conducted by various researchers as described in chapter 2. However, none of these studies mimics the conditions specific to the Hybrid Monopile. The assumed values for the axial and lateral pile-group factor are chosen according to the situations most resembling the situation for the pin piles of the Hybrid Monopile. However uncertainties arise concerning the precise pile-group factor.

This study primarily focused on the feasibility of implementing the Hybrid Monopile in the North Sea. To assess whether this concept could be feasible in other global regions, two critical factors must be considered: wave characteristics and soil conditions. If a region exhibits wave heights and periods similar to those studied, the Hybrid Monopile might be applicable there; however, if the maximum wave heights exceed those considered, the resulting forces would increase the structure's dimensions, weight, and costs. Additionally, a longer wave period than in the North Sea would generally be less problematic, as it would reduce the likelihood of resonance with the structure's natural frequency. Conversely, a significantly shorter wave period could lead to resonance issues, increasing the dynamic amplification factor. Soil conditions are also crucial; the Hybrid Monopile is unlikely to be feasible in areas with soft clay, as it would not provide sufficient soil resistance and might collapse. Further assessments are needed to ensure structural integrity in different locations, and additional research is required to address challenges such as floating ice, seismic activity, or rocky soil.

The final design, based on the structural analysis, aims to bring the occurring stresses in the structure as close as possible to the stress threshold. However, the stress analysis of the Hybrid Monopile has revealed several potential design improvements. For instance, it was observed that the upper and lower flanges do not contribute significantly to the stiffness of the structure. Despite these insights, the subsequent results of the study are based on the original design of the Hybrid Monopile, including the structural components identified for potential adaptation in the structural analysis chapter. Consequently, it should be noted that the results obtained for the Hybrid Monopile are not based on a fully optimized structure. In contrast, the monopiles and jacket structures from other projects, which serve as comparisons, are assumed to be optimized. Nevertheless, the design of the Hybrid Monopile is considered representable for technical and economic improvement regarding shape and structure to compare with the existing structure.

7.1.2. Installation assessment

This study primarily focuses on the installation of a single Hybrid Monopile, assuming that the vessel can start operations immediately upon arrival at the installation site.

Various installation strategies for the Hybrid Monopile were established based on qualitative research into the installation methods of different offshore structures. However, no quantitative analysis was conducted to assess the lifting capabilities of specific vessels under various crane angles. Additionally, a big bubble curtain is considered the most effective and commonly used noise mitigation system to reduce noise pollution during the installation of pin piles and monopiles, according to the literature. Nonetheless, certain projects employ location-specific noise mitigation systems that could potentially offer greater noise reduction and more feasible installation processes than assumed in this study. Whenever a (double) bubble curtain is available, it is generally preferable to project-specific measures.

The results indicate that the installation time for the Hybrid Monopile is approximately 30% longer compared to a jacket structure. This is because the assumed time spans for driving pin piles into the subsurface, regardless of size, lead to a longer overall installation time for the Hybrid Monopile, which has six pin piles, compared to the jacket structure, which has four pin piles. It is important to note that the number of pin piles required for the Hybrid Monopile and the jacket structure can significantly affect the installation time per structure.

This study assumes fixed time spans for the installation of pin piles without considering specific project data, which is often not available in open sources. The actual installation time heavily depends on the

penetration depth required for the pin piles and the soil type, which can influence the installation time for Hybrid Monopiles, jacket structures, or traditional monopiles.

Another limitation of this research is the assumption that the transportation and positioning of the Hybrid Monopile on top of the piles will be similar to that of the jacket. This approach does not significantly reduce the time compared to jacket installation. This study qualitatively explained that horizontal transportation of hybrid monopiles is not feasible due to wave slamming on the interface piece, which overhangs the vessel. However, a quantitative determination of the exact limitations based on significant wave height, wave period, and required weather window is needed to check whether this is the case for every location.

Finally, the installation analysis in this study focuses on a single structure, assuming the installation vessel is already on site. Considering factors such as distance to shore, potential need for barges, transferring foundations from barge to installation vessel, or a vessel needing to return to the harbor to get the foundation, these assumptions would increase the installation time per foundation if multiple foundations need to be installed. Nevertheless, analyzing the installation of a single foundation provides a reliable estimation of the installation time per structure, allowing for a comparison of the Hybrid Monopile with the jacket and traditional monopile to evaluate its potential.

7.1.3. Economic evaluation

The economic evaluation in this research primarily focuses on the manufacturing and installation of a single structure.

The manufacturing cost per metric ton for hybrid monopiles, jacket structures, and monopiles is based on public sources and influenced by steel- and labor prices. Jacket structures tend to have higher labor costs due to the extensive welding required. Additional factors affecting manufacturing costs include yard usage fees, available space, and production and storage capacities, which can lead to manufacturing interruption. The largest interface size has a diameter of 26 meters, while jackets installed in water depths of 80 meters have footprints of around 35x35 or 40x40 meters. Consequently, jackets typically need more storage space and a larger piling template. However, location-specific costs, such as those influenced by site-specific conditions around the North Sea, are not considered in this research.

The installation costs are based on the expenses of an installation vessel and its required equipment. The potential costs of a barge for the transportation are not included in this calculation because the installation location is not specified, making these costs difficult to determine reliably. The use of barges and the distance to shore can significantly influence the installation costs per foundation. Therefore, it is important to note that the results of this research cannot be directly applied to any specific situation in or around the North Sea. The cost evaluation provides an overview based on manufacturing and installation costs, regardless of the installation site. To make a direct comparison, the design of the three foundations should be optimized for a specific site, along with considerations for the location and yard exploitation for manufacturing.

Both manufacturing and installation costs are heavily influenced by fluctuations in demand and supply in the offshore energy market. This includes the costs of steel, labor, and day rates for vessels and equipment required for installing the Hybrid Monopile, jacket structure, or traditional monopile. Therefore, these costs have significant uncertainties, and contacting suppliers to verify day rates is recommended to mitigate these uncertainties.

Additionally, the cost of the interface piece is based on the design established in this research. Due to its limited space requirements and limited required welding, it is assumed that the labor hours needed to produce the interface piece are lower compared to the jacket. However, since the interface piece has never been manufactured before, providing an exact manufacturing cost ratio for the Hybrid Monopile is challenging.

Despite the uncertainties addressed in this economic evaluation, the cost comparison is considered reliable, as most uncertainties apply to all three structures in this research. A sensitivity study is conducted to see the influence of the most uncertain parameter in this research, the interface piece. Therefore, the cost ratio between the structures is deemed reliable.

7.2. Conclusion

This study investigates the feasibility of the Hybrid Monopile, which is a new concept for the foundation of offshore wind turbines. The main research questions of this research is formulated as below:

"Can the technical and economic aspects of bottom-fixed foundations be improved by implementing the Hybrid Monopile as a bottom-fixed foundation in comparison to jacket structures and traditional monopiles in the North Sea?"

To answer this research question three subquestions are formulated. First all the three subquestions are carefully answered. The answer on the main question will be formulated so the final conclusion of this research can be drawn.

1. *Up to what water depths, soil conditions, and wind turbine sizes can the Hybrid Monopile be feasibly manufactured and installed?*

In the first part of this research, a structural analysis is conducted. A preliminary design for the Hybrid Monopile is created, followed by checks on its bearing capacity, natural frequency, dynamic amplification factor, and stresses within the structure. Based on these checks, the design of the structural components of the Hybrid Monopile is evaluated. This evaluation, along with identified limitations, determines the feasible manufacturing and installation conditions for the Hybrid Monopile.

Given that a new factory in Germany can manufacture monopiles with a diameter of up to 14 meters and a length of 140 meters, it is concluded that the Hybrid Monopile can be installed in both sand and clay soils, at water depths up to 80 meters, and with a wind turbine capacity of 22 megawatts. Larger water depths for the same wind turbine size would require a diameter exceeding 14 meters, making it currently economically unfeasible to produce, and would it hardly be possible to install. Therefore, the Hybrid Monopile is technically suitable for installation in water depths up to 80 meters with a wind turbine size of 22 megawatts.

2. *Is it possible to reduce the installation cycle time of the Hybrid Monopile compared to traditional monopiles and jacket structures*

In the second part of this research, the installation assessment of the Hybrid Monopile is conducted by introducing three different strategies for its installation. Based on the design from the structural analysis, the preferred installation strategy is determined, including the leveling and connection of the Hybrid Monopile. The structural analysis also informs the type of actions required for installation and the installation type per action.

Given that the Hybrid Monopile is installed with support from six pin piles and is lifted from a barge and positioned atop the already installed pin piles, its installation closely resembles that of the jacket structure, which requires only four pin piles. Therefore, as long as the Hybrid Monopile requires more pin piles than the jacket structure, the installation cycle, assuming the vessel is already on site and ready to operate, is not faster than that of the jacket structure. However, if the number of piles for the jacket structure increases or the number of pin piles for the Hybrid Monopile decreases, the installation cycle of the Hybrid Monopile could potentially outperform that of the jacket structure.

Comparing the installation of the Hybrid Monopile with that of the traditional monopile, the Hybrid Monopile's installation is significantly more time-consuming. This is because the installation process for a pin pile and a monopile is similar, with only the hammer size varying. Considering that the Hybrid Monopile requires six piles for installation, its installation cycle takes considerably more time, making it highly unlikely to outperform the installation cycle of the traditional monopile. From the results on the installation times it can be concluded that the installation time of the monopile is 80% faster compared to the Hybrid Monopile. Compared to the jacket structure, there is potential to reduce the installation time, mainly based on the number of pin piles required for each structure. However, in this study the installation time of the jacket structure is 28% faster.

3. *Are there achievable cost savings in manufacturing and installation processes of the Hybrid Monopile compared to traditional monopiles and jacket structures?*

In the final part of this research, a cost evaluation is conducted for the manufacturing and installation of the Hybrid Monopile, compared to the traditional monopile and the jacket structure. The manufacturing

costs are based on the structural design of each type, while the installation costs are based on the use of vessels and the required equipment for installation.

For the manufacturing costs, it is assumed that the cost of producing the interface piece, the most uncertain structural component of the Hybrid Monopile, is lower than that of the jacket structure. The manufacturing costs depend on steel prices and labor costs per metric ton of steel for each type of structure. If the interface piece is indeed cheaper to manufacture, the overall manufacturing costs of the Hybrid Monopile are lower than those of the jacket structure. This is mainly because the weight and size of the interface piece are significant components of the Hybrid Monopile. According to the costs evaluation, a 20% reduction in the manufacturing cost of this component could significantly decrease the overall costs. However, if the manufacturing costs of the interface piece are equal to or higher than those of the jacket structure, the Hybrid Monopile becomes less cost-effective, particularly for larger turbines. This is due to the fact that the increase in size for the jacket and for the Hybrid Monopile the trend goes slightly exponential. The deeper the water depth, the more the costs of the Hybrid Monopile equals each other. Therefore it can be concluded that the manufacturing costs for the Hybrid Monopile are lower compared to the jacket in case the costs of the interface piece is lower than the jacket per metric ton

The installation costs for the Hybrid Monopile are higher than those for the jacket structure, primarily because the installation cycle is longer due to the greater number of pin piles needed for the Hybrid Monopile. Additionally, the type of vessel required for the Hybrid Monopile cannot be significantly reduced in cost, as the weight of the Hybrid Monopile (including the assembled monopile and interface piece) is comparable to that of the jacket. Consequently, similar vessels with similar day rates are used for both structures. Therefore, it can be concluded that as long as the Hybrid Monopile requires more pin piles compared to the jacket, the installation costs cannot the reduced significantly.

Comparing the manufacturing costs of the Hybrid Monopile with a traditional monopile, the Hybrid Monopile is not more cost-effective. A traditional monopile is relatively simple and inexpensive to manufacture compared to the more complex geometries of jackets or the interface piece of the Hybrid Monopile. Therefore, it can be concluded that the Hybrid Monopile will not be more cost-effective to produce than the traditional monopile for water depths up to 40 meters.

Regarding installation costs, the Hybrid Monopile is always more expensive to install than the traditional monopile for water depths up to 40 meters. This is mainly due to the time-consuming process of installing pin piles. Therefore it can be concluded that the using a Hybrid Monopile does not reduce the installation costs compared to the traditional monopile.

Based on the answered subquestions the main research question can be answered.

This study concludes that the Hybrid Monopile is suitable for installation in water depths of up to 80 meters, extending its applicability to deeper waters compared to the traditional monopile. However, in scenarios where the traditional monopile is a viable option, it always remain more cost-effective to install compared to the HMP. It should be acknowledged, however, that an increasing number of countries are imposing stricter sound exposure limit during installation, potentially making the installation of monopiles more challenging due to restrictions on pile driving. In this kind of situation the Hybrid Monopile would be a interesting alternative since the diameter of the pin piles required for the Hybrid Monopile are significant smaller compared to the diameter of the traditional monopile

When comparing the Hybrid Monopile to the jacket structure, the Hybrid Monopile does not exceed the allowable installation depth of the jacket, which can be installed in deeper waters compared to the Hybrid Monopile. Nevertheless, the economic evaluation suggests that the Hybrid Monopile has the potential to be more cost-effective than the jacket structure when installed in North Sea conditions up to water depth of around 70 meter. This indicates that the Hybrid Monopile could economically outperform the jacket structure in specific scenarios, despite the jacket's broader technical applicability.

In conclusion, the Hybrid Monopile presents a promising alternative foundation for offshore wind turbines in the North Sea conditions. With further research and optimization, it has the potential to enhance the feasibility and cost-effectiveness of offshore wind energy projects, contributing to the transition towards renewable energy sources.

7.3. Future recommendations and opportunities

The future recommendations highlight opportunities for further research and improvements in the Hybrid Monopile's design, installation, economic evaluation. These recommendations aim to enhance the research on the Hybrid Monopile's feasibility and competitiveness in the offshore wind energy market.

Structural analysis recommendations
Future research should focus optimizing the number of pin piles and exploring alternative configurations for the interface piece. This can further enhance the Hybrid Monopile's structural performance and cost-effectiveness.

Future research on the structural analysis also consist of a fatigue analysis which is not conducted in the feasibility study. Most offshore structure are relatively vulnerable to fatigue due to the fluctuating wind and wave forces. For the optimized design, an extensive fatigue analysis should be conducted.

Installation assessment recommendations
Optimizing installation strategies for the Hybrid Monopile, including potential horizontal transportation and dynamic positioning, should be explored to reduce installation time and costs. Quantitative analysis of specific vessel capabilities and noise mitigation systems should be conducted to enhance the accuracy of the installation assessment. Future research should also consider the impact of installing multiple Hybrid Monopiles in an offshore wind farm.

Economic evaluation recommendations
Optimizing the Hybrid Monopile's design for specific offshore wind farm sites, considering location-specific factors and market fluctuations, is essential for enhancing its economic competitiveness. Future research should involve detailed cost assessments based on specific project sites by taking into account the distance to shore and potential yard and transport costs.

Overall recommendation
In the paragraphs above, specific recommendations were provided for various sections discussed in this thesis. This final paragraph presents overall recommendations to make the concept of the Hybrid Monopile more feasible.

As previously addressed, the structural design of the Hybrid Monopile is not fully optimized. Structural optimization can lead to significant weight reduction and, consequently, cost reduction. The cost comparison indicates that the structural components significantly impact the total costs of the structure. A lighter structure will likely result in an overall reduction in the weight of multiple structural components of the Hybrid Monopile. Therefore, the first step is to optimize the structural design of the Hybrid Monopile.

Regarding the installation of the Hybrid Monopile, it would be beneficial to investigate whether the Hybrid Monopile can be transported horizontally on a barge. This would allow more Hybrid Monopiles to fit on a barge, thereby reducing transport costs. Additionally, determining the optimal number of pin piles per situation could potentially reduce installation time. It is also recommended to conduct a site-specific study and include a transport model to evaluate the required time, number of barges, and specific use of yards. This would provide a better estimation of the total installation costs of the Hybrid Monopile compared to traditional monopiles and jackets.

From an economic perspective, it is recommended to identify a yard where the Hybrid Monopile can be manufactured. Currently, yards only exist for the fabrication of either monopiles or jackets. Investigating the possibilities and potential costs of establishing a yard dedicated to fabricating the Hybrid Monopile is highly recommended.

Opportunities
It could be interesting to check for ice-regions where jacket structures are not structurally feasible for the foundation of offshore wind turbines. In these regions the Hybrid Monopile potentially has to compete with the gravity-based structure. In these regions it would also be interesting to check whether the Hybrid Monopile could be installed where the traditional monopile is not feasible to be installed. In addition, certain regions in the world are subjected to earthquakes. It would be interesting to see how to structure responds to the loads created by earthquakes.

Additionally, Heerema Marine Contractors recently introduced a silent pile-driving system. Instead of vibrating or hammering piles into the subsurface, this system pushes them in. It would be interesting

to explore the feasibility of using this technology for the Hybrid Monopile, as multiple piles need to be installed. The push hammer can leverage the other piles to assist in installation. This method can be performed without any noise pollution and has the potential to significantly reduce installation time [84].

Bibliography

[1] Deltares, *Advances in water replenishment studies of offshore monopile foundations*, [Online; accessed March 22, 2024]. [Online]. Available: https://www.deltares.nl/en/expertise/areas-of-expertise/energy-transition/advances-in-water-replenishment-studies-of-offshore-monopile-foundations.

[2] K.-Y. Oh, W. Nam, M. S. Ryu, J.-Y. Kim, and B. I. Epureanu, "A review of foundations of offshore wind energy convertors: Current status and future perspectives," *Renewable and Sustainable Energy Reviews*, vol. 88, pp. 16–36, 2018, ISSN: 1364-0321. DOI: 10.1016/j.rser.2018.02.005. [Online]. Available: https://www.sciencedirect.com/science/article/pii/S136403211830025X.

[3] *Offshore wind patents on the rise, new study by irena and epo shows*, Accessed: 2024-03-01. [Online]. Available: https://www.irena.org/News/articles/2023/Nov/Offshore-wind-patents-on-the-rise-new-study-by-IRENA-and-EPO-shows#:~:text=The%20global%20renewable%20power%20capacity,increase%20in%20comparison%20to%202020..

[4] *Renewable energy – powering a safer future*, Accessed: 2024-03-01. [Online]. Available: https://www.un.org/en/climatechange/raising-ambition/renewable-energy.

[5] M. Freeman, "Offshore wind can lower energy prices and beat out oil and gas," Tech. Rep., 2022, pp. 714–728. [Online]. Available: https://www.americanprogress.org/article/offshore-wind-can-lower-energy-prices-and-beat-out-oil-and-gas/.

[6] W. Musial, P. Spitsen, P. Duffy, *et al.*, "Offshore wind market report: 2023 edition," U.S. DEPARTMENT OF ENERGY, Tech. Rep., 2023.

[7] Heerema Engineering Solutions, *Internal documents*.

[8] F. van der Stap, M. Nielsen, C. Owen, and H. van der Male P. an Hendrikse, "On the feasibility of monopile foundations for offshore wind in the baltic sea," p. 15, 2023.

[9] Y. E. Liu, "Monopile forever," Technical University of Delft, Tech. Rep., Aug. 2021.

[10] A. Kielkiewicz, A. Marino, C. Vlachos, F. López Maldonado, and I. Lessis, "A comparison study of offshore wind support structures with monopiles and jackets for u.s. waters," Tech. Rep., 2015.

[11] M. Keene, *Comparing offshore wind turbine foundations*, Jan. 2021. [Online]. Available: https://www.windpowerengineering.com/comparing-offshore-wind-turbine-foundations/.

[12] R. He, J. Ji, J. Zhang, W. Peng, Z. Sun, and Z. Guo, "Dynamic impedances of offshore rock-socketed monopiles," *Journal of Marine Science and Engineering*, vol. 7, p. 134, May 2019. DOI: 10.3390/jmse7050134.

[13] B. O'Kelly and M. Arshad, "Offshore wind turbine foundations – analysis and design," C. Ng and L. Ran, Eds., pp. 589–610, 2016. DOI: 10.1016/B978-0-08-100779-2.00020-9. [Online]. Available: https://www.sciencedirect.com/science/article/pii/B9780081007792000209.

[14] V. Negro, J.-S. López-Gutiérrez, M. D. Esteban, P. Alberdi, M. Imaz, and J.-M. Serraclara, "Monopiles in offshore wind: Preliminary estimate of main dimensions," *Ocean Engineering*, vol. 133, pp. 253–261, 2017, ISSN: 0029-8018. DOI: 10.1016/j.oceaneng.2017.02.011. [Online]. Available: https://www.sciencedirect.com/science/article/pii/S0029801817300690.

[15] R. Damiani, K. Dykes, and G. Scott, "A comparison study of offshore wind support structures with monopiles and jackets for u.s. waters," Tech. Rep., Oct. 2016.

[16] S. Horwath, J. Hassrick, R. Grismala, and E. Diller, "Comparison of environmental effects from different offshore wind turbine foundations," Tech. Rep., Aug. 2020.

[17] SKI-Consults, “Monopile,” [Online; accessed July 3, 2024]. [Online]. Available: https://ski-consult.de/en/taetigkeitsbreiche/offshore-windenergieanlagen/monopile/.

[18] B. Zhao, *Jacket Platform*. Springer Singapore, Oct. 2020, vol. 3, pp. 1–4. DOI: 10.1007/978-981-10-6963-5_6-1.

[19] L. Ramirez, D. Fraile, and G. Brindley, “Offshore wind in europe - key trends and statics 2020,” WindEurope, Tech. Rep., 2021.

[20] J. Wilson, *Offshore Structures (Marine Engineering)*. 2003, pp. 161–168, ISBN: 9780122274107.

[21] K. Davis, *Guide to offshore wind foundations*. [Online]. Available: https://www.empireengineering.co.uk/wp-content/uploads/2021/08/The_Empire_Engineering_Guide_to_Offshore_Wind_Foundations_eBook-1.pdf.

[22] M. Seidel and S. Kelma, “Stochastic modelling of wind and wave induced loads on jacket piles,” *Stahlbau*, vol. 81, 2012. DOI: 10.1002/stab.201201599.

[23] G. Hou, K. Xu, and J. Lian, “A review on recent risk assessment methodologies of offshore wind turbine foundations,” Tech. Rep., 2022, p. 112469. DOI: 10.1016/j.oceaneng.2022.112469. [Online]. Available: https://www.sciencedirect.com/science/article/pii/S0029801822017528.

[24] X. Wang, X. Zeng, J. Li, X. Yang, and H. Wang, “A review on recent advancements of substructures for offshore wind turbines,” *Energy Conversion and Management*, vol. 158, pp. 103–119, 2018, ISSN: 0196-8904. DOI: 10.1016/j.enconman.2017.12.061. [Online]. Available: https://www.sciencedirect.com/science/article/pii/S019689041731213X.

[25] A. Tsouvalas, “Underwater noise emission due to offshore pile installation: A review,” *Energies*, vol. 13, no. 12, p. 3037, 2020. DOI: 10.3390/en13123037.

[26] S. K. Chakrabarti, *Hydrodynamics of Offshore Structures*. WIT Press, 1987.

[27] T. Sarpkaya, “In-line and transverse forces on cylinders in oscillatory flow at high reynolds-numbers,” *Journal of Ship Research*, vol. 21, no. 4, pp. 200–216, 1977.

[28] M. W. O’Neill, “Group action in offshore piles,” in *Proceedings of Conference on Geotechnical Practice in Offshore Engineering*, New York: ASCE, 1983, pp. 25–64.

[29] L. C. Reese, W. R. Cox, and F. D. Koop, “Field testing and analysis of laterally loaded piles in stiff clay,” in *Proceedings, 7th Offshore Technology Conference*, 1975, pp. 671–690.

[30] M. Rouholamin, S. Bhattacharya, and D. Lombardi, *Winkler Springs (p-y Curves) for Liquefied Soil from Element Tests*. CRC Press, 2015, ISBN: 978-1-138-02707-7. DOI: 10.1201/b17395-170.

[31] L. C. Reese, W. R. Cox, and F. D. Koop, “Analysis of laterally loaded piles in sand,” in *All Days*, Offshore Technology Conference (OTC), 1974.

[32] L. C. Reese and R. C. Welch, “Lateral loading of deep foundations in stiff clay,” *Journal of the Geotechnical Engineering Division, ASCE*, vol. 101, no. GT7, pp. 633–649, 1975.

[33] G. M. Norris, “Theoretically based bef laterally loaded pile analysis,” in *Proceedings of the 3rd International Conference on Numerical Methods in Offshore Piling*, TECHNIP, Ed., 1986, pp. 361–386.

[34] American Petroleum Institute, *Recommended Practice for Planning, Designing, and Constructing Fixed Offshore Platforms - Working Stress Design, API RP 2A-WSD, Twenty-Second Edition*. 2014, p. 310.

[35] M. A. Bellmann, J. Brinkmann, A. May, T. Wendt, S. Gerlach, and P. Remmers, “Underwater noise during the impulse pile-driving procedure: Influencing factors on pile-driving noise and technical possibilities to comply with noise mitigation values,” Supported by the Federal Ministry for the Environment, Nature Conservation et al., Tech. Rep., 2020.

[36] J. von Pein, T. Lippert, S. Lippert, and O. von Estorff, “Scaling laws for unmitigated pile driving: Dependence of underwater noise on strike energy, pile diameter, ram weight, and water depth,” *Applied Acoustics*, vol. 198, p. 108986, 2022, ISSN: 0003-682X.

[37] A. Memija, *Titan wind to build xxxl monopile production facility in northern germany*, 2024. [Online]. Available: https://www.offshorewind.biz/2024/06/24/titan-wind-to-build-xxxl-monopile-production-facility-in-northern-germany/.

[38] V. Negro, J. Lopez-Gutierrez, M. D. Esteban, and C. Matutano, "Uncertainties in the design of support structures and foundations for offshore wind turbines," *Renewable Energy*, vol. 63, pp. 125–132, Mar. 2014. DOI: 10.1016/j.rene.2013.08.041.

[39] M. Karimirad, *Offshore Energy Structures: For Wind Power, Wave Energy and Hybrid Marine Platforms*. Springer International Publishing, 2014, ISBN: 9783319121741. DOI: 10.1007/978-3-319-12175-8.

[40] R. Rahmani, A. Khairuddin, S. Cherati, and M. Pesaran, "A novel method for optimal placing wind turbines in a wind farm using particle swarm optimization (pso)," *IEEE Transactions on Power Electronics and Conference Record of the 2010 IEEE 26th International Power Engineering Conference (IPEC)*, pp. 134–139, Oct. 2010. DOI: 10.1109/IPECON.2010.5697144.

[41] T. Corke and R. Nelson, *Aerodynamic performance*.

[42] K. von Terzaghi, "Evaluation of coefficients of subgrade reaction," *Géotechnique*, vol. 5, no. 4, pp. 41–50, 1995.

[43] J. M. Murchison and M. W. O'Neill, "An evaluation of p-y relationships in sands," University of Houston-University Park, Report, 1983.

[44] W. M. Isenhower, S.-T. Wang, and L. G. Vasquez, *Technical Manual for LPile 2016 (Using Data Format Version 9): A Program for the Analysis of Deep Foundations Under Lateral Loading*. 2016.

[45] A. Haiderali and G. Madabhushi, *Evaluation of the p-y Method in the Design of Monopiles for Offshore Wind Turbines*. 2013, vol. 3. DOI: 10.4043/24088-MS.

[46] H. Matlock, "Correlations for design of laterally loaded piles in soft clay," in *Proceedings, 2nd Offshore Technology Conference*, vol. I, 1970, pp. 577–594.

[47] H. M. Coyle and L. C. Reese, "Load transfer for axially loaded piles in clay," *J. Soil Mech. Found. Div.*, vol. 92, no. 2, pp. 1–26, 1966. [Online]. Available: https://doi.org/10.1061/JSFEAQ.0000850.

[48] H. M. Coyle and I. H. Sulaiman, "Skin friction for steel piles in sand," *J. Soil Mech. Found. Div.*, vol. 93, no. 6, pp. 261–278, 1967. [Online]. Available: https://doi.org/10.1061/JSFEAQ.0001055.

[49] V. N. Vijayvergiya, "Load movement characteristics of piles," in *Proc., Ports'77: The 4th Annual Symp. of the Waterway, Port, Coastal and Ocean Division*, Reston, VA: ASCE, 1977, pp. 269–284.

[50] American Petroleum Institute (API), "Geotechnical and foundation design considerations," American National Standards Institute (ANSI), Recommended Practice 2GEO, Apr. 2011.

[51] L. M. Kraft, R. P. Ray, and T. Kagawa, "Theoretical t-z curves," *J. Geotech. Eng. Div.*, vol. 107, no. 11, pp. 1543–1561, 1981. [Online]. Available: https://doi.org/10.1061/AJGEB6.0001207.

[52] Y. K. Chow, "Analysis of vertically loaded pile groups," *Int. J. Numer. Anal. Methods Geomech.*, vol. 10, no. 1, pp. 59–72, 1986. [Online]. Available: https://doi.org/10.1002/nag.1610100105.

[53] M. F. Randolph, "Design methods for pile groups and piled rafts," in *Proc., 13th Int. Conf. of Soil Mechanics and Foundation Engineering*, New Delhi, India: Oxford and IBH Publishing Company, 1994, pp. 61–82.

[54] M. Pando, C. Ealy, G. Filz, J. Lesko, and E. Hoppe, "A laboratory and field study of composite piles for bridge substructures," Mar. 2006.

[55] K. Nering and A. Kowalska-Koczwara, "Determination of vibroacoustic parameters of polyurethane mats for residential building purposes," *Polymers*, vol. 14, p. 314, 2022. DOI: 10.3390/polym14020314.

[56] Y. Zhang, F. N. Rochmann, Y. Teng, and Y. Lai, “A numerical study on the group effect for offshore piles in clay under lateral loading,” *Marine Structures*, vol. 84, p. 103 238, 2022, ISSN: 0951-8339. DOI: 10.1016/j.marstruc.2022.103238. [Online]. Available: https://www.sciencedirect.com/science/article/pii/S0951833922000776.

[57] R. H. Jongbloed, S. C. V. Geelhoed, M. Huisman, *et al.*, “Efficient and effective use of bubble curtains for noise mitigation in offshore installation projects: Wp1: Defining the starting conditions,” Wageningen Marine Research, Wageningen Marine Research report C021/23, 2021. [Online]. Available: https://doi.org/10.18174/629724.

[58] APE China, *Ape drives the world’s largest pile!* May 2011. [Online]. Available: https://www.americanpiledriving.com/wordpress/2011/05/17/the-worlds-largest-pile-is-driven/.

[59] A. Buljan, *Heerema, iqip produce 24 db less noise during monopile installation at enbw’s he dreiht offshore wind farm*, 2024. [Online]. Available: https://www.offshorewind.biz/2024/07/04/heerema-iqip-produce-24-db-less-noise-during-monopile-installation-at-enbws-he-dreiht-offshore-wind-farm/.

[60] Copernicus, *Era5 monthly averaged data on single levels from 1940 to present*, 2024. [Online]. Available: https://cds.climate.copernicus.eu/cdsapp#!/dataset/reanalysis-era5-single-levels-monthly-means?tab=form.

[61] D. Apsley, *Waves: Random waves and statistics - 11*, 2023.

[62] DNV, *Offshore standards, dnv-os-c101, structural design of offshore units*, 2023.

[63] Spinergie, *Access in-depth market insights*, 2024.

[64] N. Faizi and Y. Alvi, “Chapter 6 - correlation,” in *Biostatistics Manual for Health Research*, N. Faizi and Y. Alvi, Eds., Academic Press, 2023, pp. 109–126, ISBN: 9780443185502. DOI: 10.1016/B978-0-443-18550-2.00002-5. [Online]. Available: https://www.sciencedirect.com/science/article/pii/B9780443185502000025.

[65] F. N. Kudu, Ş. Uçak, G. Osmancikli, T. Türker, and A. Bayraktar, “Estimation of damping ratios of steel structures by operational modal analysis method,” *Journal of Constructional Steel Research*, vol. 112, pp. 61–68, 2015, ISSN: 0143-974X. DOI: 10.1016/j.jcsr.2015.04.019. [Online]. Available: https://www.sciencedirect.com/science/article/pii/S0143974X15001339.

[66] T. Raktate and R. Choudhary, “Design of monopile foundation for offshore wind turbine,” pp. 4–6, 2020. DOI: 10.1051/conf/202017001024.

[67] S. Sánchez, J.-S. López-Gutiérrez, V. Negro, and M. D. Esteban, “Foundations in offshore wind farms: Evolution, characteristics and range of use. analysis of main dimensional parameters in monopile foundations,” *Journal of Marine Science and Engineering*, vol. E28040,

[68] Seagreen Wind Energy, *Offshore wind farm piling strategy*, 2020.

[69] M. Semenyuk, “Offshore wind farm installation planning: Decision-support tool for the analysis of new installation concepts,” Technical Report, 2019.

[70] IQIP, *Pre-piling jacket template*.

[71] Oil States Industries. “Swage and/or level fixed structures in a single trip!” Youtube. (2023), [Online]. Available: https://www.youtube.com/watch?v=wo2SfB1A6mU.

[72] Oil States, *Structural integrity & abandonment services hydra-lok connections*, [Online; accessed March 13, 2024], 2024.

[73] J. E. corporation, *How to connect the piles and the jacket (welding and grouting)*, [Online; accessed March 14, 2024], 2024.

[74] offshoreWIND.biz, *Macgregor and kongsberg maritime launch pile-gripper solution*, [Online; accessed March 14, 2024], 2018. [Online]. Available: https://www.offshorewind.biz/2018/05/07/macgregor-and-kongsberg-maritime-launch-pile-gripper-solution/.

[75] IRM Offshore and Marine Engineers PVT. LTD., *Irm pile grippers*, [Online; accessed March 14, 2024], 2021. [Online]. Available: https://www.irmome.com/irm-pile-grippers.php.

[76] UltraTech, *What is grouting in construction?* 2021. [Online]. Available: https://www.ultratechcement.com/for-homebuilders/home-building-explained-single/descriptive-articles/grouting-and-types-of-grouting-materials#:~:text=Grouting%2C%20in%20the%20context%20of,elements%20of%20a%20construction%20project..

[77] MAMMOET, *Monopile marshaling*, [Online; accessed March 06, 2024], 2024. [Online]. Available: https://www.mammoet.com/offshore-wind/monopile-marshaling/.

[78] Huisman, *Huisman to equip seaway7 jack-up vessel seaway ventus with monopile installation spread*, [Online; accessed June 18, 2024]. [Online]. Available: https://www.huismanequipment.com/en/media_centre/press_releases/163-197_Huisman-to-equip-Seaway7-jack-up-vessel-Seaway-Ventus-with-monopile-installation-spread.

[79] BOA Offshore AS, *Van oord east angelia one- jacket transport and related engineering*, [Online; accessed March 07, 2024], 2018. [Online]. Available: https://www.boa.no/van-oord-east-angelia-one-jacket-transport-and-related-engineering/.

[80] K. Sarah, *Sleipnir wraps up hornsea two jacket installation*, [Online; accessed March 07, 2024], 2020. [Online]. Available: https://www.heerema.com/news/sleipnir-wraps-up-hornsea-two-jacket-installation.

[81] University of Strathclyde, *Cost analysis*, 2015.

[82] BVGAssociaties, *Interactive guide*, 2024.

[83] CBS, *Inflation rate 3.8 percent in 2023, excluding energy at 6.5 percent*, 2024.

[84] M. Ottolini, *Shh! silent piling in progress*, Jun. 2023. [Online]. Available: https://www.heerema.com/insights/shh-silent-piling-in-progress.

A

Trend lines for the monopile and jacket

Appendix A provides the curve fit trend plots for the higher orders, this appendix shows them for the monopile and jacket structure. In the report the linear trend line is used in all cases.

Curve fit Monopile

For each of the six different wind turbine groups, three polynomial fits are plotted along with their respective least-squares errors (LSE). The polynomial fits are represented by solid lines up to the last known data point, beyond which they are depicted as dashed lines to indicate extrapolation. This extrapolation extends the trend beyond the available data points to predict how the relationship might continue based on existing monopile foundation data for offshore wind turbines.

Curve fit for 3 MW < WTG ≤ 5 MW

In the plot for the wind turbines bigger than 3 MW and smaller or equal to 5 MW wind turbines, the first and second order plots are the most representative, the third order shows a downward trend which end up with negative values for the diameter in deeper water. The deepest water where the 3-5 MW turbines is installed or an assessment is conducted is around 45 meter. Figure A.1 represents the curve fits of the wind turbines bigger than 3 MW and smaller or equal than 5 MW.

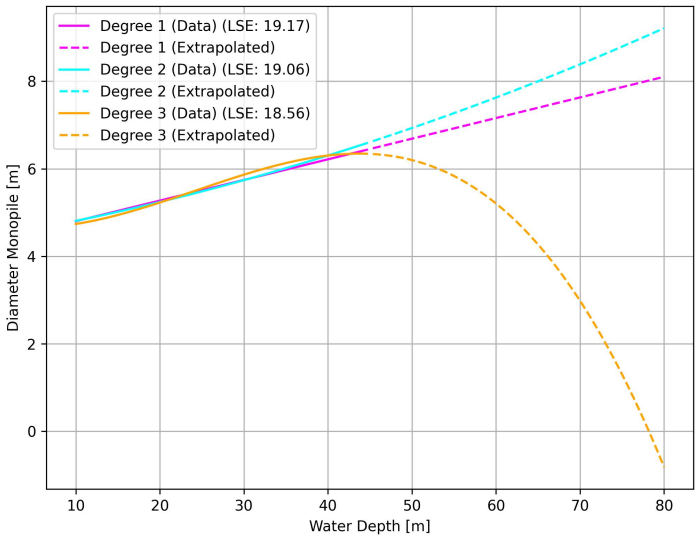

Figure A.1: First, second and third order curve fit for 3 < WTG ≤ 5 MW

Curve fit for 5 MW < WTG ≤ 8 MW

In the plot for the wind turbines bigger than 5 MW and smaller or equal to 8 MW wind turbines, the first order curve fit is the most representative, the second order curve fit shows a steep upward trend while around 30 meter water depth is the diameter decreases slightly, and third order shows a downward trend for the diameter in deeper water. The deepest water where the 5-8 MW turbines is installed or an assessment is conducted is around 65 meter. Figure A.2 represents the curve fits of the wind turbines bigger than 5 MW and smaller or equal than 8 MW.

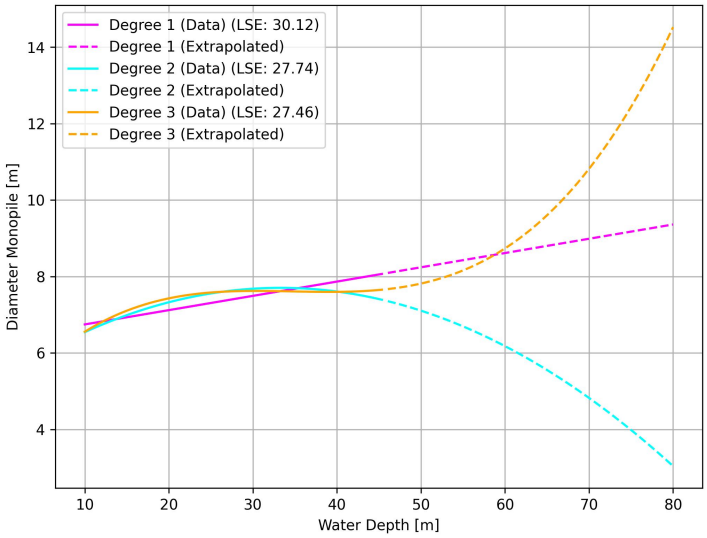

Figure A.2: First, second and third order curve fit for 5 < WTG ≤ 8 MW

Curve fit for 8 MW < WTG ≤ 10 MW

In the plot for the wind turbines bigger than 8 MW and smaller or equal to 10 MW wind turbines, the first and second order curve fit is the most representative, both the curves have exactly the same LSE. The third order shows a similar trend, however shows a more tempering trend after 65 meter. The deepest water where the 8-10 MW turbines is installed or an assessment is conducted is around 65 meter. Figure A.3 represents the curve fits of the wind turbines bigger than 8 MW and smaller or equal than 10 MW.

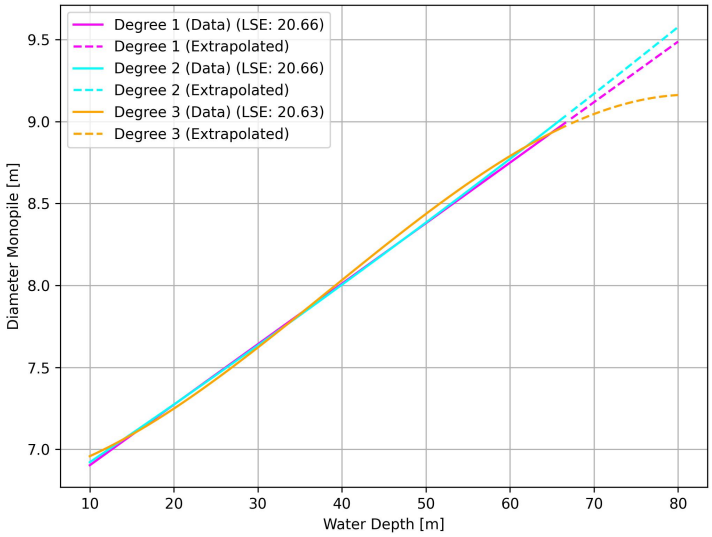

Figure A.3: First, second and third order curve fit for 8 < WTG ≤ 10 MW

Curve fit for 10 MW < WTG ≤ 15 MW

In the plot for the wind turbines bigger than 10 MW and smaller or equal to 15 MW wind turbines, the first and second order curve fit is the most representative, both the curves have exactly the same LSE. The third order shows decreasing trend including going beyond negative values. The deepest water where the 10-15 MW turbines is installed or an assessment is conducted is around 49 meter. Figure A.3 represents the curve fits of the wind turbines bigger than 10 MW and smaller or equal than 15 MW.

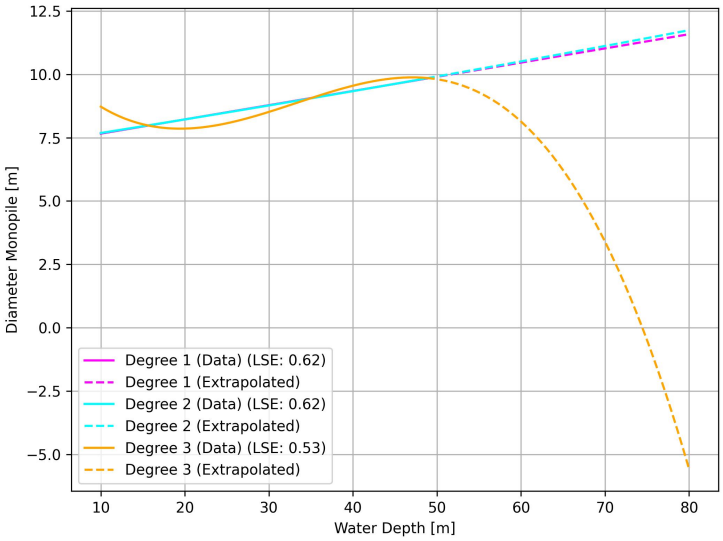

Figure A.4: First, second and third order curve fit for 10 < WTG ≤ 15 MW

Curve fit for 15 MW < WTG ≤ 22 MW

In the plot for the wind turbines bigger than 15 MW and smaller or equal to 22 MW wind turbines, the first and second order curve fit is the most representative, both the curves have exactly the same LSE.

The third order shows a tempering trend around 60 meter water depth. The deepest water where an assessment is conducted for the 15-22 MW turbines is around 67 meter. Figure A.5 represents the curve fits of the wind turbines bigger than 15 MW and smaller or equal than 22 MW.

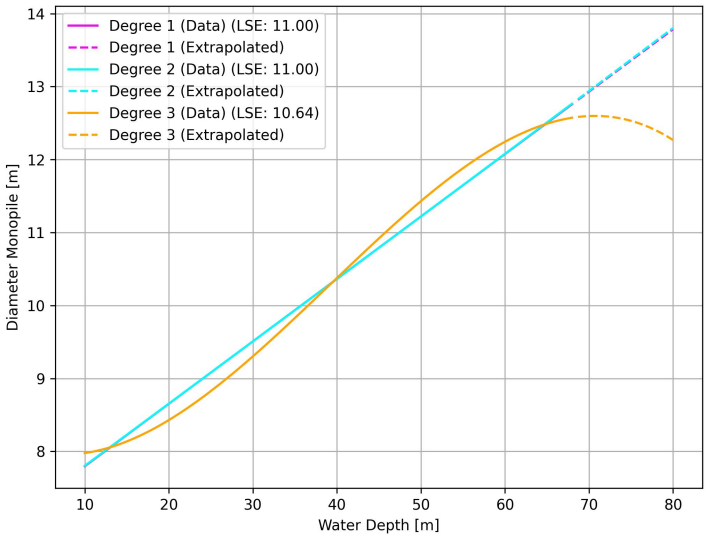

Figure A.5: First, second and third order curve fit for 15 < WTG ≤ 22 MW

Curve fit Jacket

In this section of in the appendix the first, second and third order of the curve fit of the jacket are represented including there least square error. Only the plots for the 5-8 MW, 8-10 MW and 15-22 MW. There is not enough data available of jackets built, developed or assessed in the North Sea for wind turbines smaller than 3 MW and in between 10-15 MW

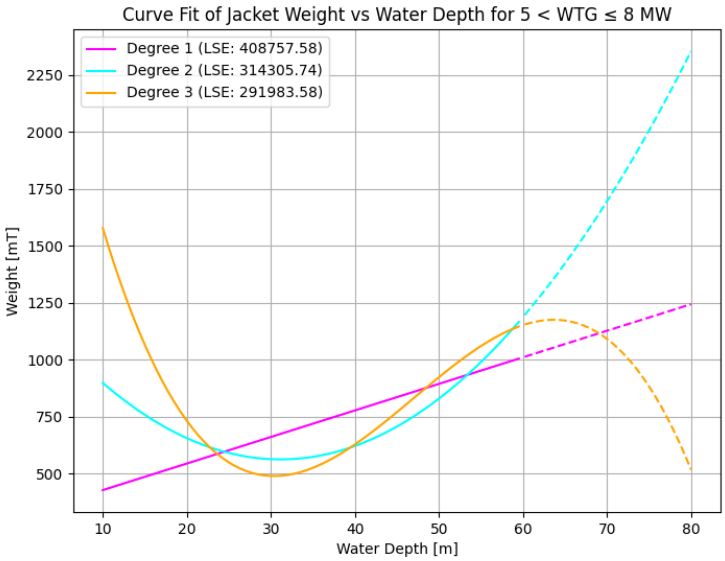

Figure A.6: First, second and third order curve fit for 5 < WTG ≤ 8 MW

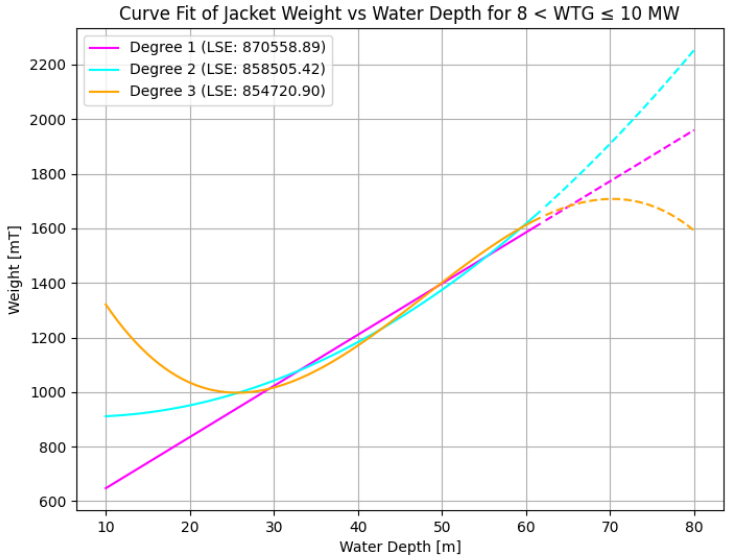

Figure A.7: First, second and third order curve fit for 8 < WTG ≤ 10 MW, for the jacket

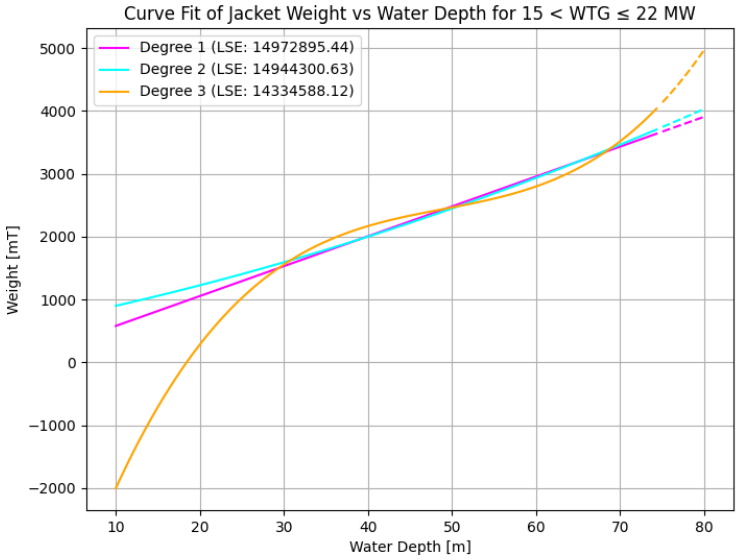

Figure A.8: First, second and third order curve fit for 15 < WTG ≤ 22 MW, for the jacket

B

Abaqus model

In appendix B the explanation of the assumption and algorithm is outlined for the Abaqus model is outlined.

The Abaqus suite comprises several modules, with Abaqus/Standard and Abaqus/Explicit being the most prominent. Abaqus/Standard is used for static and low-speed dynamic events (quasi-static), such as stress analysis, while Abaqus/Explicit handles high-speed dynamic events, such as crash simulations and complex contact problems. Both of these modules are numerical solvers based on the Newton-Raphson method. Another key module, Abaqus/CAE (Complete Abaqus Environment), provides a comprehensive environment for modeling, visualization, and managing simulation data.

Finite Element Analysis

To assess the stresses induced by wind and wave forces, a finite element analysis (FEA) is conducted. This section will outline the approach for the FEA and explain the setup of the Abaqus model. The forces exerted by wind and wave loading will be detailed in the subsequent subsection. The objective of this analysis is to determine the deflection of the various structural components of the Hybrid Monopile, from which the stresses can be derived.

The second analysis conducted using Abaqus focuses on determining the natural frequency of the structure. To achieve this, reference turbines are modeled atop the Hybrid Monopile to obtain a reliable response regarding the natural frequency and corresponding modal shape.

To conduct the FEA of the Hybrid Monopile a numerical model is created to verify the design of the foundation of the Hybrid Monopile. Abaqus is a finite element analysis software used to analyse the model. The structure is discretized with a certain amount of nodes, which are connected by elements. Every element is modelled as an quad shell element, and every node has 6 DOF, resulting in an element with 24 DOF.

Approach

To model the displacement and stresses in the structure, the structure is 3D-modelled in the software Abaqus. Which allows to accurately model the response of the structure subjected to the forces of the waves and wind. The elements are quad shells consisting of 24 DOF. Each node is subjected to three displacement degrees of freedom and three rotation degrees of freedom.

To investigate the foundation of the Hybrid Monopile and reduce the computational time, the monopile is cut-off a few meter above sea bed level. Therefore it is assumed that the monopile itself is structurally stable and will not fail. The part that is modelled in Abaqus is the interface piece and the pin piles. The resulting environmental forces exerting on the monopile and tower structure are concentrated on top of the interface piece at the model.

Assumptions and limitations

The finite element model is a representation of a real world situation, where it tries to mimic it as much as possible. However, by creating such a model, some limitation arises which can lead to insecurities of the model.

As mentioned in the former subsection, the Hybrid Monopile will be cut-off right above the interface piece. The resulting forces on the monopile and tower structure are centralised and simplified as point loads and moments. Three forces are placed in the exact middle of the 3D-model where the monopile is cut-off. These three forces are a horizontal, vertical and overturning moment. This assumption is made to simplify the exerting forcing on the model.

Additionally, the assumptions regarding material properties, such as the homogeneity and isotropy of the quad shell elements, may not accurately reflect the actual characteristics of the foundation of the Hybrid Monopile. Real-world materials often exhibit nonlinear behavior, anisotropic properties, and other complexities that are not accounted for in the simplified model. While incorporating nonlinear material models would provide more accurate representations, it would also increase the complexity and computational time the analysis.

The soil-spring stiffness's from the p-y curves, t-z curves and q-z curves are added to the model as extra stiffness's in the global assembly matrix. The springs are providing extra stiffness only for the horizontal and vertical displacement of the nodes where they are assigned to. This assumption may not fully incorporate the complex behaviour and interaction of the foundation of the Hybrid Monopile with the subsurface.

Additionally, it is expected that during the installation the monopile itself will penetrate the soil due to the self weight of the monopile. This will cause some extra stiffness to the model. It is however assumed that the p-y curves does not any stiffness based on the resistance of the soil to the tip of the monopile. The empirical data where the p-y curves are based on are not verified for such large diameters as a monopile has. Therefore in real-world it would add extra stiffness to the structure, in the model no extra stiffness is added to the tip of the monopile

During installation, the monopile naturally penetrates the soil under its own weight, contributing additional stiffness to the overall system. However, in the model, it is assumed that the p-y curves do not incorporate this added stiffness from soil resistance at the monopile tip. This assumption is based on empirical data that hasn't been verified for monopiles with such large diameters. Consequently, while real-world scenarios would experience increased stiffness due to this soil resistance at the tip, the model does not account for it.

It is important to acknowledge that mesh size significantly affects the model's accuracy. Finer meshes yield more precise models, but they also demand more computational time, which can be a limitation. However, at this design stage, using a somewhat coarser mesh still provides a good representation.

Model set-up

The finite element analysis for designing the Hybrid Monopile follows a specific sequence of steps. Initially, the structure's geometry is constructed, and governing equations are established based on plate theory. Subsequently, structural elements are discretized into nodes and elements. The next step involves assigning properties to represent the actual material of these elements and create the soil-stiffness springs according to theory described in section 2.3. Local mass and stiffness matrices are then defined using shape functions derived from the governing equations for the shell elements. These local matrices are aggregated into global matrices for both mass and stiffness. Boundary conditions are applied to specific nodes within the global matrix. Finally, a linear system is formulated and solved numerically using the implicit Newton-Raphson method.

Step 1: Discretize the domain

A file is created to make the model parametric, this allows to manually adapt the geometry, discretization, soil conditions etc. This file prevents the user from adapting the and drawing the abaqus model in Abaqus itself. Based on the geometry and meshing grip, the amount of nodes is determined. The model is discretized with a mesh size of 0.5. The amount varies dependent on the length and diameter

of the foundation of the Hybrid Monopile. Figure B.1 shows the discretized domain of the structure in Abaqus.

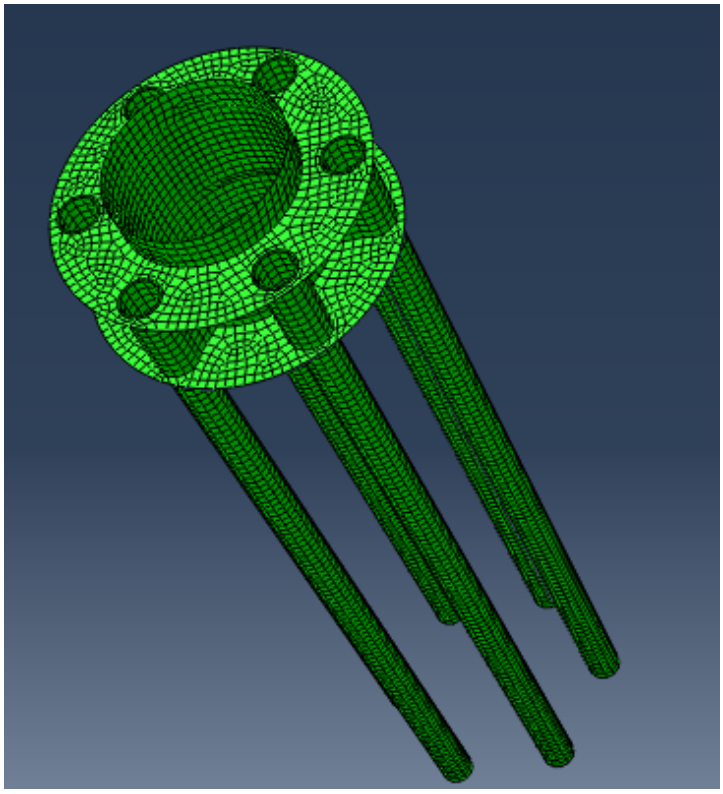

Figure B.1: Discretization of the model in Abaqus

Step 2: Define element properties

The Abaqus model requires a parameterized input file where the geometry of the structure is defined. The allows to run the model in multiple runs in once, instead of adapting the model in Abaqus self, which is difficult and time consuming. The element properties are based on the geometry input of the the structure and are calculated according to Equation B.1 until Equation B.4

$$A = \frac{pi}{4}\left(D_{out}^2 - D_{in}^2\right) \tag{B.1}$$

$$I = \frac{pi}{64}\left(D_{out}^4 - D_{in}^4\right) \tag{B.2}$$

$$J = 2 * I \tag{B.3}$$

$$Im = \frac{pi}{32}\left(D_{out}^4 - D_{in}^4\right) \tag{B.4}$$

On top of that, the material properties are assumed to be:

$G_{steel} = \frac{E_{steel}}{2*(1-\nu_{steel})}$

ν_{steel} = 0.3 [-]

ρ_{water} = 1025 $[\frac{kg}{m^3}]$

ρ_{steel} = 7850 $[\frac{kg}{m^3}]$

E_{steel} = 2.1 E^5 $[\frac{N}{mm^2}]$

Step 3: Create soil-springs

The third step is creating the soil-springs according to the p-y, t-z and q-z springs. This is done by describing how the soil layers are built up. The soil characteristics are as described at the beginning of the chapter. The soil-springs are simulated based on the depth of the layer where they are assigned. The deeper the springs occur in the subsurface, the stiffer they are. The amount of springs can be chosen dependent on the input. Limitations arise when the spring distance becomes to small compared to the meshing size. When the spring distance for example becomes smaller compared to the meshing size, multiple springs are assigned to one node, this leads to an unreliable stiff node and so are the results.

The third step involves creating soil-springs based on the p-y, t-z, and q-z models. This requires detailing the composition of the soil layers. The soil characteristics, as described at the beginning of the chapter. Soil-springs are assigned according to the depth of the layer they correspond to, with deeper springs being stiffer. The number of springs can be adjusted based on the input. However, limitations arise when the spring spacing becomes too small relative to the meshing size. If the spring distance is smaller than the mesh size, multiple springs may be assigned to a single node, resulting in an unrealistically stiff node and unreliable results.

Step 4: Solve the system

In the last step the local K matrices of every elements are defined and solved, dependent on the complexity of the system, Abaqus is making weak form of the partial differential equation (governing equations) based on the principles of linear algebra. After defining the local matrices, the global matrix is assembled, where it is important to connect the correct nodes to each other.

Based on the connectivity matrix, which allows elements to rotate over a certain axis, the global matrix is assembled. Since the forces are static and the structure is not allowed to move in the water the linear formulation is derived as described in Equation B.5. Where K is the force matrix and K the global stiffness matrix.

$$\mathbf{F} = \mathbf{K}u \tag{B.5}$$

In relatively simple systems, Abaqus can determine displacement (u) by inverting the global stiffness matrix (K matrix). However, for large and complex systems, Abaqus uses a linear solver based on the iterative implicit Newton-Raphson method to solve for displacement (u). For the Monopile, which is considered a large system, Abaqus employs this iterative method.

The process involves assigning forces at different time steps. In the first 20% of the total time, Abaqus checks the soil-stiffness spring curves to determine where soil resistance and displacement converge. This process continues at 40%, 60%, 80%, and finally 100% of a total time span of 1 seconds. Thus, static loads are applied over a 1-second period.

If the applied forces on the structure exceed the available soil resistance, the model fails to converge because displacement continues to increase without a corresponding increase in soil resistance. Consequently, the foundation cannot withstand the applied forces.

After confirming the ULS check of the structure, the natural frequency of the structure is checked. Since it is an static situation the natural frequency of the system is calculated.

In Abaqus, the natural frequency of a structure is calculated using a modal analysis through an eigenfrequency extraction procedure. This involves creating the finite element model by defining the geometry, specifying material properties, assigning sections, and meshing the structure. Appropriate boundary conditions are applied to accurately represent constraints. An eigenfrequency extraction step is then created, typically using the Lanczos solver, to specify the number of eigenvalues to be

extracted. Abaqus formulates the equation of motion, $\mathbf{Ku} = \lambda\mathbf{Mu}$, and solves for the eigenvalues λ, which are used to determine the natural frequencies $f = \frac{\sqrt{\lambda}}{2\pi}$.

C

Frequency spectrum

In appendix C the overview of the frequency spectrum of every wind turbine type in the various water depths are shows.

Frequency spectrum in 30 and 40 meter water deph

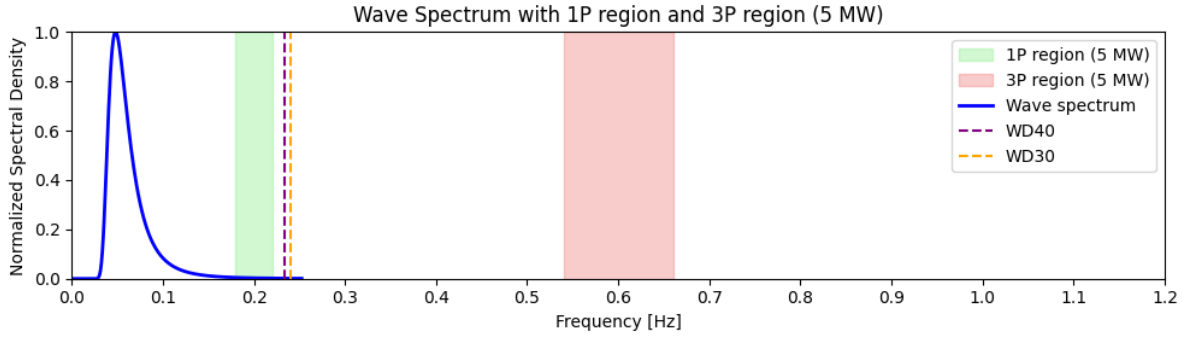

Figure C.1: 5 MW frequency spectrum in water depth of 30 and 40 meter

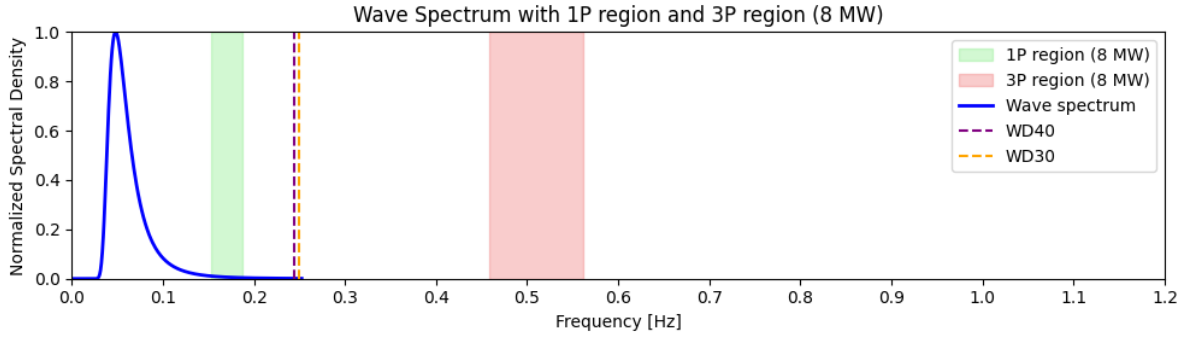

Figure C.2: 8 MW frequency spectrum in water depth of 30 and 40 meter

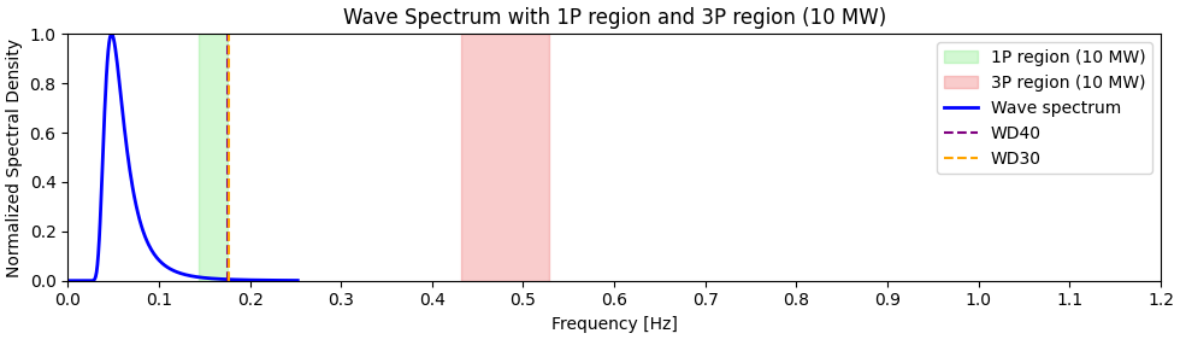

Figure C.3: 10 MW frequency spectrum in water depth of 30 and 40 meter

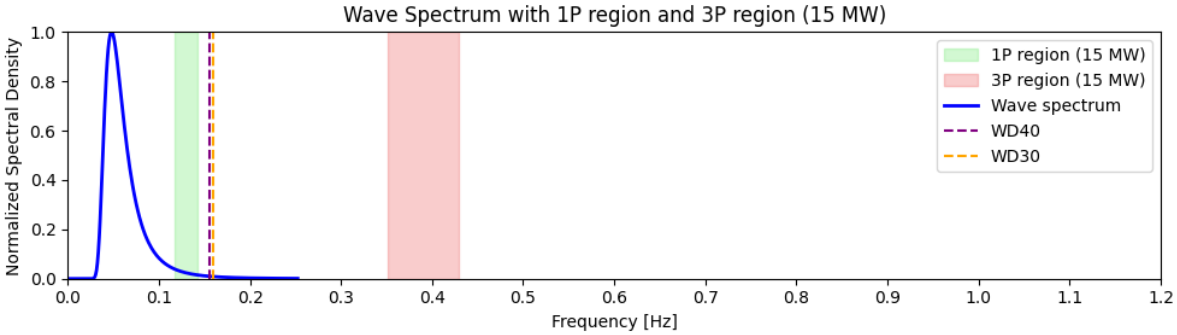

Figure C.4: 15 MW frequency spectrum in water depth of 30 and 40 meter

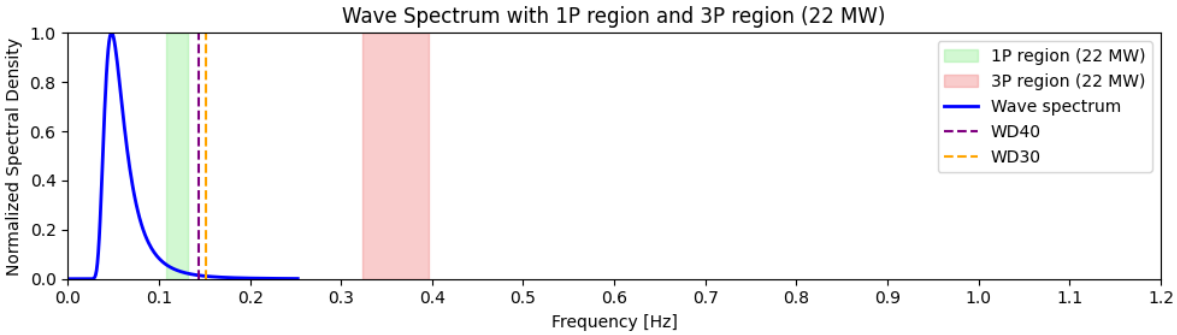

Figure C.5: 22 MW frequency spectrum in water depth of 30 and 40 meter

Frequency spectrum in 50 and 80 meter water depth

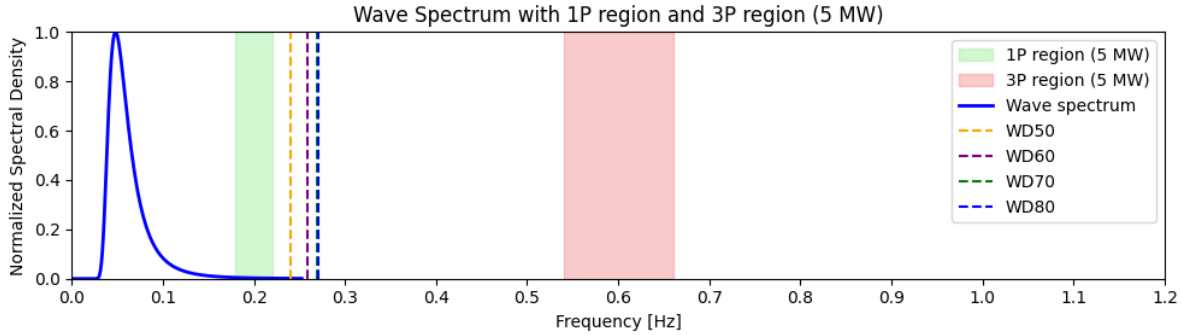

Figure C.6: 5 MW frequency spectrum in water depth of 50 till 80 meter

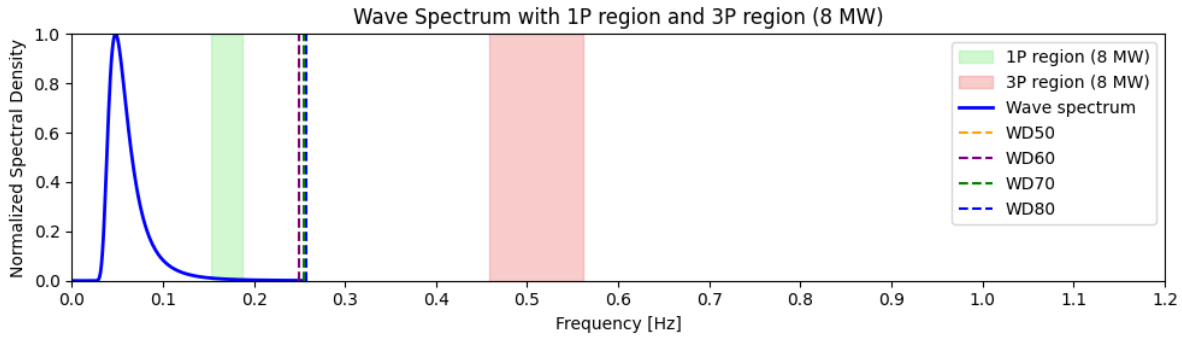

Figure C.7: 8 MW frequency spectrum in water depth of 50 till 80 meter

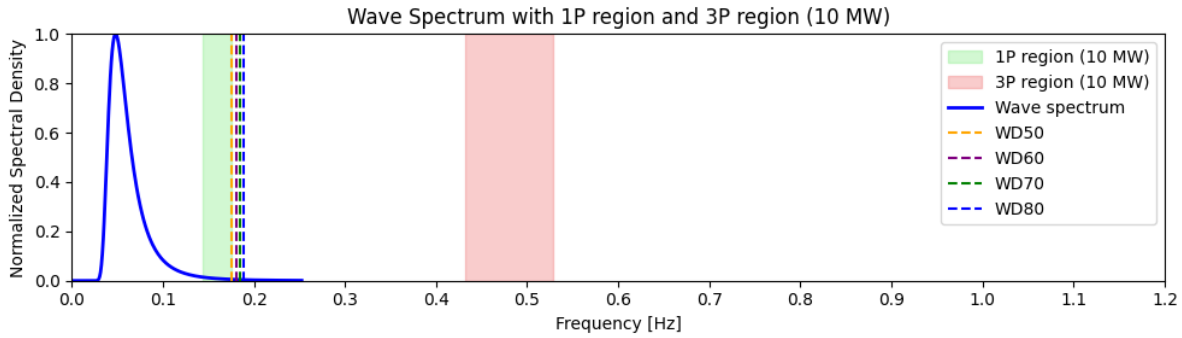

Figure C.8: 10 MW frequency spectrum in water depth of 50 till 80 meter

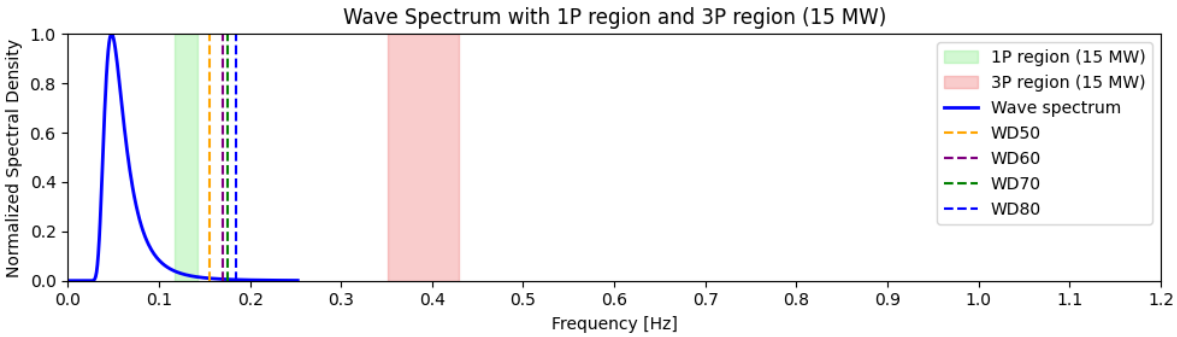

Figure C.9: 15 MW frequency spectrum in water depth of 50 till 80 meter

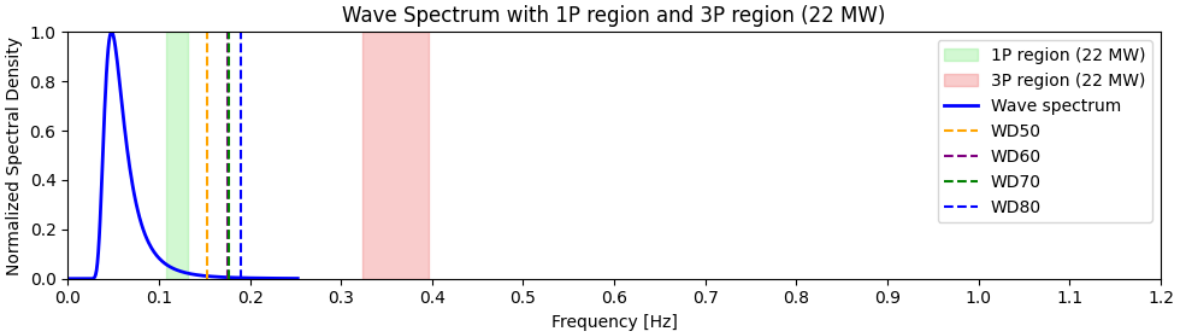

Figure C.10: 22 MW frequency spectrum in water depth of 50 till 80 meter

D

Cost overview for clay

Appendix D represents the graph's for the economic comparison

Manufacturing costs

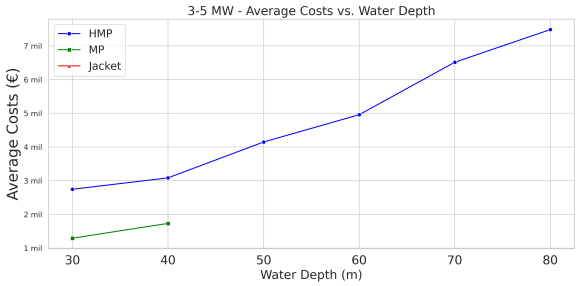

Figure D.1: WTG Range 3-5 MW (clay)

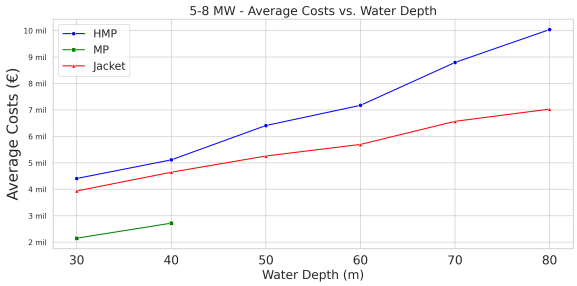

Figure D.2: WTG Range 5-8 MW (clay)

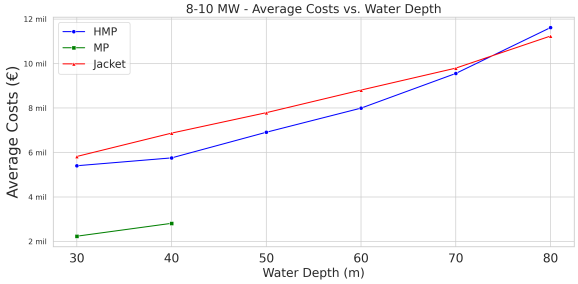

Figure D.3: WTG Range 8-10 MW (clay)

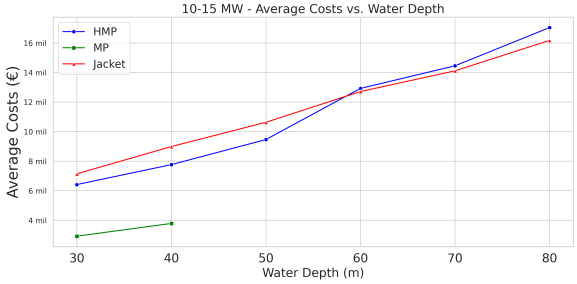

Figure D.4: WTG Range 10-15 MW (clay)

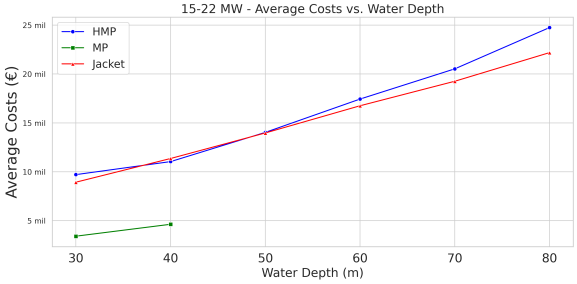

Figure D.5: WTG Range 15-22 MW (clay)

Installation costs

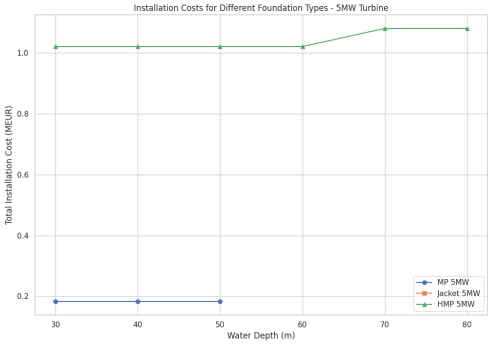

Figure D.6: WTG Range 3-5 MW (clay)

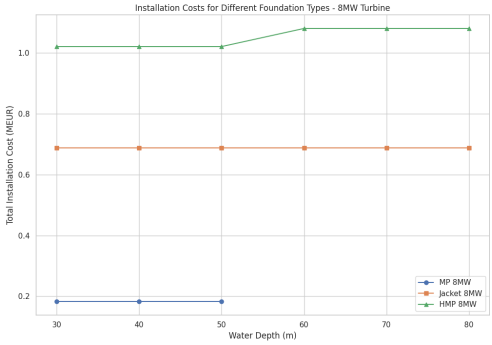

Figure D.7: WTG Range 5-8 MW (clay)

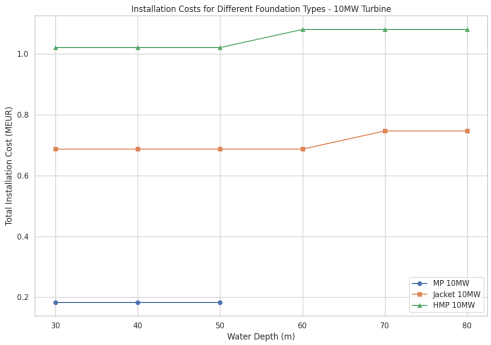

Figure D.8: WTG Range 8-10 MW (clay)

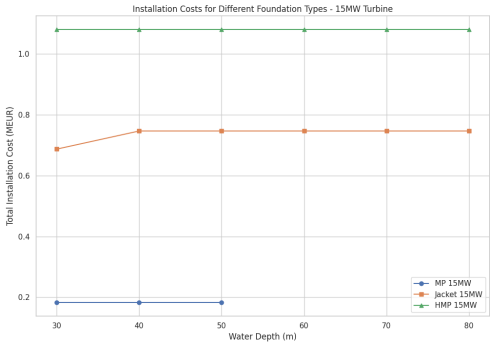

Figure D.9: WTG Range 10-15 MW (clay)

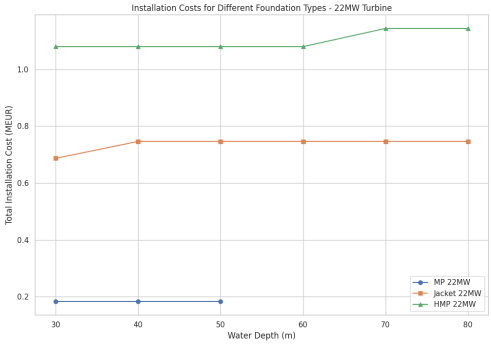

Figure D.10: WTG Range 15-22 MW (clay)

Total costs

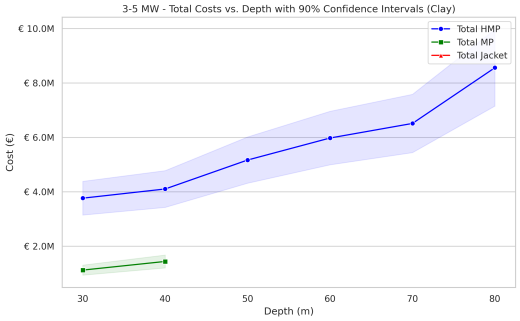

Figure D.11: 3-5 MW Total Costs vs. Depth with CI (clay)

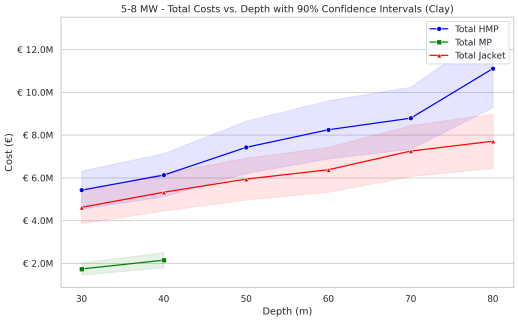

Figure D.12: 5-8 MW Total Costs vs. Depth with CI (clay)

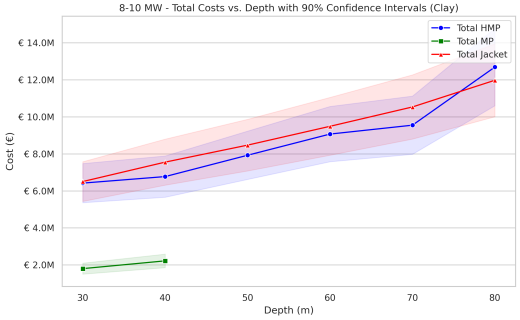

Figure D.13: 8-10 MW Total Costs vs. Depth with CI (clay)

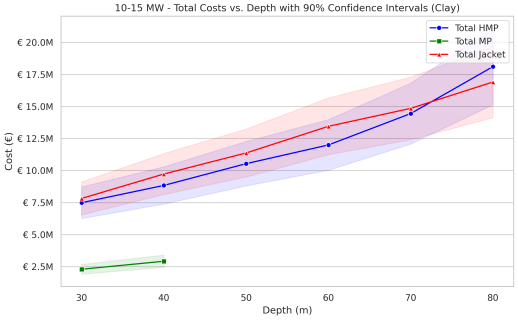

Figure D.14: 10-15 MW Total Costs vs. Depth with CI (clay)

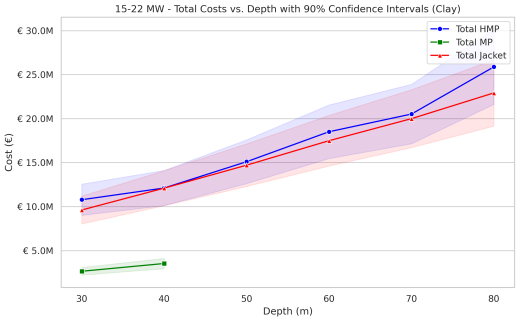

Figure D.15: 15-22 MW Total Costs vs. Depth with CI (clay